TAMPEREEN TEKNILLINEN YLIOPISTO
TAMPERE UNIVERSITY OF TECHNOLOGY

Muhammad Usman Sheikh

Aspects of Capacity Enhancement Techniques in Cellular Networks

Julkaisu 1261 • Publication 1261

Tampere 2014

Tampereen teknillinen yliopisto. Julkaisu 1261
Tampere University of Technology. Publication 1261

Muhammad Usman Sheikh

Aspects of Capacity Enhancement Techniques in Cellular Networks

Thesis for the degree of Doctor of Science in Technology to be presented with due permission for public examination and criticism in Tietotalo Building, Auditorium TB109, at Tampere University of Technology, on the 14th of November 2014, at 12 noon.

Tampereen teknillinen yliopisto - Tampere University of Technology
Tampere 2014

Doctoral advisor
Professor Jukka Lempiäinen, D.Sc.(Tech)
Department of Electronics and Communications Engineering
Tampere University of Technology
Tampere, Finland
email: jukka.lempiainen@tut.fi

Pre-examiner
Vice Head of Department, Associate Professor Jyri Hämäläinen, D.Sc.(Tech)
Department of Communications and Networking
Aalto University
Espoo, Finland
email: jyri.hamalainen@aalto.fi

Pre-examiner and opponent
Associate Professor Mario Garcia Lozano, D.Sc.(Tech)
Department of Signal Theory and Communications
Universitat Politecnica de Catalunya
Barcelona, Spain
email: mariogarcia@tsc.upc.edu

Opponent
Professor Risto Wichman, D.Sc.(Tech)
Department of Signal Processing and Acoustics
Aalto University
Espoo, Finland
email: risto.wichman@aalto.fi

ISBN 978-952-15-3402-7 (printed)
ISBN 978-952-15-3430-0 (PDF)
ISSN 1459-2045

PREFACE

The research work for this doctoral thesis was carried out during the years 2010-2014 at European Communications Engineering Ltd, and at the Department of Electronics and Communications Engineering in Tampere University of Technology, Finland.

First of all, I am thankful to God Almighty Allah for being benevolent, for giving me strength to complete this milestone in my life, and for the countless blessings on me. Then, I am thankful to Hazrat Muhammad (P.B.U.H) for being so kind and generous. I would like to express my genuine appreciation and deepest gratitude to my supervisor and custos Prof. Jukka Lempiäinen for his continuous guidance and support, invaluable advises, cooperative supervision, discussions and feedback, and for the confidence he has shown over me. Working under his supervision was a pleasure and a great experience for me. I would also like to express my regard to Prof. Markku Renfors for his support and encouragement. I would like to thank Tampere Doctoral Program in Information Science and Engineering (TISE) for financially supporting my conference trips. I would like to thank Dr. Jussi Turkka for encouraging me and making me believe that I can make my doctoral study. I would like to thank Dr. Jarno Niemelä for introducing me to Radio Network Planning (RNP) group, and for helping me in carrying out my initial research work at preliminary stage. I would like to pay appreciations to all my current and ex-colleagues at RNP group especially Dr. Panu Lahdekorpi, and Dr. Tero Isotalo. Moreover, I would also like to thank my colleagues at European Communications Engineering Ltd, and special thanks to Hans Ahnlund for his fruitful discussions, Krista Laine for her care and Marja Enomaa for her motherly behavior.

I would like to thank whole Pakistani community at Tampere and Espoo for supporting me, for giving me so many moments of joy and fun, and for making my stay in Finland unforgettable. I would especially like to acknowledge the help and support of Haider Ali and Adnan Kiani in the early days of my stay in Finland.

I would like to express my greatest and warmest thanks to my parents Fahmida Begum and Muhammad Akhtar Sheikh (Late), for their

unconditional support and love, for always being kind, encouraging and cheering me, and for their endless love and countless prayers, without whom it was not possible for me to achieve this milestone. I am profoundly thankful to my siblings, Imran Sheikh, Ejaz Sheikh, Riaz Sheikh, Nagina Aurangzeb, and Bhabies for their infinite support in every thick and thin of my life, and for their sincere prayers.

At last but not the least, I am extremely thankful to my beloved wife Sehrish Usman for her enormous love, unlimited patience, for helping me to maintain a good balance in my life, and for giving me the priceless gifts in the form of two daughters Areesha Usman and Eshal Usman. Thanks to my lovely daughters for providing me tons of joy, and for filling the colors in my life.

Tampere, Finland
November 2014,

Muhammad Usman Sheikh

Dedicated to my beloved Prophet
Hazrat Muhammad Sallallahu Alaihi Wa Aalihi Wa Sallam

"Your Paradise lies under the feet of your mother"
Muhammad Ibn-e-Abdullah

TABLE OF CONTENTS

LIST OF PUBLICATIONS

This thesis is the compilation of the following publications:

[P1] Sheikh, M.U., and Lempiäinen, J., "UMTS900 Deployment with Different Call Handling Strategies", in *Proc. 6th IEEE International Symposium on Wireless Communication System (ISWCS)*, Tuscany, Italy, pp. 590-594, 7-10 September 2009.

[P2] Sheikh, M.U., and Lempiäinen, J., "Assessment of Smart Traffic Handling Schemes in Multimode Multiband Cellular Network" in *Wiley's Journal on Wireless Communication and Mobile Computing*, vol. 11, pp: 1618-1627, December 2011.

[P3] Sheikh, M.U., and Lempiäinen, J., "Impact of Penalty Time on Multilayer Network Along with UMTS900 Deployed with Smart Traffic Handling Scheme", in *Proc. IEEE Student Conference on Research and Development (SCOReD)*, Serdang, Malaysia, pp. 12-15, November 2009.

[P4] Sheikh, M.U., Jagusz, R., and Lempiäinen J., "Performance Evaluation of Adaptive MIMO Switching in Long Term Evolution", in *Proc. IEEE 7th International Wireless Communication and Mobile Computing (IWCMC'11) Conference*, Istanbul, Turkey, pp. 866-870, 4-8 July 2011.

[P5] Sheikh, M.U., and Lempiäinen J., "Performance Analysis of Dual-Cell HSDPA plus MIMO and LTE along with Adaptive MIMO Switching at Cellular Level", *in Elsevier Journal on Physical Communication (Special Issue),* vol. 9, pp. 288-298, December 2013.

[P6] Sheikh, M.U., and Lempiäinen J., "A Flower Tessellation for Simulation Purpose of Cellular Network with 12-Sector Sites", in *IEEE Wireless Communications Letters*, vol.2, no.3, pp.279-282, June 2013.

[P7] Sheikh, M.U., Lempiäinen J., and Ahnlund, H., "Advanced Antenna Techniques and High Order Sectorization with Novel Network Tessellation for Enhancing Macro Cell Capacity in DC-

HSDPA Network", in *AIRCC International Journal of Wireless & Mobile Networks (IJWMN)*, vol. 5, no. 5, pp. 65-84, October 2013.

[P8] Sheikh, M.U., and Lempiäinen J., "Will New Antenna Materials Enable Single Path Multiple Access (SPMA)?", *in Springer Journal on Wireless Personal Communications*, vol. 78, no. 2, pp. 979-994, September 2014.

LIST OF FIGURES

LIST OF TABLES

LIST OF ABBREVIATIONS

2G	Second Generation
3G	Third Generation
3GPP	3rd Generation Partnership Project
4G	Fourth Generation
5G	Fifth Generation
AICH	Acquisition Indicator Channel
AMC	Adaptive Modulation and Coding
AMS	Adaptive MIMO Switching
DC-HSDPA	Dual-Cell HSDPA
AoA	Angle of Arrival
AoD	Angle of Departure
BCCH	Broadcast Control Channel
BS	Base Station
CCCH	Common Control Channel
CDF	Cumulative Distribution Function
CMA	Constant Modulus Algorithm
CNR	Carbon Nanoribbon
CNT	Carbon Nanotube
CPICH	Common Pilot Channel
CS	Circuit Switched
CSI	Channel State Information
D2D	Device-to-Device
DCH	Dedicated Traffic Channel
DD	Decision Directed
DL	Downlink
DMI	Direct Matrix Inversion
DoA	Direction of Arrival
DoD	Direction of Departure
DTX	Discontinuous Transmission
EGC	Equal Gain Combining
Er	Erlang
FDMA	Frequency Division Multiple Access
FH	Frequency Hopping

G	Generation
GSM	Global System for Mobile Communication
HSDPA	High Speed Downlink Packet Access
HS-PDSCH	High Speed Physical Downlink Shared Channel
IM	Interference Margin
ISD	Intersite Distance
IT	Image Theory
LMS	Least Mean Square
LTE	Long Term Evolution
LTE-A	LTE-Advanced
M2M	Machine-to-Machine
MIMO	Multiple Input Multiple Output
MRC	Maximum Ratio Combining
MS	Mobile Station
Multi-RAT	Multiple Radio Access Technology
NLMS	Normalized Least Mean Square
NLOS	Non Line of Sight
OFDMA	Orthogonal Frequency Division Multiple Access
PC	Power Control
PG	Processing Gain
PICH	Paging Indicator Channel
PS	Packet Switch
P-SCH	Primary Synchronization Channel
PSD	Power Spectral Density
QoS	Quality of Service
RAT	Radio Access Technology
RB	Resource Block
RE	Resource Element
RF	Radio Frequency
RLS	Recursive Least Squares
RR	Round Robin
RRM	Radio Resource Management
SBR	Shoot and Bouncing Ray
SC-FDMA	Single Carrier Frequency Division Multiple Access
SDR	Software Defined Radio
SINR	Signal to Interference plus Noise Ratio

SISO	Single Input Single Output
SM	Spatial Multiplexing
SPMA	Single Path Multiple Access
S-SCH	Secondary Synchronization Channel
TDMA	Time Division Multiple Access
UE	User Equipment
UL	Uplink
UMTS	Universal Mobile Telecommunication System
WCDMA	Wideband Code Division Multiple Access

LIST OF SYMBOLS

$(.)^T$	Transpose operation
H_{IID}	Random fading channel matrix with independent and identically distributed entries
I_{other}	Interference coming from other cell
I_{own}	Interference coming from own cell
L_j	Path loss of jth user between user and base station
M_{max}	Maximum number of users scheduled per TTI
N_{rf}	Noise spectral density
P_{AICH}	Power of Acquisition Indicator Channel in downlink direction
P_{CCCH}	Common Control Channel power in downlink direction
P_{CPICH}	Common Pilot Channel Power in downlink direction
P_{P_SCH}	Power of primary synchronization channel in downlink direction
P_{PICH}	Power of Paging Indication Channel in downlink direction
P_{P-SCH}	Primary Synchronization Channel power in downlink direction
P_{S_SCH}	Power of secondary synchronization channel in DL direction
P_{S-SCH}	Secondary Synchronization Channel power in downlink direction
P_{max}	Maximum available transmission power in DL direction
Pr_{data}	Probability of no data transfer
Pr_{speech}	Speech blocking probability
R	User bit rate
R_R	Receive covariance matrix
R_T	Transmit covariance matrix
$SF_{HS-PDSCH}$	Spreading factor of High Speed Physical Downlink Shared Channel in HSDPA
β_j	Individual user loading factor
η_{CCCH}	Cell loading due to Common Control Channel

η_{CPICH}	Cell loading due to Common Pilot Channel
η_{DCH}	Cell loading due to Dedicated Channel
η_{DL}	Downlink cell loading
η_{HSDPA}	HSDPA cell loading
$\eta_{HS-PDSCH}$	Cell loading due to High Speed Physical Downlink Shared Channel
$\eta_{HS-SCCH}$	Cell loading due to High Speed Shared Control Channel
η_{UL}	Uplink cell loading
$\eta_{non-HSDPA}$	Loading of non-HSDPA cell
η_{total}	Total cell loading
δ	Orthogonality
H	Channel Matrix
$SINR$	Signal to Interference plus Noise Ratio
W	Chip rate
i	Interference factor
v	Activity factor

1. INTRODUCTION

1.1. Background and motivation

Evolution of the mobile networks has been extremely fast during the last two decades, and a tsunami of data traffic is expected to grow even more rapidly in the coming years. Mobile data traffic is expected to increase thirteen fold between 2012 and 2017 [1]. In the coming years, the number of mobile devices connected to networks will surpass the number of people on the planet earth, and by the year 2017 there will be nearly 1.4 mobile devices per person [1].

Since the deployment of Global System for Mobile Communication (GSM) in early 1990's, a drastic and rigorous development was observed in the field of cellular communications. The Second Generation (2G) of wireless technology was dominated by GSM. In 1998, Wideband Code Division Multiple Access (WCDMA) was selected as radio access technology for Universal Mobile Telecommunication System (UMTS). UMTS belongs to Third Generation (3G) cellular system. To cope with the demand of high data rates and improved spectral efficiency, 3rd Generation Partnership Project (3GPP) responsible for the standardization of Third Generation (3G) systems introduced High Speed Downlink Packet Access (HSDPA) in Release 5. HSPA+ was introduced in 3GPP Release 7, and peak data rates were further improved by adding the support of dual stream transmission with Multiple Input Multiple Output (MIMO) antennas, and higher modulation and coding scheme e.g. 64QAM. The evolution of the High Speed Downlink Packet Access (HSDPA) system continued in Release 8 of 3GPP, and the concept of aggregating the radio resources of two HSDPA carriers also known as Dual-Cell HSDPA (DC-HSDPA) with the help of a joint scheduler was floated. In parallel with the development and evolution of 3G cellular system, 3GPP has also been working as a standardization body for

Orthogonal Frequency Division Multiple Access (OFDMA) based Long Term Evolution (LTE) technology. LTE was introduced in Release 8 of 3GPP [2].

The main target of the radio network planner is to provide the maximum coverage with the minimal infrastructure, and to ensure the good Quality of Service (QoS). Intelligent radio network planner tries to efficiently utilize, and competently optimize the usage of radio resources i.e., frequency and power resources. In this regard, better radio propagation, large coverage print and low cost capital investment make UMTS900 deployment an attractive option for radio engineers. In the existing UMTS2100 deployed coverage area, the UMTS900 layer can serve as an overlay to provide continuous indoor coverage for data users. In this way cellular operators not only minimize the capital investment of the network, but also bring down the operational cost of a network.

Peak capacity of a traditional macro cellular network can be increased by adding more carriers (Frequency), by adding sectors [3, 4, 5], by network densification [6, 7, 8] or by adding femto (small) cells [9]. To improve the capacity, spectral efficiency and Signal to Interference plus Noise Ratio (SINR), advanced antenna solutions such as spatial multiplexing through conventional Multiple Input Multiple Output (MIMO) antenna system, distributed antenna system, higher order sectorization, multiple fixed beam antennas, switched beam antennas, smart antennas for beamforming, advanced adaptive antenna [10], and massive MIMO system [11] can be employed. Adopting an optimized network tessellation also helps in achieving better results [12].

Fifth Generation (5G) technology is not a standardized technology yet, and currently it is in the early research phase. Ultimately, 5G is about a supreme user experience, a user can think of. 5G wireless network is expected to offer thousand times more capacity compared to capacity offered by fourth generation of wireless networks. Couple of Gbps of download speed for individual users with extremely low latency and response time is anticipated in 5G. It is an enormous challenge for the future 5G wireless networks to offer such a huge capacity and massive connectivity for an increasingly diverse set of applications and services with different requirements. It will be a big challenge for 5G wireless

technology to ensure the efficient utilization of available non-contiguous spectrum, and to ensure the absolute level of security and reliability [13, 14].

Extremely high data rates, gigantic capacity needs, much lower latency, and simple network architecture required by 5G cannot be achieved only by the evolution of the status quo technologies [13].

1.2. Objectives and scope of the thesis

The scope of this thesis is to provide the aspects for the efficient utilization of the radio resources, which includes traffic handling in a multilayer network, efficient power allocation, and optimize network tessellations. The other objective of this thesis is to validate the viability of different antenna technologies in enhancing the network capacity, and finally to present the innovative antenna solution for the fifth generation of cellular network for thousand fold more capacity. The multilayer network considered in this thesis consists of GSM900, GSM1800, UMTS900 and UMTS2100 layer. HSDPA and LTE were not considered in the multilayer network study.

The structure of this thesis can be divided into three parts: efficient and optimal utilization of the radio resources, advanced antenna techniques for enhancing the capacity of the system, and the novel and innovative antenna concept for 5G network. The first part of the thesis will concentrate on the impact of different traffic handling schemes on load balancing among the different layers in a multilayer network. Impact of smart traffic handling scheme on the capacity of the network, and on the interference margin in UMTS system is evaluated in a macrocellular environment. The role of optimal power allocation scheme in HSDPA system for efficient utilization of power resources is also included in the first part. The second part of the thesis will concentrate on the performance of MIMO antennas in LTE and DC-HSDPA system. Firstly, the importance of deploying Adaptive MIMO Switching (AMS) in LTE will be highlighted, and its performance is assessed. Secondly, a performance comparison of conventional antennas with different sectorization and advanced antenna techniques i.e., switched beam smart

antenna and fully adaptive beam antenna is provided. Impact of different network tessellations on the different order of sectorization was also investigated. The third part of the thesis introduces a novel concept of Single Path Multiple Access (SPMA), using a highly sophisticated antenna made up of advanced electrical metamaterials. Antenna requirements for SPMA are found by using indigenous 3D MATLAB simulator.

Throughout my research work towards this thesis, I address the following research questions:

1) Does proposed smart traffic handling scheme help in enhancing the traffic handling capacity of the multilayer network for a mix type of traffic i.e., for voice and Packet Switch (PS) data?
2) Does proposed smart traffic handling scheme help in balancing the load among the different layers in a multilayer network for a mix type of traffic?
3) Does proposed smart traffic handling scheme help in improving the interference margin provided in UMTS system link budget?
4) Does proposed smart traffic handling scheme efficiently utilize the resources of each layer in a multilayer network.
5) Does Adaptive MIMO Switching (AMS) give significant gain over diversity techniques and spatial multiplexing?
6) What is the performance comparison of LTE and DC-HSDPA system in a macrocellular environment?
7) How much gain can be achieved by employing smart switched beam antennas and adaptive beam antennas over conventional wide beam antennas?
8) Which layout provides the best signal to interference plus noise ratio for different order of sectorization?
9) How do the proposed "Flower" tessellation and "Snowflake" tessellation differ from other tessellations from the radio network performance point of view?
10) What are the antenna requirements for the proposed concept of Single Path Multiple Access (SPMA)? How does SPMA work?
11) Can SPMA be a potential candidate for 5G technology?

1.3. Author's contribution

The author of this doctoral thesis is the main contributor of the publications [P1]-[P8] and had the leading role in developing the concepts, and simulator. The author of this thesis carried out the simulations, analyzed the results and was a responsible person for writing all the publications. The study of this doctoral thesis was fully supported by Prof. Jukka Lempiäinen, the supervisor of this thesis. Prof. Jukka Lempiäinen was also involved during brainstorming sessions, and in writing and proofreading of the publications [P1]-[P8].

2. MULTILAYER CELLULAR NETWORK

A multilayer cellular network is a mix of cells with different characteristics like radio access technology, base station power, size of the cells, frequency of operation, height and location of the base station antenna. A heterogeneous network is a blend of overlay macro cells with underlay micro, small or femto cells [15]. In densely populated areas, hot spot regions, city centre, or in cosmopolitan areas, multilayer networks are deployed to meet the capacity requirement, and to provide better quality of services with improved coverage. In the current mobile market, smart cellular phones capable of handling Multiple Radio Access Technology (multi-RAT) like LTE, HSPA, UMTS, GSM/EDGE, CDMA and WiFi are already available.

2.1 Overlay - Underlay Configuration

Overlay – Underlay configuration is utilized to meet the requirement of increasing traffic demand in hot spot areas in an efficient way [16, 17]. Underlay layer adds capacity to the network, whereas the overlay layer provides improved coverage. In GSM system, the underlay layer has squeezed frequency reuse factor and hence provides enhanced network capacity. Generally, the cellular layer operating at higher frequency band acts as a capacity layer, and a cellular layer operating at lower frequency band acts as a coverage layer. In a multimode multiband band radio network e.g. GSM900/1800 deployed along with UMTS900/2100, the GSM900 and UMTS900 layers act as coverage layers and the GSM1800 and UMTS2100 layers act as capacity layers. Due to better radio propagation at 900MHz band, UMTS900 can serve as an overlay to provide continuous indoor coverage for data users. Illustration of the overlay – underlay configuration with co-siting is shown in Fig.2.1. It can be seen in Fig.2.1, that seamless coverage area with no coverage holes is provided by the overlay, and underlay adds capacity to the network. In

Fig.2.1, only two layered network was considered, but in a multilayer network several layers of different radio access technologies operating at different frequency bands can be present.

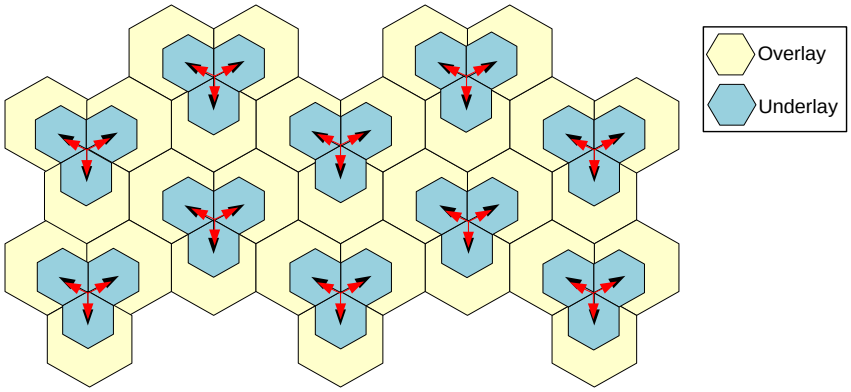

Fig.2.1 Illustration of overlay – underlay configuration

2.2 UMTS Load Equations

UMTS is an interference sensitive system; rise in interference causes decrease in the capacity of the network. In a soft blocked network e.g. UMTS, the cell capacity is limited by the rise in interference in the cell, and is referred to as "soft capacity". Whereas, in a hard blocked TDMA/FDMA network e.g. GSM, the maximum cell capacity is limited by the number of available traffic channels. For a soft capacity limited system, a conventional Erlang B table cannot be used to estimate the capacity of the system. For UMTS system, load equations are generally used to estimate the average load of the cell in the uplink as well as in the downlink direction [17, 18, 19, 20, 21]. The downlink load factor η_{DL} can be used to estimate the loading of a cell in the downlink direction, which is given by the equation (2.1).

$$\eta_{DL} = \sum_{j=1}^{Nu} \frac{(E_b/N_0)_j}{\frac{W}{R_j}} * v_j * [(1-\delta_j) + i_j] \qquad \textbf{(2.1)}$$

where in equation (2.1), Nu is the number of users connected in downlink direction, W is the chip rate which is fixed in UMTS system at 3.84Mchip/sec, R_j is the bit rate of the j^{th} user, $(E_b/N_0)_j$ is the quality

requirement of the j^{th} user for the required service, v_j is the activity factor of the j^{th} user, δ_j is the orthogonality factor of the j^{th} user, and i_j is the interference factor of the j^{th} user. An interference factor is defined as the ratio between the other cell interference to the own cell interference. Code orthogonality is affected by the multipath propagation, which in turn depends on the propagation environment, speed of the mobile user, and the user location. Similarly, uplink load factor η_{UL} is used to estimate the loading of a cell in the uplink direction, which is given by the equation (2.2).

$$\eta_{UL} = \sum_{j=1}^{N_u} \frac{1}{\frac{W}{(E_b/N_0)_j . R_j . v_j}} * [1 + i_j] \qquad \textbf{(2.2)}$$

2.3. Interference Margin as a function of cell loading in UMTS

The Interference Margin (IM) also known as noise rise, is the margin provided in uplink link budget to account for the system degradation. The interference margin takes into account the noise coming from the own cell as well as the noise coming from the neighbour cell. The interference margin depends upon the expected loading of the cell; higher the loading of a cell the higher will be the IM [17, 18]. The relation between the interference margin and the cell loading is given by the equation (2.3). In equation (2.3), IM is the interference margin and η_{UL} is the uplink loading of UMTS cell. Interference margin is generally given in dB values. In Fig.2.2, the interference margin approaches infinity as the cell load in the uplink direction approaches unity, where the unity load means 100% loading of the cell. In practice, the maximum cell load is always less than a unity. It can be seen in Fig.2.2, that after 70% cell loading the interference margin curve starts to go exponential. Thus, it is recommended to dimension the system with the load factor of 0.5 (50%) to guarantee the stable behaviour of a network [22].

$$IM = \frac{1}{1 - \eta_{UL}} \qquad \textbf{(2.3)}$$

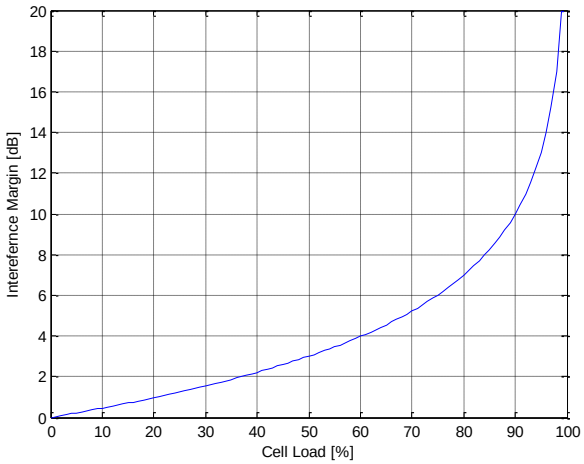

Fig.2.2 Interference margin versus uplink cell load

2.4. Power sharing in UMTS system

Total available power at NodeB is one of the limiting factors of downlink capacity. In UMTS, total available power at NodeB is shared between the channels used for carrying data traffic and channels used for signalling purposes. The required downlink transmission power in UMTS depends upon the number of active users, their required service type (bit rates), and on the interference coming from the own and neighbour cells. In UMTS, coverage prediction is done by Common Pilot Channel (CPICH). Typically 5-10% of the total available power is reserved for CPICH [17]. Other channels that share the transmission power are Common Control Channels (CCCHs), Primary and Secondary Synchronization Channel (P-SCH and S-SCH), Paging Indicator Channel (PICH), Acquisition Indicator Channel (AICH), and Dedicated Traffic Channels (DCHs). Power control mechanism is not applied at pilot channel and other common channels. Activity of DCHs and CCCHs varies with the change in the load of a cell. Signalling required for call establishment will increase with the increase in number of call attempts. Therefore, the total power of CCCHs fluctuates with the change in a loading of a cell. The total required power at NodeB for N_u users can be computed by the equation (2.4) [21, 23].

$$P_{Total} = \frac{(P_{CCCH} * \eta_{DL}) + N_{rf} \sum_{j=1}^{N_u} \frac{(E_b/N_0)_j}{\frac{W}{R_j}} * v_j * L_j}{1 - \eta_{DL}} + P_{CPICH} + P_{P-SCH} + P_{S-SCH} + P_{AICH} + P_{PICH} \quad \textbf{(2.4)}$$

In equation (2.4), N_{rf} is the noise spectral density, L_j is the path loss between UE and NodeB of the j^{th} user. UMTS is a power and interference sensitive system. One of the target of the radio network planner is to minimize the interference coming from other cells, which can be achieved by optimizing the base station power and cell loading [17]. To achieve a better performance at the air interface, both the UE and NodeB should transmit with as low power as possible to avoid causing the interference. In UMTS system, both in uplink and downlink a fast power control mechanism with 1500Hz frequency is supported, whereas in GSM the slow power control with 2Hz frequency is available [18, 24, 25].

2.5. Frequency reuse factor and GSM capacity

Frequency reuse factor specifies the number of cells after which the same frequency resources (spectrum) can be reused [26]. Carrier to interference ratio plays a vital role in determining the minimum frequency reuse factor. With a small reuse factor, high capacity can be achieved but a small reuse factor leads to a high interference in a system. There are different reuse factors like 1x1, 1x3, 3x9, 4x12 etc. In reuse factor 1x3, all available frequencies are divided in three cells of one site, in 4x12 all frequencies are divided in 12 cells of four sites, and 1x1 corresponds to the use of whole frequency band in every cell [24].

Fig.2.3 shows different frequency reuse patterns. FB represents the frequency band used in a cell. It is possible to use a different reuse factor for Broadcast Control Channel (BCCH) and Traffic Channel (TCH) frequencies. BCCH requires a large reuse factor to meet the requirement of co-channel and adjacent channel interference as they are transmitted with no power control. Discontinuous transmission (DTX) and frequency hopping are not applied to the BCCH [24].

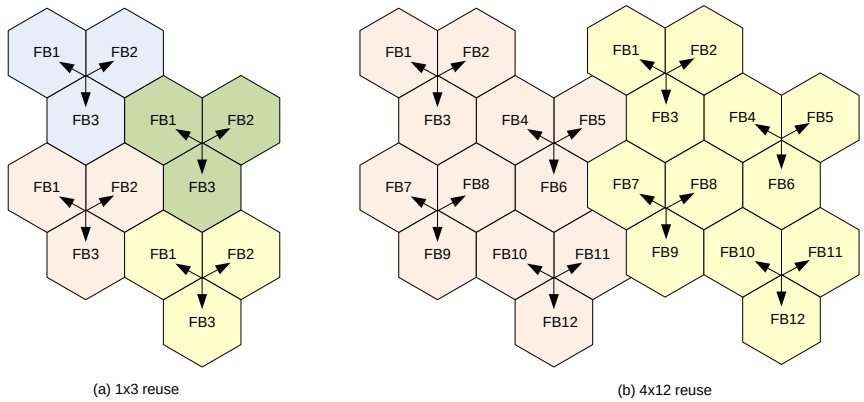

Fig.2.3 Frequency reuse pattern (a) 1x3 reuse (b) 4x12 reuse

2.6. UMTS900 in co-existence with GMS900

UMTS was initially deployed around 2GHz spectrum. But, better propagation, and improved coverage with low cost capital investment make UMTS900 deployment quite attractive [27, 28, 29]. The spectrum available for UMTS900 deployment is already in use by GSM900, and it has made the UMTS900 deployment challenging, as the spectrum needs to be shared between UMTS900 and GSM900. In this kind of multilayer network, the refarming of the GSM900 band is required to free the band for UMTS900. Amount of spectrum for UMTS900 should be minimized so that the remaining spectrum can be used by the GSM900 layer. The nominal channel bandwidth for UMTS system is 5MHz. There are two modes of UMTS900 deployment, uncoordinated deployment and coordinated deployment.

In uncoordinated deployment, the locations of UMTS900 and GSM900 sites are different and can be off as extreme as being at the cell edge of each other. The worst condition is when a GSM base station is located at the cell edge of UMTS NodeB, and the UMTS user equipment operates close to a GSM base station, or a GSM mobile station operates next to the UMTS NodeB [30].

In coordinated deployment, GSM900 and UMTS900 sites are located at the same location and can doing site sharing. Adjacent channel interference is less significant in coordinated deployment, since

UMTS900 and GSM900 are co-located. 3GPP recommends a carrier separation of 2.8MHz between UMTS900 and GSM900 carrier for uncoordinated deployment [31]. However, by coordinated deployment, carrier spacing can be pushed smaller than 2.8MHz. In coordinated deployment, isolation is required from other operators' carrier as well. Other operators' site with the adjacent carrier can be placed any where independent of own operator's site, which can be a source of significant interference. Therefore, for deploying UMTS900 in co-existence with GSM900, the suggested frequency plan is sandwich type deployment as shown in Fig.2.4. In a sandwich type deployment, the UMTS900 carrier is placed in between the GSM900 carriers of the same operator, and thus provides isolation between the operators and helps in minimizing the adjacent channel interference [30, 31].

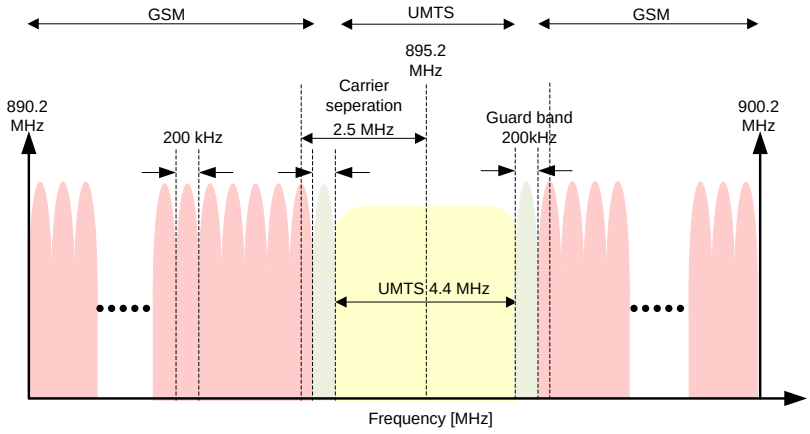

Fig.2.4 Sandwich deployment of UMTS900

In Fig.2.4, out of total 10MHz band, 5.2MHz is reserved for GSM900 and 4.4MHz is reserved for UMTS900, and the rest of the available spectrum is used for placing the guard bands. Guard bands of 200 kHz are placed at the starting and at the ending of UMTS900 band. The carrier separation between the GSM900 and UMTS900 layer is 2.5MHz.

2.7. Traffic handling schemes

One scope of this thesis is to investigate two traffic handling schemes named as *Random Layer Selection Strategy* and *Smart Traffic Handling Scheme* in a multimode multiband network. A multilayer network consists of GSM900, GSM1800, UMTS900 and UMTS2100 was considered for this purpose. These traffic handling schemes are valid for two types of services i.e., speech and data services.

2.7.1. Random layer selection strategy (Case1)

The name ”random layer selection strategy” itself implies the basis for this scheme. This scheme allows data users to connect either of the UMTS layer i.e., UMTS900 or UMTS2100 depending upon the availability, and restricts to use the GSM layers for data services. For speech users, random selection is made by the user equipment to connect any of the GSM layers or UMTS layers, as there is no restriction in choosing any of the available layers for speech service. In case, if the selected layer has already reached its maximum capacity limit, then the process of layer reselection continues until all the available layers are tried atleast once. The process of layer selection and reselection for speech and data users is random, independent, with no priority, and has uniform probability of selection for all available cellular layers.

2.7.2. Smart traffic handling scheme (Case2)

In a smart traffic handling scheme, information about the user location i.e., distance of the user from the base station, and information about the required service type is used for layer selection. The concept of overlay-underlay was exploited by smart traffic handling scheme. The essence of this scheme is to use GSM900 and UMTS900 as coverage layer, and GSM1800 and UMTS2100 as capacity layer, with high priority of using GSM layers for speech users. It was made mandatory for speech users to connect GSM layers until GSM layers reached their maximum traffic handling capacity. Speech users in the close vicinity of a base station were compelled to connect GSM1800 layer, and away users were forced to connect GSM900 layer. For speech users, once the GSM layers reach

their capacity limit, then UMTS layers can also be used to serve them. In case of GSM layers reaching their limit, UMTS2100 was given higher priority over UMTS900 to serve the speech users in the close vicinity of the base stations. With the help of smart traffic handling scheme, UMTS resources were made available for serving more data users, by avoiding the speech users from utilizing them. Similar to speech users, for data users the approach of using the UMTS2100 as a capacity layer near the base station, and UMTS900 as a coverage layer for the far users is adopted. But, the layer selection and reselection for data users is only allowed between UMTS900 and UMTS2100.

2.8. Simulation approach

In general, radio network simulations are done at two different levels, known as link level simulations and system level simulations. Link level simulations are performed to provide the information about the receiver performance at a bit level. This approach requires high computation, and gets much complicated when we need to simulate the large number of mobiles and NodeBs. To simulate the complicated behavior of a radio network, system level simulations are required. System level simulations are high level simulations where interference situations, mobility scenario, different services and environment impact are modelled. System level simulations also enable us to model the effect of random variables, and parameters on system performance.

A simulation approach can be again categorized into static simulation and dynamic simulation. Static simulation offers a promising way for assessing the network behavior, tessellation performance, and topology assessment by using a given network configurations, parameters, radio resource management strategies, traffic handling schemes, user distribution, service types and their requirements. In static simulation, a network performance is analyzed after regular intervals of time by taking a snapshot of the network. Each snapshot is independent of each other, and has no correlation between them in time domain. The impact of user mobility in the network is not included in the static simulations. A Monte-Carlo simulation is an example of high level static system simulation,

which is used to estimate the system level performance with respect to defined network configurations [17, 32].

Whereas, the mobility of the user is tracked in dynamic simulation, and it also includes the time dimension. Dynamic simulators are more complex and require more time for simulation compared to static simulators. However, dynamic simulations are more appropriate for analyzing the Radio Resource Management (RRM) functionalities such as fast power control, dynamic scheduling of resources, and handover functionality in a system.

2.8.1. Static planning tool

Impact of two different traffic handling schemes on the performance of a multilayer network is analyzed in the thesis with the help of system level simulations. Simulations were performed in the indigenous planning tool, and the platform of MATLAB was used to make the indigenous static simulator. Network properties are modelled in the simulator as realistically as possible to have an accurate and precise result. Parameters regarding the radio resources, maximum transmit power; coverage and capacity thresholds are provided as an input to the simulator. The Okumura Hata model is used as a radio propagation model for calculating the path loss between the transmitter and a receiver. The user activity for speech and data users in the uplink and downlink direction is not modelled as the random process in the simulator. The terminal speed is neglected and only the static users are assumed, therefore the mobility of the users is not modelled in the simulator. The slow fading is modelled with log-normal distribution. Receiver antenna height is set at 1.5m, and omni-directional antenna with zero dB gain is used at UE terminal.

2.8.2. Service type and user distribution

Terminals with two service types i.e., terminal with voice service of 12.2kbps, and terminal with data service of 384kbps at the application layer were created to load the network. Speech and data users were randomly and homogeneously distributed over the coverage area of the cell, independent of the clutter information. Number of speech and data users in a cell in each snapshot has uniform and flat distribution between

the minimum and maximum number of speech and data users. Minimum number of speech and data users in a cell is set to twelve and one, respectively. Whereas, the maximum number of data users in a cell is set to 5. The total number of data users per site was fixed at twelve for all simulations, but the maximum number of speech users was variable.

2.8.3. Simulation methodology

A Monte-Carlo approach is adopted for carrying out the campaign of these simulations. In each snapshot, users with voice and data services are distributed over the area under consideration. Each user tries to establish a connection to the network by using either of the traffic handling schemes. Users which are not able to connect to the network are considered as ”blocked users”. This process of placing users, connecting to different layers and saving the result is called a *snapshot*. In each snapshot, for the users connected to UMTS layers the downlink transmit power required to achieve the target (E_b/N_0) for the required service type is computed. The required transmit power for each link depends on the downlink cell load, neighbor cell load and path loss. Downlink (DL) radio link powers are calculated iteratively, by adding one user at the time to the network in coordination with admission and load control. This iteration is continued until users are getting connection to UMTS layers. Simulator saves different parameters of the network like number of speech call attempts, successful call attempts, fail call attempts, data transfer attempts, data transfer failure, NodeB transmission power, required interference margin, penalty time, downlink load, uplink load etc. Finally, the post processing of results is done to analyze the results in a better way. The results presented in this thesis are the averaged results over a certain number of snapshots. The flow chart of a simulation procedure adopted in MATLAB is presented in Fig.2.5.

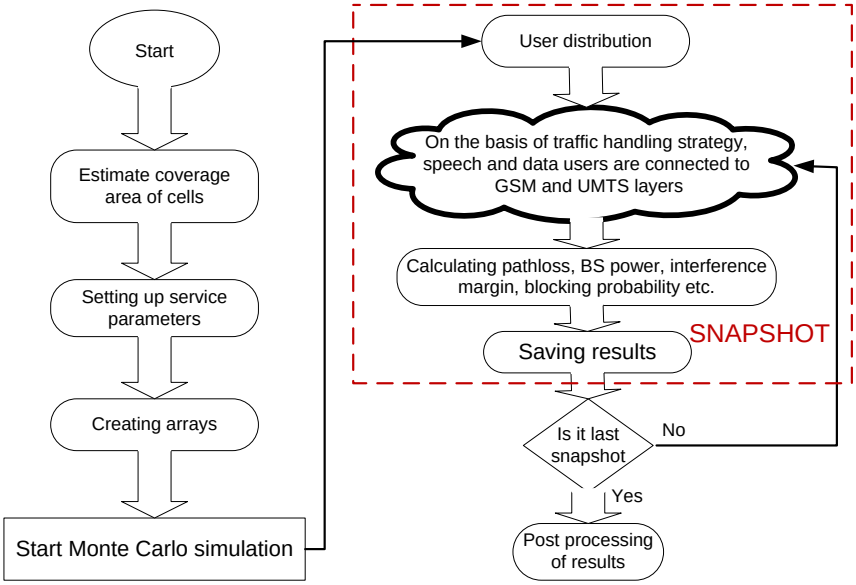

Fig.2.5 Flow chart of simulation procedure in MATLAB

2.9. Simulation results with different traffic handling schemes

In this section, performance comparison of two different traffic handling schemes is presented, and the importance of deploying UMTS900 is highlighted. Impact of traffic handling schemes on the system capacity and other parameters is analyzed with extensive set of simulations. Details of the traffic handling strategies are presented in section 2.7. The results presented in this section are taken from publications [P1- P3].

2.9.1. Maximum supported users with defined blocking probabilites

In [P1-P3], speech blocking probability (Pr_{speech}) is defined as the probability of new speech call being blocked, and is given by the equation (2.5).

$$Pr_{speech} = \frac{Number\ of\ speech\ call\ connection\ failure}{Number\ of\ speech\ call\ attempts} \qquad \textbf{(2.5)}$$

Similarly, for data connections the probability of no data transfer is defined as the probability of new data connection being failed, and is given by the equation (2.6).

$$Pr_{data} = \frac{Number\ of\ data\ connection\ failure}{Number\ of\ data\ connection\ attempts} \quad \textbf{(2.6)}$$

In [P1], for predefined speech blocking probability of 2%, and 10% of probability of no data transfer, the maximum supported number of users by a multilayer network composed of GSM900, GSM1800, UMT2100 and possible UMTS900 was found. All relevant simulation parameters and description of simulation environment can be found at [P1]. Results presented in Table 2.1 shows that the UMTS900 deployment not only helps in improving the coverage, rather it also helps in enhancing the network capacity, and the impact of having better traffic handling strategy is evident. UMTS system being more spectrum efficient than GSM system offers more capacity for the speech and data users. UMTS900 deployed with random layer selection adds capacity to the system, but smart traffic handling scheme shows remarkable improvement in the traffic handling capacity of the network by doing load balancing among the different layers, and by efficiently utilizing the available resources.

Table 2.1Maximum supported users with different traffic handling schemes

CASE	Speech users per site	Speech users per cell	Data users per site	Data users per cell
W/o UMTS900 random layer selection	76	45	9	5
W/o UMTS900 smart traffic handling	104	57	9	5
With UMTS900 random layer selection	91	51	13	7-8
With UMTS900 smart traffic handling	146	92	17	9-10

In [P2], speech blocking probability was found against the variable number of speech users per site while keeping the number of data users per site fixed. In Fig.2.6, red and blue lines show the cases of a multilayer network without UMTS900, and it was found to have high blocking probability compared to purple and black lines which represent cases with UMTS900. Case1 and Case2 represent random layer selection and smart

traffic handling scheme, respectively. Smart traffic handling scheme with UMTS900 outperforms, shows top notch performance and offers lowest speech blocking probability compared to other cases. Smart traffic handling scheme balanced the load optimally among the layers, avoid the speech users to utilize the resources of UMTS layers, and kept the GSM900 resources to serve speech users near the cell edge area. Whereas, with random layer selection scheme most of the blocked users were found near the cell edge area, as random layer selection scheme did not forbid the users near the base station from using the GSM900 resources.

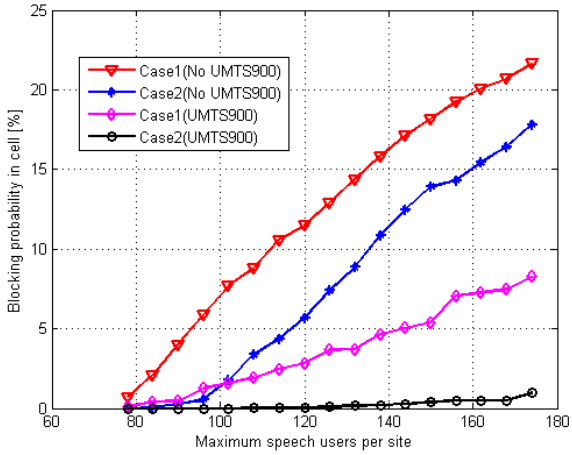

Fig.2.6 Speech blocking probability in cell

2.9.2. Impact of traffic handling strategies on cell loading and interference margin of UMTS layer

Parameter planning is required to optimize the usage of a network. It is of the utmost importance to keep the load under the predefined threshold to guarantee the required quality of service. Admission and load control together optimizes the quality and capacity of the UMTS network. Admission Control (AC) takes care of new connections, and it checks whether the new user can be admitted into the system or not. Load control manages a situation when system load exceeds the threshold and takes a feasible measure to bring the load back to normal; it maximizes the throughput without deteriorating the quality of a network [17, 18]. Smart traffic handling scheme performs both these functionalities of admission control and load control, and helps in doing the load balancing.

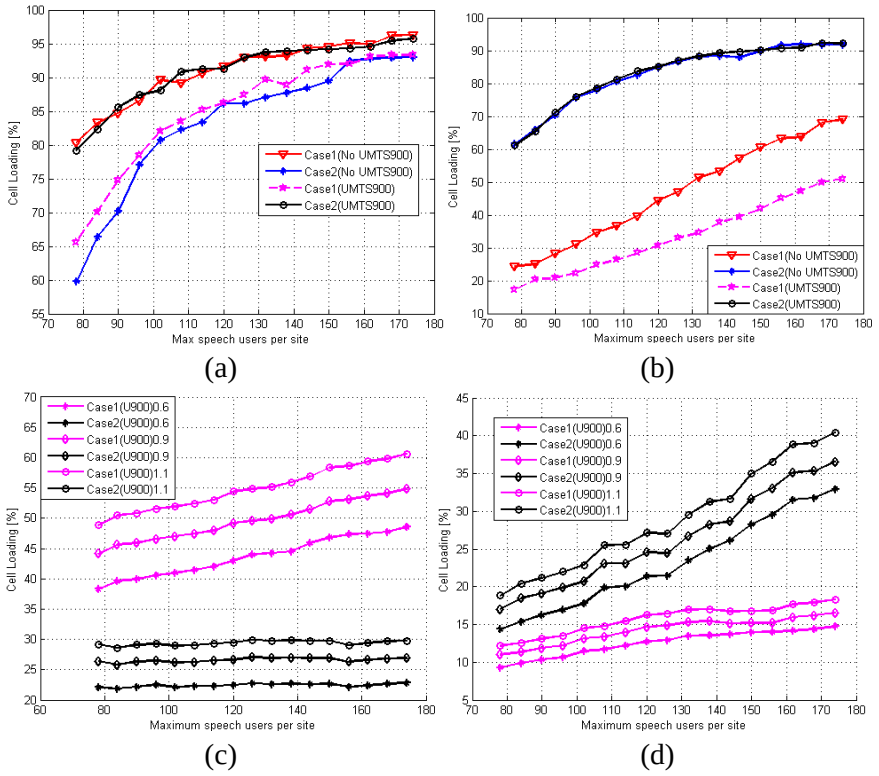

Fig.2.7 (a) Downlink loading of GSM900 cell (b) Downlink loading of GSM1800 cell (c) Uplink loading of UMTS900 cell and (d) Uplink loading of UMTS2100 cell

Fig.2.7(a) shows the downlink loading of GSM900 layer as the percentage of its maximum handling capacity. For the cases without UMTS900, due to large coverage print of GSM900 layer it was found heavily loaded in Case1, but smart traffic handling scheme utilized GSM1800 as capacity layer and offload the traffic to GSM1800 layer, which results in the low loading of GSM900 layer. For the cases with UMTS900, the coverage area of UMTS900 is almost the same as GSM900, and UMTS900 share the same spectrum of 900MHz band leaving small band for GSM900 which means less capacity for GSM900. With random layer selection strategy, as the coverage print of UMTS900 is the same as GSM900, therefore fair a number of speech users are connected to UMTS900 layer, which results in the low percentage of GSM900 loading despite its low maximum handling capacity. Finally, in

Case2 with UMTS900, the GSM900 layer was effectively used for carrying the speech users.

Simulation results presented in Fig.2.7(b) show that for Case1 with and without UMTS900, the GSM1800 layer was found lightly loaded because of its small coverage area, hence it was not efficiently utilized. By analyzing the results presented in Fig.2.7(a) and Fig.2.7(b) it was found that with random layer selection scheme the loading of GSM layers is proportional to the coverage area of the corresponding layer. Larger the coverage area the higher will be the loading of the cell, and vice versa. Interestingly, GSM1800 was utilized efficiently and showed high loading percentage in case of smart traffic handling scheme with and without UMTS900. Unlike random layer selection, the smart traffic handling scheme exhibits the feature of load balancing and accommodated the speech users with GSM layers, leaving the resources of UMTS layers for data users.

In Fig.2.7(c), uplink loading of UMTS900 layer with a different interference factor is shown. It can be seen that high interference factor causes a high loading of a cell. For any particular interference factor, the uplink loading of UMTS900 layer with smart traffic handling scheme is almost flat due to the fact that in simulations the number of data users were kept fixed, and smart traffic handling scheme gives higher priority to UMTS2100 layer for serving the speech users once the GSM layers approach their maximum limit. Whereas, an ascending curve of loading can be witnessed with random layer selection as speech users share the resources of UMTS layer.

Fig.2.7(d) shows the uplink loading of UMTS2100 layer with different interference factor. Like in GSM layers, a similar trend of cell loading is observed in UMTS layers with random layer selection, that a layer with large coverage area has high loading and vice versa. The UMTS900 layer was found far more loaded compared to UMTS2100 layer with random layer selection. But, smart traffic handling scheme makes the right use of layers and utilizes “capacity layers” (GSM1800 and UMTS2100) for offering more capacity and “coverage layers” (GSM900 and UMTS900) for giving better coverage, whereas random layer selection does opposite.

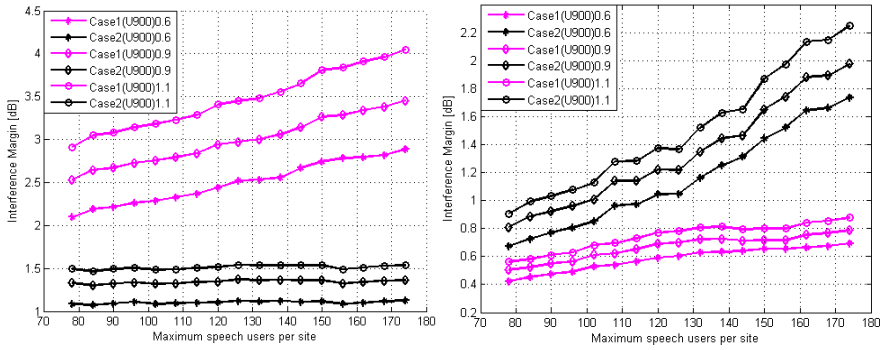

Fig.2.8 Interference margin in uplink (a) UMTS900 and (b) UMTS2100

In UMTS, interference margin is the function of uplink cell loading. A high interference factor causes a high cell loading which corresponds to a large value of required interference margin in uplink direction. As discussed in section 2.3, interference margin increases exponentially after 70% cell loading, therefore it is recommended to keep the cell loading under control to assure a stable network. In Fig.2.8(a), a required interference margin for UMTS900 layer with different interference factor is shown. For Case2, even for a large number of users per site along with a high interference factor of 1.1, the required interference margin is about 1.5dB only. Whereas, with Case1 required interference margin is around 4.5dB, which is around 3dB more compared to Case2. Fig.2.8(b) shows required interference margin of UMTS2100 layer. For Case1 due to low and inefficient cell loading, the small interference margin is needed compared to Case2 for UMTS2100. But, still the interference margin needed with Case2 is under the controlled safe region. More detailed results can be found at [P2].

2.9.3. Impact of traffic handling strategies on penalty traffic in GSM networks

In a GSM network, the maximum traffic handling capacity with given traffic channels and required blocking probabilities can be estimated through Erlang B and Erlang C tables [33, 34]. Erlang (Er) is a unit of traffic intensity, and it is a unit less quantity. In practice one erlang is defined as the amount of traffic generated by a user occupying a traffic

channel for one hour. GSM is a hard blocked system, where calls are blocked due to lack of available traffic channels. GSM only supports hard handover, which means it breaks the connection with the source cell before it makes connection with the target cell [26, 35]. In [P3], the penalty traffic is defined as the extra traffic in a GSM network due to reservation or lack of release of resources. It is assumed that time slot remain reserved for a certain period of time called "penalty time" after the call ended, and before it can be re-allocated to other user. The resources are reserved in a source cell to ensure that in case of un-successful handover to a target cell, user can return to a source cell, and call does not drop due to lack of traffic channel. In this way, more priority is given to handover cases compared to new incoming calls at the cost of some capacity loss. From a user's point of view the termination of an ongoing call is considered worse than blocking a new incoming call.

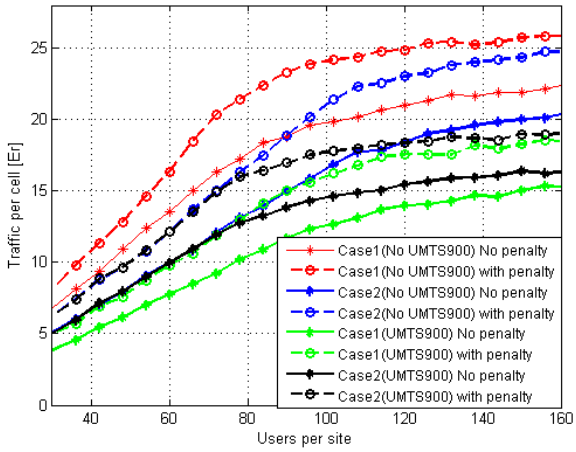

Fig.2.9 GSM900 cell load without and along with penalty traffic in erlangs

In Fig.2.9 and Fig.2.10, cell traffic with and without penalty traffic is shown for GSM900 and GSM1800, respectively. It can be seen that in both figures, the penalty traffic increases with the increase in the loading of a cell. In Fig.2.9, GSM900 layer loading is almost identical for Case2 with and without UMTS900 till 78 users per site, but afterwards for the Case2 without UMTS900 the traffic trend continued to rise as there are more traffic channels available for GSM900. Similarly, in Fig.2.10, the GSM1800 layer follows the same traffic loading curve for Case2 with and

without UMTS900, as GSM1800 needs no frequency refarming due to UMTS900 deployment.

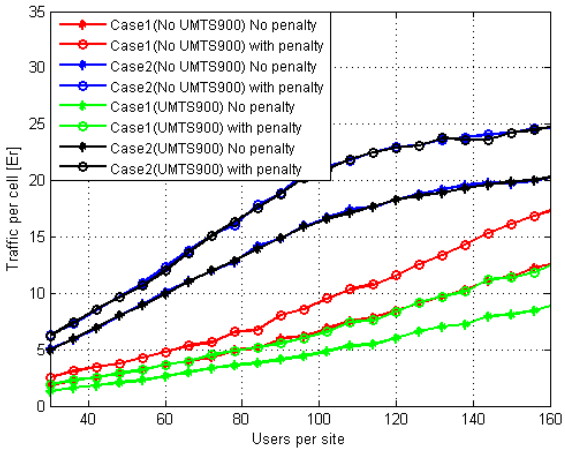

Fig.2.10 GSM1800 cell load without and along with penalty traffic in erlangs

It is interesting to see in Fig.2.11(a) and (b) that despite of increase in penalty traffic with an increase in a loading of a cell, the relative percentage of penalty traffic does not always increase. It is evident from the results presented in Fig.2.11 that smart traffic handling scheme helps in keeping the penalty traffic low in comparison with random call selection strategy especially in GSM1800 layer. The average percentage of penalty traffic in GSM1800 layer is around 26.5% and 28% for Case1 with and without UMTS900, respectively. Whereas, the percentage of penalty traffic is reduced to 19.4% in GSM1800 layer by smart traffic handling scheme.

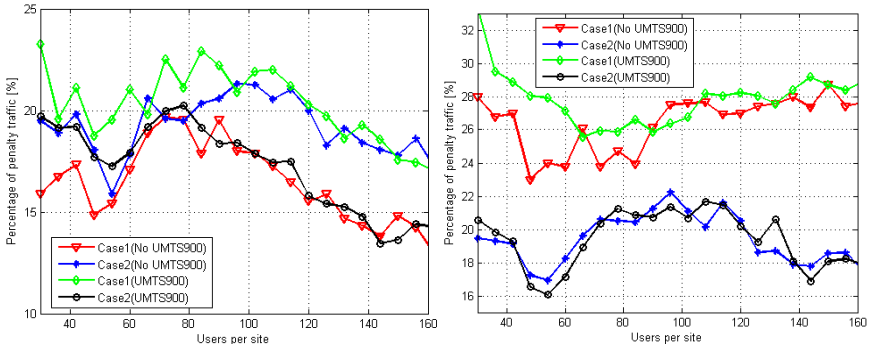

(a) (b)

Fig.2.11 Percentage of penalty traffic in (a) GSM900 and (b) GSM1800.

3. ADVANCED ANTENNA TECHNIQUES AND NEW NETWORK TESSELLATIONS

The rising trend of the packed switched traffic, and high capacity requirement in the mobile networks have urged the researchers to think about new antenna designs and possible new network layouts for high speed cellular networks. High Speed Downlink Packet Access (HSDPA), Internet HSPA, Dual Cell HSDPA (DC-HSDPA), and Long Term Evolution (LTE) are the examples of high speed cellular network. Current and future capacity demands of next generation mobile networks cannot be achieved by using traditional macro cells only. Traditional macro cells with conventional wide beam antennas are not able to offer high data rates homogeneously over the entire cell area, and most of the network capacity is lost due to the interference coming from the neighbor cells. Spectral efficiency of a system can be improved by employing advanced Multiple Input and Multiple Output (MIMO) antennas, and smart antenna solutions [10]. Regular network tessellations can be used as a guideline to make a nominal cellular network plan. New and optimized network tessellations are needed for high order sectored sites.

3.1. Dual Cell High Speed Downlink Packet Access (DC-HSDPA): The Evolution of HSDPA

To cope with the demands of high data rates and improved spectral efficiency, 3rd Generation Partnership Project (3GPP) responsible for the standardization of 3G systems introduced High Speed Downlink Packet Access (HSDPA) in Release 5. HSDPA has a fix spreading factor of 16, and has total maximum number of 16 codes available [36, 37]. At a physical layer, user data is carried by High Speed Physical Downlink Shared Channel (HS-PDSCH) with a fixed Transmission Time Interval (TTI) of 2ms. HS-PDSCH is capable of multicode transmission, and is shared by the users as a combination of time and code division

multiplexing. It means that at any instant a combination of multiple downlink codes can be allocated to any user. HS-PDSCH also supports the Adaptive Modulation and Coding (AMC) schemes. HSDPA can offer a theoretical peak data rate of 21.1 Mbps with 15 codes for HS-PDSCH [38].

In 3GPP Release 7, peak data rates were further improved by introducing the support of dual stream transmission (Spatial Multiplexing) by Multiple Input Multiple Output (MIMO) antennas, and higher Modulation and Coding Scheme (MCS) e.g. 64QAM. Supported data rates are subsequently enhanced in the downlink direction by including DC-HSDPA and Multi-Carrier HSDPA in Release 8 of 3GPP [39, 40]. The main idea of introducing the concept of dual cell operation in HSDPA is to provide improved user throughput over the whole cell area. In DC-HSDPA, two WCDMA carriers each of 5MHz are combined, and data is transmitted simultaneously over the two carriers for the single user [41]. Hence DC-HSDPA helps in almost doubling the user throughput without the expense of dual transmission antennas. DC-HSDPA can offer a theoretical peak data rate of 42.2 Mbps with 15 codes for HS-PDSCH at each carrier [38]. DC-HSDPA is claimed to offer better performance than MIMO operation, particularly in low SINR condition [40]. In Release 10, DC-HSDPA can be deployed along with MIMO, and theoretically DC-HSDPA with MIMO can provide the data rate of 84.4Mbps [42].

3.1.1. HSDPA cell loading and power sharing

Conventional load equations used for estimating the cell load in uplink and downlink direction for UMTS system cannot be used for calculating the percentage of cell load in HSDPA system. In HSDPA system, information about the allocated power for different channels is used to find the system loading in a downlink direction. In other words, cell loading is expressed as a function of transmission power of NodeB. The overall system load η_{total} is equal to P_0/P_{max}, where P_0 is the active transmit power of NodeB in the DL direction, and P_{max} is the maximum available DL transmission power [43]. In general, HSDPA is deployed in co-existence with UMTS, and the power resources of the same NodeB are shared between HSDPA and UMTS. Therefore, total cell loading η_{total} is

given by equation (3.1), which is the sum of loading caused by the HSDPA layer η_{HSDPA} and non-HSDPA layer $\eta_{non-HSDPA}$ i.e., UMTS. Non-HSDPA loading factor also includes loading caused by Common Pilot Channel (CPICH), Common Control Channel (CCCH), and Dedicated Channel (DCH), whereas HSDPA loading factor depends on loading caused by High Speed Shared Control Channel (HS-SCCH) and HS-PDSCH as shown in equation (3.3) [38].

$$\eta_{total} = \eta_{non-HSDPA} + \eta_{HSDPA} \quad \textbf{(3.1)}$$

$$\eta_{non-HSDPA} = \eta_{CPICH} + \eta_{CCCH} + \eta_{DCH} \quad \textbf{(3.2)}$$

$$\eta_{HSDPA} = \eta_{HS-SCCH} + \eta_{HS-PDSCH} \quad \textbf{(3.3)}$$

In equation (3.4), $\eta_{HS-PDSCH}$ is the sum of individual loading factor β_j caused by the j^{th} user. In equation (3.5), $P_{HS-PDSCH_j}$ is the required transmission power for HS-PDSCHs intended for the j^{th} user. The sum of the power used by HS-PDSCHs by all active HSDPA users and HS-SCCHs in a cell cannot exceed the total power reserved for HSDPA system [19].

$$\eta_{HS-PDSCH} = \sum_{i=1}^{j} \beta_j \quad \textbf{(3.4)}$$

$$\beta_j = P_{HS-PDSCH_j}/P_{max} \quad \textbf{(3.5)}$$

3.1.2. Even codes and power allocation scheme in DL

In case of conventional even codes and even power allocation scheme, the channelization codes and power resources are equally distributed among active code multiplexed users in one TTI, whereas the modulation and coding scheme for each user is adaptive to the channel condition [44]. The link adaption algorithm is based on SINR value reported by the UE. Each user computes its SINR value using equation (3.8) and sends it to NodeB. The transmission power and available channelization codes are allocated to each user as given by equation (3.6) and (3.7), respectively. In equation (3.6), $P_{HS-PDSCH_{max}}$ is the maximum power available for the HS-PDSCHs at NodeB, M_{max} is the maximum number of code multiplexed users per TTI, where in equation (3.7) N_{UE_j} is the number of

codes assigned to j^{th} user, and N_a is the maximum number of available codes. Maximum throughput achieved by the user is limited by the power and the number of channelization codes given to the user [36, 44].

$$P_{HS-PDSCH\,j} = P_{HS-PDSCH_{max}}/M_{max} \quad j = 1, \ldots . M_{max} \tag{3.6}$$

$$N_{UE\,j} = N_a/M_{max} \quad j = 1, \ldots . M_{max} \tag{3.7}$$

SINR of each user in the DL direction can be computed using equation (3.8). Where S_j is the received power of HS-PDSCH of the j^{th} user from the serving NodeB, N is the noise power, I_{other} is the sum of interference power coming from k number of interfering NodeBs, and I_{own} is the interference coming from own cell due to loss of code orthogonality [38].

$$SINR_j = \frac{S_j}{I_{other} + I_{own} + N} \tag{3.8}$$

$$S_j = \frac{P_{HS-PDSCH\,j}}{L_{S_j}} \tag{3.9}$$

$$I_{other} = \sum_{i=1}^{k} \frac{Pt_i}{L_i} \tag{3.10}$$

$$I_{own} = \frac{(Pt_S - S_j)}{L_{S_j}} * (1 - \alpha) \tag{3.11}$$

$$SINR_{HSDPA} = SF_{HS-PDSCH} * SINR \tag{3.12}$$

In equation (3.9), L_{S_j} is the loss factor i.e. pathloss between the j^{th} user and the serving NodeB. In equation (3.10), Pt_i is the active transmission power of i^{th} interfering NodeB, and L_i is the pathloss between the UE and the i^{th} interfering NodeB. In equation (3.11), Pt_S is the active (instantaneous) transmission power of the serving NodeB, and α is the downlink orthogonality factor for HSDPA system. $SINR_{HSDPA}$ is the SINR attained after the despreading of the received signal, therefore the impact of processing gain is added as shown in equation (3.12).

3.1.3. Proposed power control scheme for HSDPA in DL

With the proposed power control scheme, uneven power can be allocated to the users irrespective of the number of codes assigned to them. Proposed power control scheme would help the users at the far distance from the NodeB (cell edge users) to use high order MCS, and experience better quality of service. Required transmission power for HS-PDSCH is computed through iterative process. In conventional HSDPA, fix power is transmitted and then link adaption is used to select the modulation and coding scheme, based on the received SINR. However, in case of proposed power allocation scheme the required transmission power for each user is computed for the selected modulation and coding scheme. Required transmission power depends upon multiple factors which includes a pathloss, required SINR value for the selected MCS, interference coming from the other cells, and interference coming from own cell. To reduce the algorithm complexity and to avoid the large number of inputs to power allocation scheme, an even number of codes are allocated to the users. The essence of this approach is to equally distribute the codes among the active users, but allocate different power to each user, so that even the users at the cell edge can enjoy high bit rates. Required transmission power for HS-PDSCHs intended for the j^{th} user is computed by using equation (3.13)

$$P_{HS-PDSCH\,j} = \frac{L_{S_j}.Req\_SINR_j}{1+Req\_SINR_j(1-\alpha)}\left(\sum_{i=1}^{k}\frac{Pt_i}{L_i} + \frac{Pt_S}{L_{S_j}}(1-\alpha) + N\right) \qquad \textbf{(3.13)}$$

The flow chart of proposed power allocation scheme is shown in Fig.3.1. Power allocation for HS-PDSCHs is done in an iterative way. In case of serving M_{max} multiple users per TTI, scheduler first selects M_{max} number of users on the basis of Round Robin (RR) scheme. Arrange those users in an ascending order based on pathloss. MCS are indexed in an ascending order with MCS[1] and MCS[8] as the lowest and highest possible modulation and coding scheme, respectively. Assuming all other NodeBs are transmitting with their full power, Power Control (PC) selects the first user and computes the required transmission power with respect to lowest MCS by using the equation (3.13), and this process continues for M_{max} number of users. If the sum of required power needed by M_{max}

users is less than the maximum allowed NodeB transmission power P_m for HS-PDSCH, then the process of calculating required power again starts from the first user but with an advanced (one step higher) MCS, and this process continues until it reaches the limit defined by P_m.

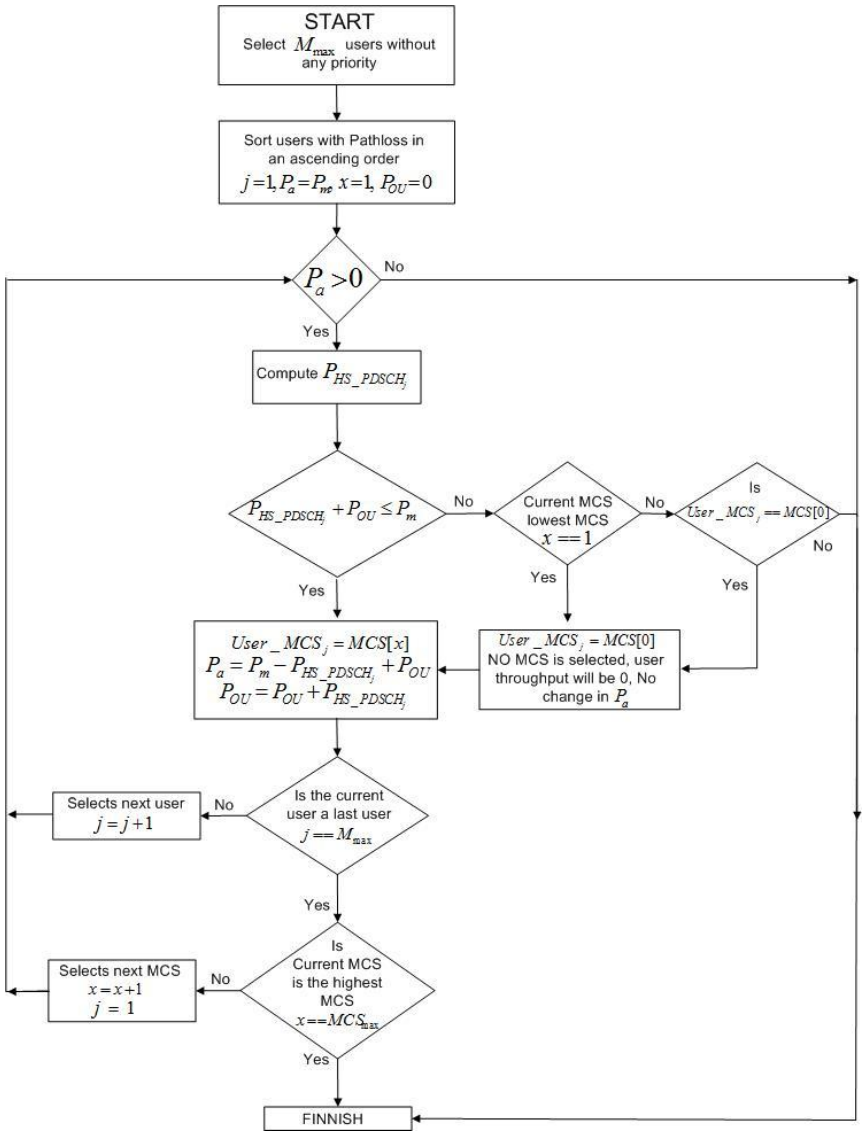

Fig.3.1 Flow chart of proposed power allocation scheme for HSDPA in DL direction

In this power allocation scheme, if any of the selected user is not able to adopt the lowest possible MCS i.e., MCS[1] due to outage of transmission power then MCS[0] is assigned to that user, which means no power is reserved for that user and there will be no data transfer. The channelization codes reserved for user with MCS[0] are not utilized for other users, but the power which was not allocated to the user with no data transfer can be used to enhance the MCS of other users with active transmission. The advantage of this scheme is that distance users can also have high QoS, high bit rates, enhanced user experience and it would help in bringing the probability of no data transfer at low level. However, the disadvantage of this approach is that if there are more users at the cell edge, then the users which are even in the close vicinity of base station would not be able to use the highest modulation scheme due to power limitation.

The following notations are used in the power allocation strategy:

M_{max}	:	Maximum number of code multiplexed users per TTI.
N_a	:	Maximum number of available codes.
N_{UE}	:	Number of codes assigned to single user.
P_m	:	NodeB maximum available power for HS-PDSCH.
P_a	:	Currently available power for HS-PDSCH.
P_{OU}	:	Power allocated to other users for HS-PDSCH.
$P_{HS-PDSCH_j}$	:	Required HS-PDSCH power for j^{th} user where, j=1,…. M_{max}
$User\_MCS_j$	:	MCS selected for j^{th} user.
MCS_{max}	:	Index of highest possible MCS.
$MCS[x]$	:	MCS with index x, where x=1,…. MCS_{max}.

3.2. Long Term Evolution (LTE): The contender of 4G Technology

Heavy penetration of smart phones capable of handling advanced applications with different Quality of Services (QoSs) demands a huge capacity with a high speed from cellular networks. LTE system is categorized as an evolved cellular network with flat IP architecture, and was introduced in Release8 of 3GPP. LTE offers low latency and provides

enhanced user experience. Essential improvements introduced in LTE system with reference to prior cellular systems are new multiple access techniques i.e., Orthogonal Frequency Division Multiple Access (OFDMA) and Single Carrier Frequency Division Multiple Access (SC-FDMA), adopted in downlink and uplink direction, respectively. MIMO is an important feature of LTE system, which helps in improving the coverage and enhancing the capacity of a system. LTE can be deployed with bandwidths ranging from 1.25MHz to 20MHz, with a fixed sub-carrier spacing of 15kHz. Flexible bandwidth deployment made LTE system an attractive choice for the operators. Radio resources are being assigned to users dynamically which leads to higher flexibility [45, 46, 2].

In LTE, Resource Block (RB) is considered as a "grid" structure in time and frequency domain. The smallest data unit which can be allocated to a single user is a pair of a resource block. Single RB consists of 12 consecutive subcarriers in a frequency domain for half a milli second in time domain. The Transmission Time Interval (TTI) is 1ms for LTE. There is parallel transmission of data with multiple subcarriers in downlink direction [47].

3.2.1. Power control and power sharing in LTE

LTE does not have a fast power control mechanism for uplink direction as in UMTS systems. LTE does not need complicated and sophisticated power control mechanism due to the orthogonal nature of the radio resources utilized by the users in the uplink direction. In LTE, the main idea of having PC in uplink direction is to minimize the terminal power consumption, and to avoid a large range of received power at eNodeB, rather than to mitigate the interference and a near far problem as encountered in UMTS system [2]. UE uses an open loop as well as closed loop power control for estimating the required transmission power in uplink direction. There is no sophisticated and fast power control in the downlink direction. Reference signal is transmitted with constant power over the entire bandwidth [48]. In case of transmitting the reference signal without power boosting, power per RE is same for those carrying the user data or reference signal. In downlink, LTE only supports static reference signal power boosting [49]. In coverage limited scenarios, RS power boosting can be used to improve the channel estimation in downlink

direction. For all the symbols of a slot except the first and the third last symbol (symbols containing the RS), a UE specific parameter ρ_a is given at [50] which is defined as the ratio of power between REs carrying the PDSCH to REs carrying the RS. Similarly for the first and third last symbol, a UE specific parameter ρ_b is specified at [50], which is also defined as the ratio of power between REs carrying the PDSCH to REs carrying the RS. Other then these two UE specific parameters, another cell specific parameter P_B defined as a ratio ρ_b/ρ_a is also given at [50]. These UE specific parameters indicate that different Power Spectral Density (PSD) can be set for different users, while keeping the cell specific parameter P_B constant. For two antenna ports, cell specific parameter P_B as a ratio of UE specific parameters is shown in Table 3.1.

Table 3.1Cell specific parameter as a ratio of UE specific parameter

P_b	ρ_b/ρ_a
0	5/4
1	1
2	¾
3	½

3.3. Antenna techniques

In quest of fuller and efficient utilization of available radio resources, scientific community is always looking for new antenna solutions. Nowadays to provide required coverage and to avoid interference to the neighbour cells, directional antennas with optimum electrical and mechanical tilts are used instead of omni directional antennas [51, 52]. Antenna configuration i.e., antenna height, azimuth, radiation pattern, number of antenna elements, beamwidth, beam shape, directivity or gain, polarization etc, has deep impact on the cell capacity [53]. Antenna techniques considered in the research work of this thesis are discussed next.

3.3.1. Higher order sectorization

High order sectorization is a promising technique for enhancing the site capacity without building additional sites. The spectral efficiency of a system can be improved through “Sectorization”, dividing the site

coverage area spatially into multiple sectors and reusing the radio resources in each sector [5, 4, 54, 3]. Six-sector sites and 12-sector sites are the examples of high order sectorization. For a macrocellular network without extensive capacity demand, 3-sector site is a practical solution with equally spaced antennas in an azimuth plane with the difference of 120^0. However, for the case of a high capacity requirement, 3-sector sites are not able to fulfill the demand, and sometimes adding another carrier in the same sector is not a viable solution for the mobile operators.

An ideal sectored antenna has a flat response within the sector and zero response outside the sector. For an ideal sectored antenna there is no overlapping between the sectors of the same site, and hence there is no inter-sector interference [5]. Practically it is not possible to achieve ideal sector response, and each sector receives co-channel interference from the neighbor sectors of the same site as well as from other sites. Performance of high order sectorization depends upon the half power beamwidth of the antenna in the horizontal plane. With optimum beamwidth antenna, 6-sector site not only provides better coverage but also gives significant capacity enhancement compared to 3-sector sites [55]. In order to avoid the installation of new sites due to high operational costs, and to improve the capacity of a cellular network, implementing high order sectorization within the existing site can be considered as a possible cost effective solution [54].

3.3.2. Multiple Input Multiple Output (MIMO) antennas

Cellular networks with Single Input Single Output (SISO) system offer limited channel capacity. Transmission and reception with multiple antennas is categorized as MIMO antenna system. Interference between the antennas can be significantly reduced by applying spatial separation between antennas. Large spatial separation between the antennas may also decrease the correlation factor between the received signals coming from different antennas [56]. MIMO transmission can be used to provide a transmit diversity with multiple transmit antennas; a receive diversity with multiple receive antennas and a spatial multiplexing with multiple antennas at the transmitter and the receiver side. Space diversity and polarization diversity are the examples of transmit diversity, where each

transmitting antenna is sending the same data. Equal Gain Combining (EGC), Maximum Ratio Combining (MRC), and Interference Rejection Combining (IRC) are the combining techniques used at receiver side to boost the SINR. Transmit and receive diversity improves the SINR level, whereas Spatial Multiplexing (SM) increases the user throughput by transmitting independent data streams from each of the transmitting antennas [56, 57].

Adaptive MIMO Switching (AMS) is a scheme of switching between antenna transmission modes to maximize the user throughput with improved coverage and quality of service (QoS). In a radio environment, channel conditions are continuously changing, and by using AMS the transmission mode is selected by switching from diversity mode to spatial multiplexing or vice versa. The target of AMS is to efficiently utilize the radio resources, and to maximize the spectral efficiency. In AMS, spatial multiplexing is selected for the users experiencing high SINR and good channel condition, whereas diversity techniques are used for the users at cell edge or with low SINR value. SINR threshold for switching between the transmission modes depends upon the throughput [2].

3.3.3. Multiple switched beam antenna

A multiple switched beam antenna is a combination of multiple narrow beams in predetermined directions, overlapping over each other. It covers the desired cell area with finite number of narrow fixed beams, where each beam can serve multiple users [10, 58]. Switched beam antenna does not steer or adapt the beam with respect to the desired signal. In this type of antenna, a RF switch connected to fixed beams controls the beam selection based on the beam switching algorithm. A switch selects the "Optimum" beam to provide service to the mobile station. The optimum beam here refers to the beam that offers the highest SINR value. In some cases, maximum received power for the user can be used as a beam selection criterion. During user mobility, a switched beam antenna tracks the user and continuously updates the beam selection to ensure high quality of service [59]. The general block diagram of a switched beam smart antenna system is shown in Fig.3.2 [60]. Switched beam antenna uses a smart receiver for detecting and monitoring the received signal power from each user at each antenna port. Based on the measurement

made by the smart receiver and beam selection algorithm, the control logic block determines the most favorable beam for specific user. The RF switch part governed by the control logic (brain of a switched beam antenna) activates the path from the selected antenna port to the radio transceiver.

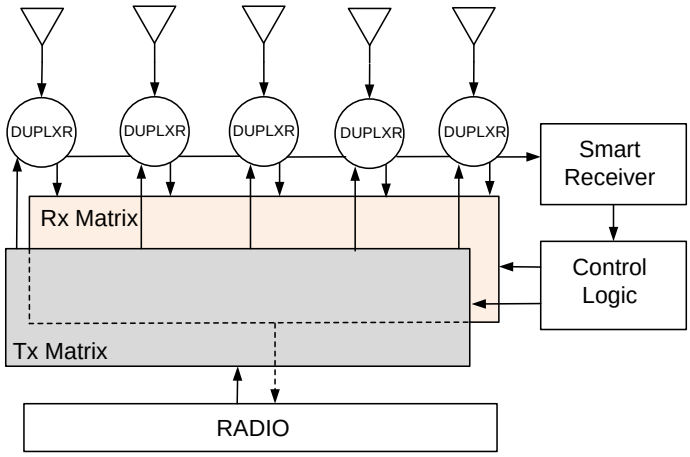

Fig.3.2 Block diagram of switched beam smart antenna system

3.3.4. Adaptive beam antenna

An adaptive antenna exploits the array of antenna elements to achieve the maximum gain in the desired direction, while rejecting the interference coming from other directions. Adaptive antenna can steer its maxima and nulls of the array pattern in nearly any direction in response to the changing environment [58]. Smart antenna employs Direction of Arrival (DOA) algorithm to track the received signal from the user, and places the nulls in the direction of interfering users and maxima in the direction of a desired user [61]. On the other hand, since adaptive antennas need more signal processing, multiple switched beam antennas are easier to implement and have the advantage of being simpler and less expensive compared with adaptive antennas.

Beam forming algorithms used in adaptive antennas are generally divided into two classes with respect to the usage of training signal i) Blind Adaptive algorithm and ii) Non-Blind Adaptive algorithm [62]. In a non-blind adaptive beam forming algorithm, a known training signal d(t) is sent from transmitter to receiver during the training period. The

beamformer uses the information of the training signal to update its complex weight factor. Blind algorithms do not require any reference signal to update its weight vector; rather it uses some of the known properties of a desired signal to manipulate the weight vector. Fig.3.3 shows the generic beam forming system based on a non-blind adaptive algorithm, which requires a training (reference) signal [61].

The output $y(n)$ of the beamformer at time n, is given by a linear combination of the data coming at the k antenna elements. The baseband received signal at each antenna element is multiplied with the weighting factor which adjusts the phase and amplitude of the incoming signal accordingly. The sum of this weighted signal results in the array output $y(n)$. On the basis of adaptive algorithms, entries of weight vector $\boldsymbol{w}$ are adjusted to minimize the error $e(n)$ between the training signal $d(n)$ and the array output $y(n)$. The output of the beamformer $y(n)$ can be expressed as given in equation (3.14), [62]

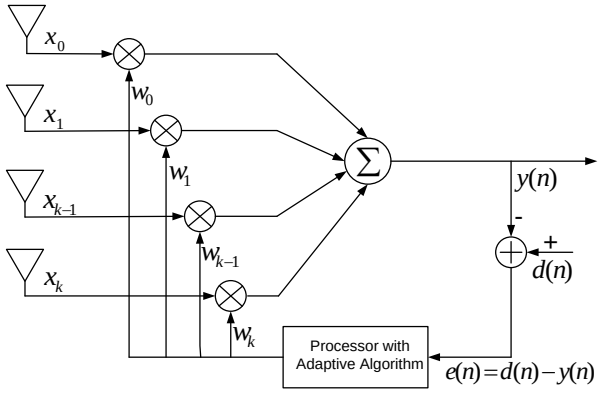

Fig.3.3 Block diagram of adaptive beamforming system

$$y(n) = \boldsymbol{w}^H(n)\boldsymbol{x}(n) \quad \textbf{(3.14)}$$

$$\boldsymbol{w}(n) = [w_1(n)\ \ w_2(n) \ldots\ldots w_{k-1}(n)\ \ w_k(n)] \quad \textbf{(3.15)}$$

$$\boldsymbol{x}(n) = [x_1(n)\ \ x_2(n) \ldots\ldots x_{k-1}(n)\ \ x_k(n)] \quad \textbf{(3.16)}$$

$$e(n) = d(n) - y(n) \quad \textbf{(3.17)}$$

where $\boldsymbol{w}(n)$ is the weight vector with $w_k(n)$ a complex weight for kth antenna element at time instant n, and $[.]^H$ denotes Hermitian (complex conjugate) transpose. $x_k(n)$ is the received baseband signal at

*k*th antenna element. Least Mean Square (LMS), Normalized Least Mean Square (NLMS), Recursive Least Squares (RLS), and Direct Matrix Inversion (DMI) are the examples of non-blind adaptive algorithm, whereas Constant Modulus Algorithm (CMA) and Decision Directed (DD) algorithms are the examples of blind adaptive algorithm [61, 62, 63]. These beamforming algorithms have their own pros and cons as far as their computational complexity, convergence speed, stability, robustness against implementation errors and other aspects are concerned.

3.4. Cellular network tessellation

To learn about the system behavior in different radio conditions, preliminary cellular system performance is evaluated through link and system level simulations. For making a nominal plan of sites for simulation purpose, it is generally assumed that the sites have regular network layout. Regular network tessellation is based on geometric shapes i.e., hexagon, triangle, square etc., fulfilling the criterion of providing continuous coverage, and forms a regular grid like structure [64]. In literature, there are several definitions for the regular layout, but the most commonly used shape for cellular network is "Hexagon" [65, 66, 67]. Network layout has significant impact on interference management, and hence on the capacity of a macrocellular network. In Fig.3.4(a), the antennas are pointed to each other, whereas in Fig.3.4(b) the antennas are pointing to the vertices of a hexagon. Layout shown in Fig.3.4(b) is known as "Cloverleaf" layout [66, 12]. In cloverleaf layout, all the interfering sites of the first tier of interferer are pointing at the null of a serving site. However, cloverleaf layout cannot be used for higher order of sectorization.

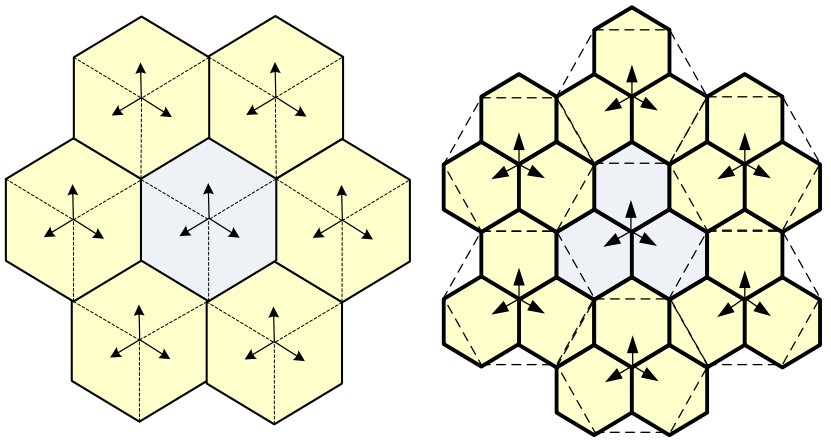

(a) (b)

Fig.3.4 Hexagonal tessellation based 3-sector layout

There also exist hexagonal tessellation for 6-sector layout as shown in Fig.3.5(a), with antennas pointing to the vertices of the hexagon [68, 69]. To enhance the performance of a 6-sector site an optimized network layout is presented in [70], where sectors do not face each other as shown in Fig.3.5(b), and hence reduce the impact of other cell interference. Onward in this thesis, the tessellation for a six-sector site presented in [70] is called "Snowflake" topology.

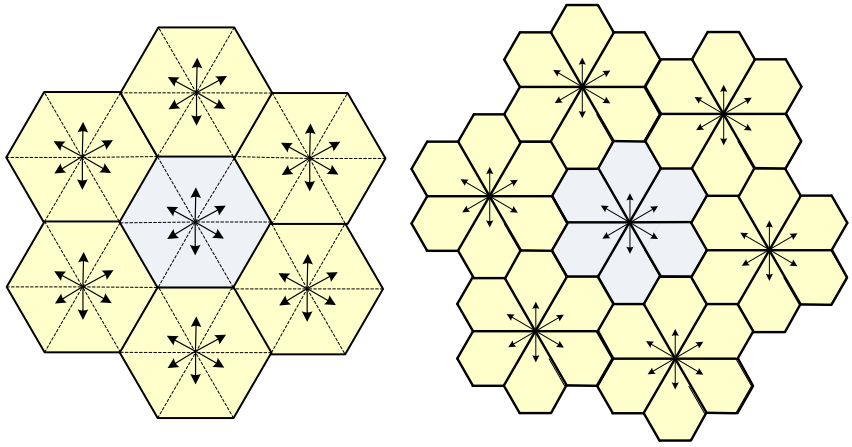

(a) (b)

Fig.3.5 Tessellations for 6-sector sites

Finally, a conventional hexagonal tessellation and a novel tessellation for 12-sector site is shown in Fig.3.6(a) and Fig.3.6(b), respectively. This

novel layout for 12-sector site was proposed in [P6] and was named as "Flower" topology due to shape of the site dominance area.

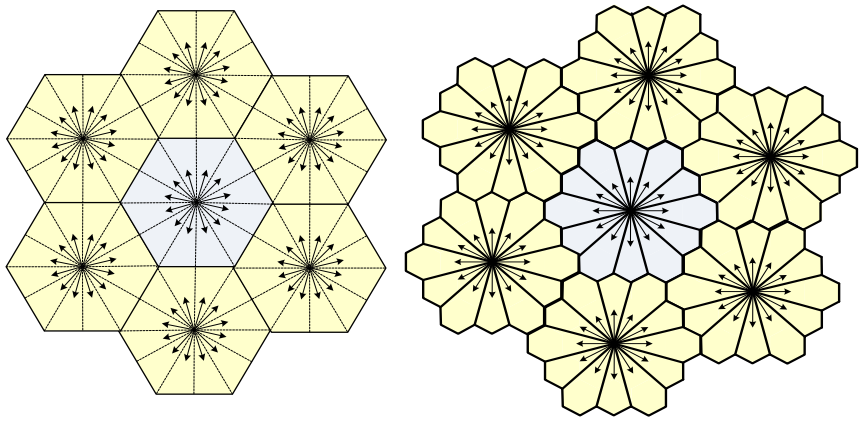

(a) (b)

Fig.3.6 Tessellations for 12-sector sites

3.5. Simulation environment and simulation results

MATLAB was used as a simulation tool for all the simulation results presented in [P4-P7]. Users with a full traffic buffer were assumed i.e. they always have data to transmit; every user tries to get as much throughput as possible. Cell resources i.e. RBs for LTE and codes for DC-HSDPA were equally divided among all the active users in a cell, leaving no unused resources at any TTI. Therefore own cell loading of 100% was assumed along with 100% other cell loading in neighboring cells. Number of users supported in any TTI was fixed, and users were homogenously distributed over the cell area. Locations of users were random, with flat distribution over the coverage area of the cell. Round Robin (RR) scheduler is considered in DL direction for scheduling purpose with no priority for any user. The COST231 Hata model was used as a radio propagation model for calculating the path loss between the user and the eNodeB.

3.5.1. Performance evaluation of AMS

In [P4], Kronecker channel model is used to model the MIMO radio channel. Kronecker model is analytical channel model and belongs to the family of random channel matrix model, and assumes no Channel State Information (CSI) at the transmitter side. This model considers scatterers located in the vicinity of the receiver and transmitter. Channel matrix is modeled by the Kronecker product of transmit and receive covariance matrix. Kronecker model defines the MIMO channel as given in equation (3.18) [71]

$$H = R_R^{1/2} * H_{IID} * (R_T^{1/2})^T \quad \textbf{(3.18)}$$

In equation (3.18), R_T and R_R are the transmit and receive covariance matrices respectively, $(.)^T$ performs the transpose operation of a matrix. H_{IID} is a random fading MIMO channel matrix whose entries are independent and identically distributed (i.i.d). Each entry has Gaussian distribution with zero mean and unit variance.

In [P4], LTE performance with different antenna transmission modes was analyzed at different Intersite Distance (ISD). Detailed simulation parameters can be found at [P4]. Fig.3.7 shows the average LTE cell throughput achieved with different antenna transmission modes against intersite distance. SIMO and MISO are representing receive diversity and transmit diversity, respectively. Whereas, MIMO2x2 and MIMO4x4 are the cases of spatial multiplexing with two and four antennas, respectively. It can be seen that the average cell throughput achieved by using AMS is better than average cell throughput by any other individual antenna configuration. In Fig.3.7, the highest cell throughput is achieved with the lowest intersite distance. By analyzing the results presented in Fig.3.7, it was found that by increasing the ISD the average cell throughput is decreased.

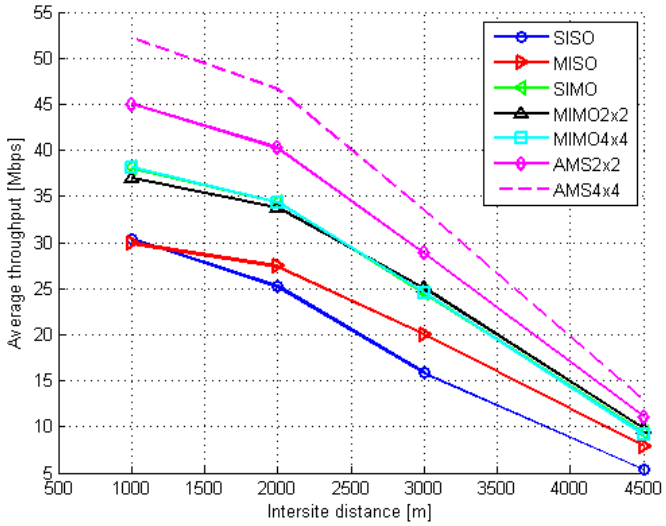

Fig.3.7 Average cell throughput against ISD for different transmission modes

3.5.2. Performance evaluation of proposed power allocation scheme in DC-HSDPA

In [P5], Monte Carlo type simulations were performed with a sample network of LTE integrated with a feature of AMS, and a DC-HSDPA enabled network along with MIMO. Impact of a variable number of users per TTI on the performance of high speed cellular networks was also analyzed. A single 3-sectored site was created, which was interfered by six other sites following a cloverleaf layout. A fading component is modelled with a log normal distribution having zero mean and 4dB of standard deviation. LTE with flat Power Spectral Density (PSD) in downlink direction is assumed i.e., total transmission power is equally distributed among all the available subcarriers in the system bandwidth. Therefore, $P_b = 1$ was chosen with $\rho_a = \rho_b = 1$, which means irrespective of the symbols containing the RS or not, there will be flat and constant power over all the RE. Key parameters related to LTE and DC-HSDPA systems used in the simulations can be found at [P5]. The results presented in Fig.3.8 and Fig.3.9 were obtained by averaging over 5000 snapshots of the network.

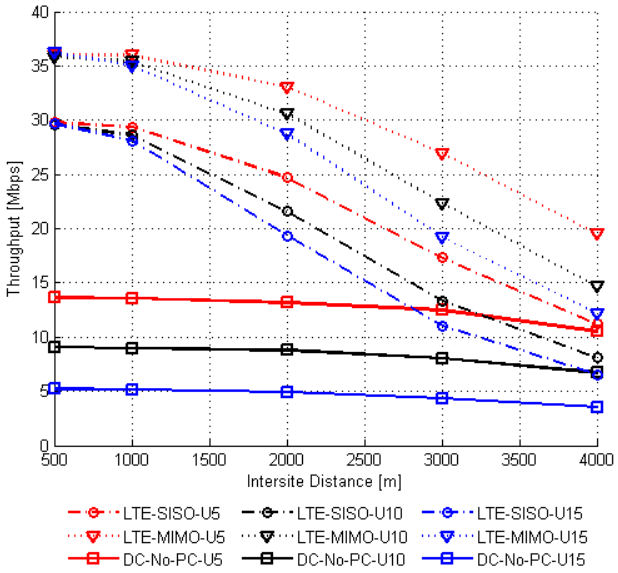

Fig.3.8 Cell throughput of LTE with SISO and MIMO, and DC-HSDPA without PC

Fig.3.8 shows average LTE cell throughput achieved with variable number of users per TTI against different ISD in macrocellular environment. Initially, LTE system with SISO and MIMO (spatial multiplexing) configuration was considered only. For the purpose of comparison, average cell throughput of DC-HSDPA without any sophisticated power allocation scheme supported with spatial multiplexing is also shown in Fig.3.8. Red, black and blue curves show results for serving 5, 10 and 15 users per TTI, respectively. It can be seen that average cell throughput declines for both systems with the increase in ISD, irrespective of the active number of users. At large intersite distances e.g. greater than 1000m, LTE throughput changes rapidly with the change in ISD and acute drop in throughput was observed, as far distance users cannot be served with high data rates. Throughput of DC-HSDPA has a mild impact of changing the intersite distance, but changes sharply with a change in active number of users. DC-HSPDA without PC offers enhanced bit rates with less number of users, as total transmission power was divided among total users. Peak average cell throughput of 36Mbps and 29.5Mbps was achieved by LTE-MIMO and LTE-SISO respectively, whereas DC-No-PC offered the peak average cell throughput of 13.73Mbps with 5 users per TTI at small ISD of 500m.

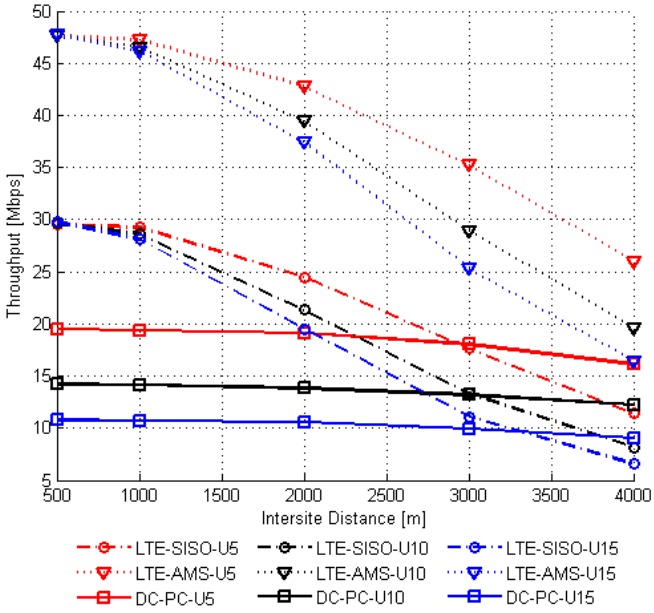

Fig.3.9 Average cell throughput of LTE with AMS, and DC-HSDPA with PC

Fig.3.9 shows average cell throughput of LTE with AMS and DC-HSDPA with proposed power allocation scheme. By comparing the results shown in Fig.3.8 and Fig.3.9, it can be seen that LTE throughput was further improved with the help of AMS compared to spatial multiplexing only. However, the cell throughput curves follow the same trend in Fig.3.9 as in Fig.3.8. On the other side, DC-HSDPA performance also enhanced by adopting a power allocation strategy proposed in this thesis. Interestingly, it was found that if the power resources in DC-HSDPA are adequately allocated and utilized, then DC-HSDPA with MIMO can compete with LTE-SISO. The advantages of AMS i.e., improving the SINR for far distance users and enhancing the throughput by multiplexing data streams for the near user are reflected in Fig.3.9. LTE-AMS outperforms at small ISDs and offered a peak averaged cell throughput of 47.66Mbps. Performance of DC-HSDPA with MIMO improves from 13.73Mbps to 19.51Mbps with the help of a fair power distribution method.

3.5.3. Assessment of Flower tessellation for 12-sector sites

It is hard to find an optimum network tessellation for 12-sector site in open literature. A novel network layout called "Flower" layout for 12-sector site is proposed in [P6].

For different network layouts presented in section 3.4, a single site in the middle interfered by two tiers of interferers i.e., 18 sites at equal intersite distance was considered for the simulation purpose. The impact of higher order sectorization i.e., 6-sector and 12-sector with different network layout was analyzed in DC-HSDPA network. Macrocellular urban environment was assumed, and Okumura-Hata pathloss model was used for estimating the path loss. Slow fading (shadowing) was modeled with lognormal distribution having zero mean and 6dB of standard deviation. Code orthogonality factor is modeled with Gaussian curve having maximum value of 0.97 at site location and 0.7 at cell edge. HPBW of antennas were scaled proportionally to the number of sectors per site i.e., 3-. 6-, and 12-sector sites were implemented with 65°, 32°, and 16° HPBW antennas, respectively. Radiation patterns of the antennas used for the simulation purpose can be found [P6].

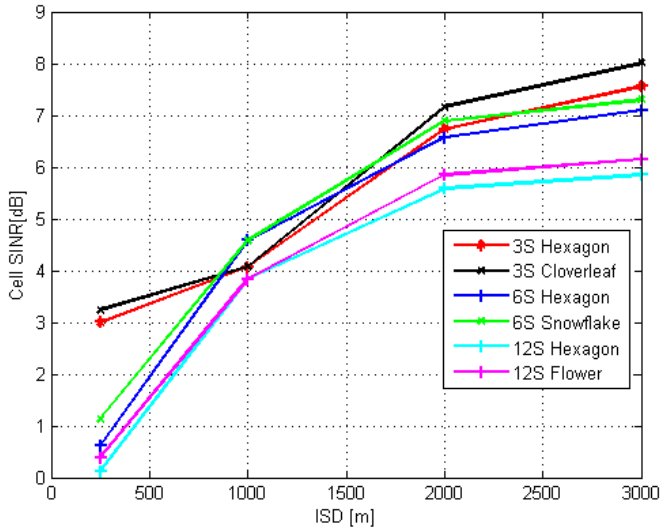

Fig.3.10 Mean cell SINR of different network layouts

Fig.3.10 shows the attained mean cell SINR for different network layouts against different intersite spacing. In each iteration (snapshot) of Monte Carlo simulation, the average SINR value over the cell is obtained by adding the linear SINR value of each user and then dividing the sum by the number of users served per TTI. It is clearly evident that cloverleaf layout performs better than hexagon layout for 3-sectors, snowflake topology performs better than hexagon layout for 6-sectors, and flower layout gives better cell SINR compared to hexagon layout for 12-sectors. Irrespective of the ISD, hexagon layout for 12-sector site offers the lowest cell SINR.

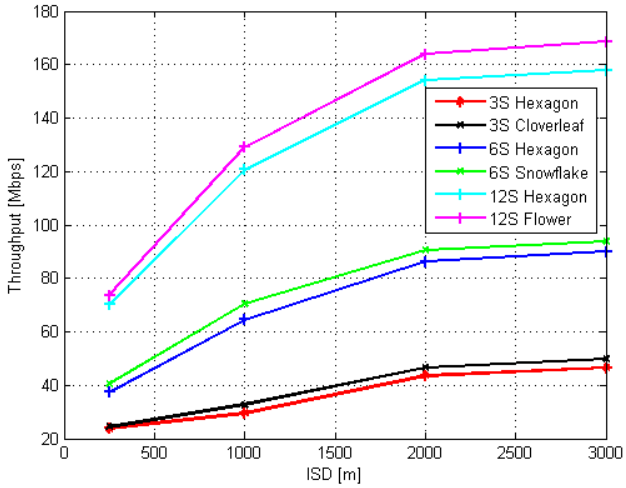

Fig.3.11 Mean site throughput for different network layouts

The results presented in Fig.3.11 highlight the gain of adopting proper network layout and spotlight the advantage of using higher order sectorization. Post simulation analysis reveals that optimized network layouts offer better system throughput compared to traditional hexagon layout. Maximum relative gain of optimized network layouts for 3-, 6-, and 12-sector sites was found at 1000m ISD. It was learned that at 1000m ISD, cloverleaf layout provides approximately 10.5%, snowflake offers 9% and flower layout tenders approximately 7.2% better throughout compared to hexagon layout for 3-, 6- and 12-sector sites respectively. To avoid the deployment of small cells, high order sectorization with optimized network layout can be considered as an alternate choice.

3.5.4. Assessment of new antenna solutions through simulations

The user SINR, user throughput and site throughput statistics were gathered from the massive simulation campaign conducted with full traffic buffer users and 100% other cell loading in DC-HSDPA network. Cell throughput in each TTI is the sum of individual users' throughput. Total transmission power for HS-PDSCH and available codes were equally distributed among the five users in each TTI. Following five cases were considered for simulations in [P7].

- **3 Sector:** It is the most common scenario where each site has three sectors and every sector has single 65° half power beamwidth antenna, with no electrical or mechanical tilt, and with the maximum antenna gain of 15.39dB. Clover leaf layout is used for this case. It acts a reference case for comparing with higher order sectorization and advanced antenna case.
- **6 Sector:** It is the case in which each site has six sectors, and every sector has single 32° half power beamwidth antenna, with no electrical or mechanical tilt, and with the maximum antenna gain of 18.20dB. Snowflake layout is used for this case.
- **12 Sector:** In this case, each site comprises 12 narrow sectors, and every sector has 16° HPBW antenna with no electrical or mechanical tilt, and with the maximum antenna gain of 21.15dB. Flower layout is used for this case.
- **7 Switched beams:** This case represents a multiple fixed switched beam scenario, where a single sector is covered by seven potential narrow beams. Each narrow beam has eight degree HPBW with spacing of 16° between the beams. No down tilting was assumed, and each beam has maximum antenna gain of 23.55dB. Three-sector site following the clover leaf layout was assumed.
- **Adaptive beam:** In this last scenario, adaptive antennas are used to form an accurate beam for each individual user. In this scenario, a narrow beam of six degree in the horizontal plane is steered precisely to the serving user, keeping user in the middle of the beam for maximum gain. Adaptive antenna has maximum gain of 24.5dB.

Details of antenna patterns used for each case and other simulation parameters can be found at [P7].

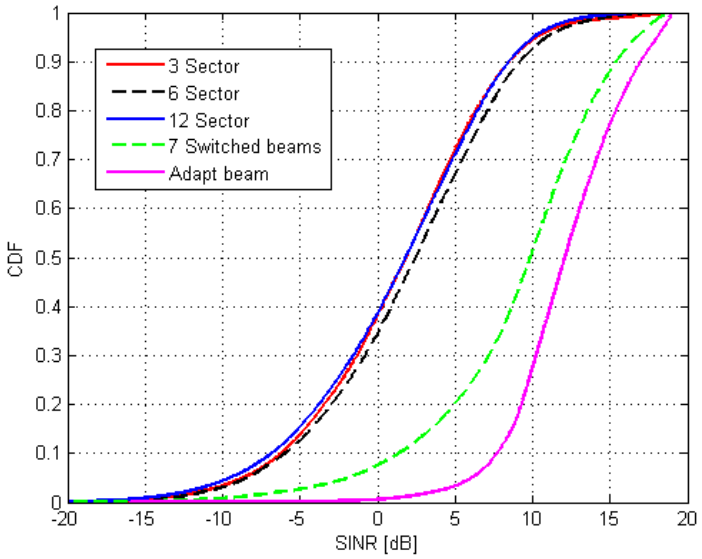

Fig.3.12 CDF plot of user SINR with 5 users per TTI at 1000m ISD

Fig.3.12 shows the Cumulative Distribution Function (CDF) of the user SINR with 5 users per TTI at 1000m ISD for different cases. Clearly switched beam antenna shows better performance in terms of offering higher SINR compared to 65°, 32°, and 16° wide beam antenna used in 3-sector, 6-sector and 12 sector sites, respectively. But an adaptive beam antenna outperforms and shows superior performance compared to all other cases. By analyzing the curves shown in Fig.3.12 it can be deduced that adaptive and switched beam antennas served the purpose of improving user experience by reducing the interference and enhancing the received SINR. The CDF curve of SINR for the case of an adaptive beam is on the extreme right position, indicating that on average the SINR for the users is improved. It is also important to note that the average user SINR does not deteriorate by increasing the order of sectorization and almost similar performance is shown by 3-sector, 6 sector and 12-sector sites. However, 6-sector site offers slightly better performance compared to 3 and 12-sector sites. An adaptive beam antenna performed well in the close vicinity of the NodeB as well as near the cell edge, as 80% of the samples are concentrated in a narrow range of 9.12dB, starting from

7.72dB to 16.84dB of user SINR. But for other traditional antenna cases, eighty percent of SINR values has wide span and spread over the range of around 14.96dB, starting from -6.3dB to 8.66dB.

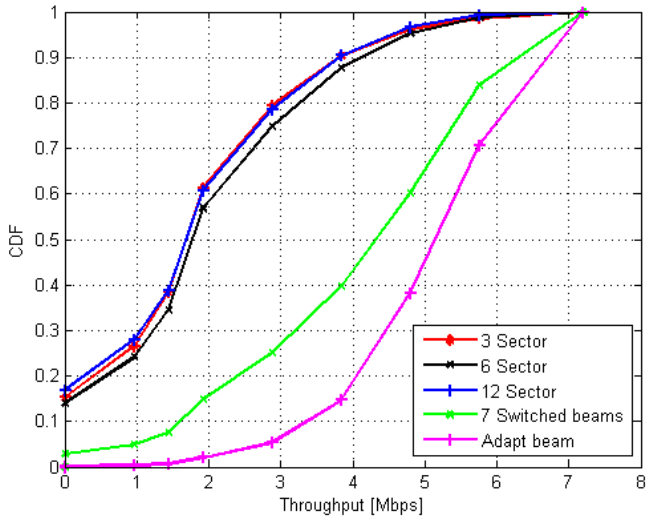

Fig.3.13 CDF plot of user throughput with 5 users per TTI at 1000m ISD

Fig.3.13 shows the CDF of the user throughput of DC-HSDPA network with 5 users per TTI at 1000m ISD. Eight marks on CDF plots represent eight different MCS. As equal codes and equal power was distributed among the users, therefore high throughput samples show that high modulation and coding scheme was used by the user. High MCS are less robust against interference and thus have a high requirement of SINR. It is interesting to note that around 4.5% of the users were able to adapt 64QAM in 3-, 6-, and 12-sector case, whereas this number was raised to 39.98% and 61.8% by switched and adaptive beam antennas, respectively. As seen from the results, more than 85% of the samples with an adaptive beam were obtained with the three highest MCS. Samples of zero throughputs in CDF plots represent the users with no data transfer due to very low SINR. It was also noted that single wide beam antenna keeps the probability of no data transfer at almost 15%. Whereas, switched beam antenna and adaptive beam antenna show remarkable improvement in the probability of no data transfer and kept it at negligible level of 2.88% and 0.16% respectively. These results clearly indicate the impact of advanced

antenna techniques in improving the user experience, when other cells are heavily loaded and are severely interfering the serving cell.

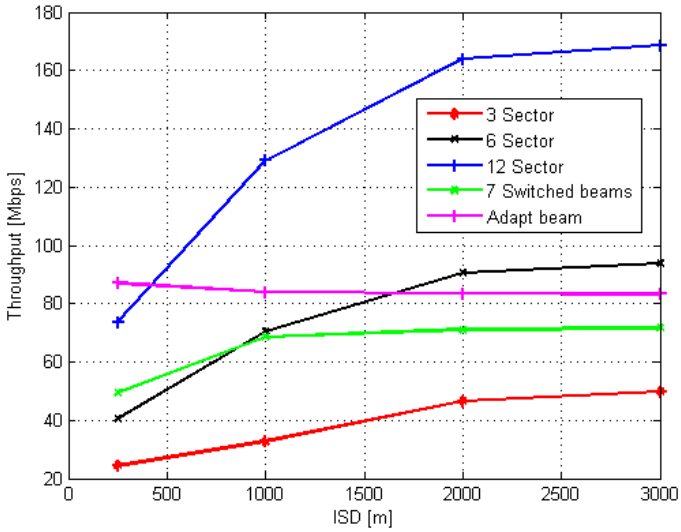

Fig.3.14 Mean site throughput with five users per TTI against ISD

It can be seen in Fig.3.14 that higher order sectorization and advance antenna techniques provide significant throughput gain over traditional 3-sector site topology. Relative site throughput gain for 6-sector and 12-sector topology is higher at large intersite distances than small ISD. Relative throughput gain of approximately 23.67% and 125.69% is achieved by 6-sector and 12-sector sites, respectively at 250m ISD, which is comparatively small, compared to 164.04% and 401.65% by 6 and 12-sector sites, respectively at 2000m ISD. Adaptive antenna beam outperformed at 250m ISD and was found more effective at small ISD. More detailed analysis of site throughput and the relative gain is presented in [P7].

4. A STEP TOWARDS 5G

The trend of wireless broadband data access is increasing significantly and is expected to ramp up even with the higher pace in the next few years. It strongly looks that recent mobile technologies will not be able to fulfill the market needs. Different ways of increasing the capacity of the cellular system are highlighted in previous sections. New capacity requirements, large data traffic in mobile networks and the requirement of high practical data rates in cellular networks have made scientific community to think about new possible access schemes and network layouts for the future. Traditional macro cells are not able to offer homogeneous data rates to the users over the entire network area, and most of the network capacity is lost due to the interference coming from the neighbors. In order to keep the macro cell layout, and to radically increase the frequency reuse, "a giant leap" is needed at concept level of radio access. This leap could be related to new antenna materials, and to new opportunities to create communication between base station and a mobile station.

4.1. 5G expectation

5G technology is not a standardized technology yet, and currently it is in the early research phase [72, 73]. Therefore, the speculation about 5G still continues as "Will 5G be an evolution of Long Term Evolution (LTE) or LTE-Advanced (LTE-A)?", or "Will there be a giant technology leap in 5G?", which would radically and abruptly change the cellular concept, the architecture of radio access, and the principles of radio network planning.

Ultimately, 5G is about a supreme user experience, a user can think of. It is about having high quality of service without any interruption, unique user experience with uniform connectivity regardless of your location. 5G wireless network is expected to offer thousand times more capacity compared to the capacity offered by LTE, the fourth generation of wireless networks. Couple of Gbps of download speed for individual

user, with extremely low latency and response time is anticipated in 5G [72, 73, 74, 75]. One can potentially expect a "Click and Bang" response from the future generation of a wireless network. It will offer new, innovative and smart ways to people to connect each other, and experience the prime quality of service. 5G is expected to support a vast range of capabilities from very fast moving devices to ultra-low energy sensors with high energy efficiency [14]. Essentially, 5G will show support for different kinds of network deployment and will be inter-operable with other Radio Access Technologies (RATs). It will also be able to simultaneously use multiple radio access technologies, and will provide seamless connectivity amongst multiple RATs and different devices. 5G is supposed to use spectrum efficiently by utilizing the unused spectrum, and by adopting cognitive radio or Software Defined Radio (SDR). One can also expect that 5G will natively support Device-to-Device (D2D) connectivity and Machine-to-Machine (M2M) communication [14]. Interference has always been a major issue in wireless networks. Thus, in 5G networks it is assumed that high level of interference coordination is utilized between the nodes to mitigate the problem of inter-cell interference. As a result an advanced interference cancelling receiver architecture will be an integral part of 5G. Integration of cloud computing capability will allow a user to have an unprecedented speed of computation, with easy access to huge data without carrying big data storage devices. Expectations about 5G from user's point of view are concentrated in Fig.4.1.

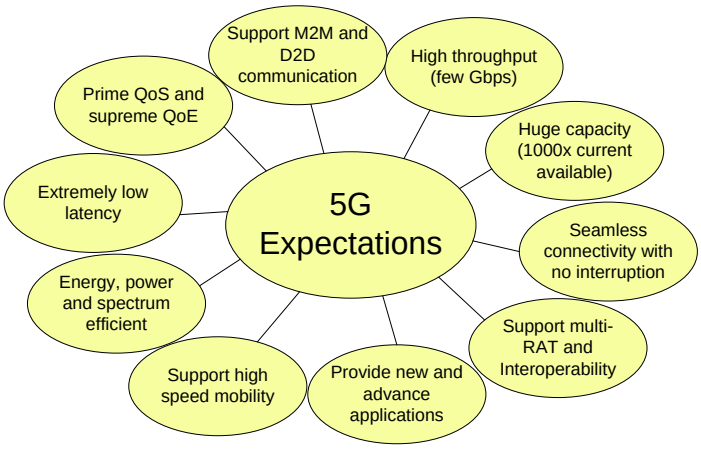

Fig.4.1 User's expectation about 5G.

4.2. Single Path Multiple Access Concept

Single Path Multiple Access (SPMA) is a novel multiple access technique proposed in [P8], which utilizes the characteristics of independent propagation paths at particular geographical location. For each geographical location, a received power is the sum of independent multipath components between the base station and mobile stations. Thus, a single independent multipath component can be used to represent a single BS – MS connection, sharing the radio resources or utilizing the whole available frequency spectrum. When frequency resources can be reused after every couple of meters, then frequency spectrum can be reused more than 1,000 times per square kilometer, enhancing a huge network capacity.

Researchers have been trying to control the Electromagnetic (EM) radiations, and they have made substantial progress at microwave and a terahertz band, but it seems much more complicated at the cellular band. Graphene has recently gained much popularity and has got enormous attraction by the research industry due to its exceptional electrical, mechanical, thermal and chemical properties [76]. Potential antenna and RF applications of graphene at microwave and at terahertz frequencies are proposed by the researchers [76]. It gives radically new possibilities to have narrow radiation pattern using graphene based antenna at nano scale level. It will not only reduce the size of antenna rather will also be able to serve the purpose of SPMA concept by employing narrow beams like "needle". In [77], an arrangement was proposed for controlling the electromagnetic radiations at microwave frequencies by hiding (covering) a copper cylinder inside the cloak. The cloak was constructed by using artificially structured metamaterials. Graphene and other structures that are based on graphene like Carbon Nanotube (CNT) and Carbon Nanoribbon (CNR) are the major candidate to become the silicon of the 21st century [78]. In [78, 79, 80], it was shown that Carbon Nanotube (CNT) can be used as nano dipole antenna, and Carbon Nanoribbon (CNR) as nano patch antenna for a terahertz band.

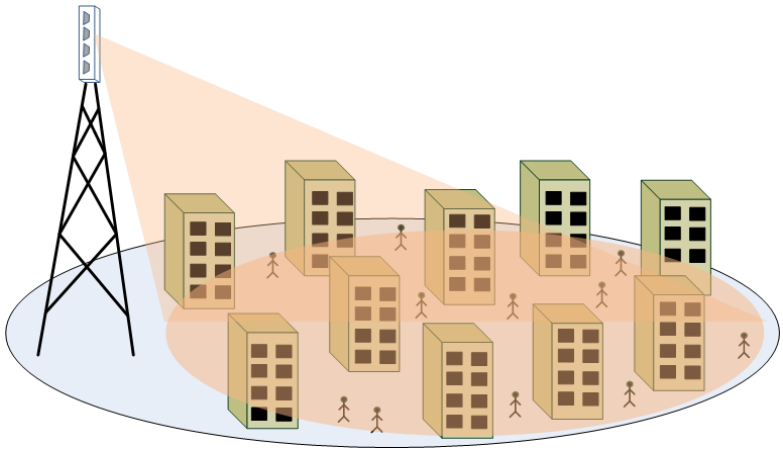

Fig.4.2 Illustration of conventional wide beam antenna.

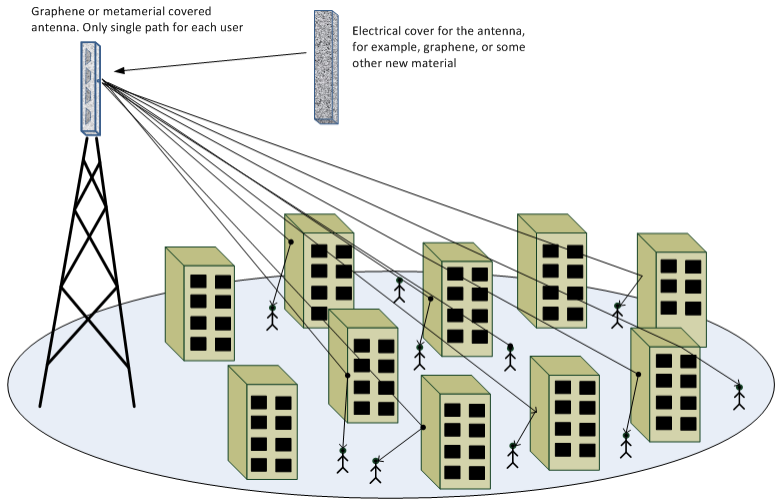

Fig.4.3 New antenna concept: a normal antenna covered with new electrical material.

A key assumption for SPMA concept is based on the expectation that new electrical materials (meta-materials, graphene, etc. [81, 82]) will be used for antenna manufacturing. This new electrical material should enable an antenna to radiate in a certain direction of interest, and prevent radiation in other unwanted directions. Such a material would act as a screen for electromagnetic (EM) radiation, restricting the propagation and creating a highly directive beam. A conventional wide beam antenna covering the cell area is shown in Fig.4.2 New antenna concept may

mean, for example, a normal base station antenna covered by a new electrical material as shown in Fig.4.3 (geometry is arbitrary). A single and independent communication path to each user can be seen in Fig.4.3. The abovementioned approach can be considered as a first generation of a advanced antenna design. Advanced technology must be developed for manufacturing such antennas. Performance of SPMA strongly depends on the directional properties of a channel such as Direction of Departure (DoD), Angle of Departure (AoD), Direction of Arrival (DoA) and Angle of Arrival (AoA), and it needs to be accurately estimated.

4.3. 3D ray tracing

Ray tracing techniques have been extensively employed as a theoretical prediction tool, and for the characterization of the radio propagation environment. Determination of multipath components between the transmitter and receiver is the first step towards the computation of a received electric field or power at the receiver. By using ray tracing techniques based on Shoot and Bouncing Ray (SBR), or Image Theory (IT) algorithm, possible multipath components can theoretically be found between each Transmitter/Receiver locations. In SBR algorithm, a large number of rays are launched with constant angular separation between neighboring rays from the transmitter. Next, intersection and reception tests need to be performed on each ray to determine the valid rays between the transmitter and a receiver. Moreover, the separation angle between the rays has major impact on the accuracy of SBR algorithm. In general, Image Theory is more accurate, precise and rigorous in comparison with SBR, as it can found all possible ray path components with finite reflections and diffractions without redundancies [83]. However, the determination of multipath components by image based ray tracing may require large computation time as it requires computing the children of images, and the level of computation increases with the increase in number of supported reflections and diffractions [83, 84, 85].

4.4. Simulations with 3D ray tracer in MATLAB

MATLAB was used as a simulation tool for implementing an indigenous 3D ray tracer based on Image Theory (IT) algorithm. Unlike a quasi three dimensional environment, transmitter height was set above the height of buildings so that diffraction from the rooftops can be supported. Simulations with ray tracing were performed in 3D arbitrary environment to show the preliminary requirements of the new proposed antenna concept, and to highlight the requirements of an extremely narrow directed beam to avoid unwanted multipath components. All available multipath components with maximum of four reflections and two diffractions, single rooftop diffraction and single ground reflection were studied, and analysis was done to select only a single strong path, not necessarily the strongest one but an appropriate multipath in the direction of interest.

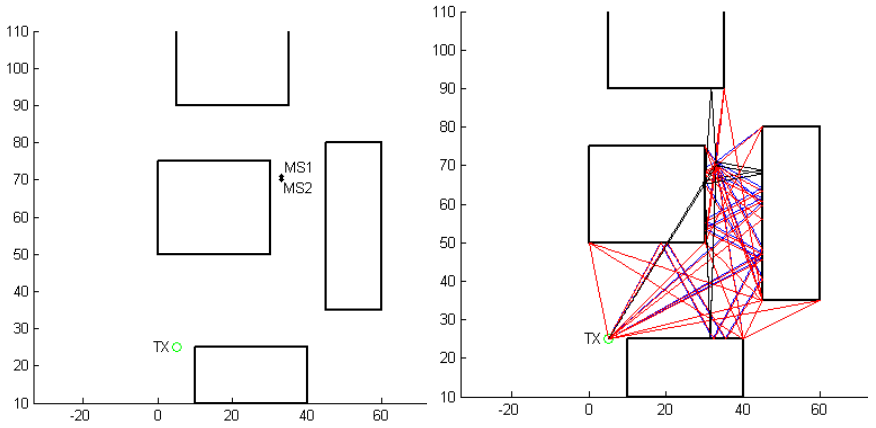

(a) (b)

Fig.4.4 (a) NLOS radio propagation channel between base station, and two mobile stations MS1 and MS2 (b) Multipath propagation in 2D environment.

In order to show the degree of independence between two geographical locations 1m apart from each other as shown in Fig.4.4(a), the power, DoD, AoD, and AoA of received multipath components were analyzed. Fig.4.4(b) shows the multipath components in 2D environment, whereas Fig.4.5 shows the multipaths components in 3D environment.

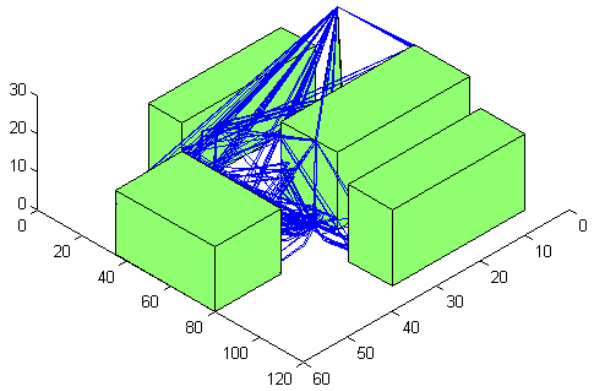

Fig.4.5 Multipath propagation in 3D environment.

Fig.4.6 shows the amplitude and angle of departure (AoD) of the ten strongest multipath components of MS1 and MS2 against the direction of departure (DoD), at transmitting end. For each geographical location, AoD along with DoD of interested multipath components defines the narrow beamwidth of the transmitting antenna for each particular user. Fig.4.6 shows that the strongest multipath component for MS1 has 41.5° of DoD with 71.3° of AoD, whereas for MS2 the strongest multipath has 40.87° and 71.13° of DoD and AoD, respectively. Strongest multipath components for MS1 and MS2 were separated by 0.63° and 0.17° in the horizontal and vertical plane, respectively.

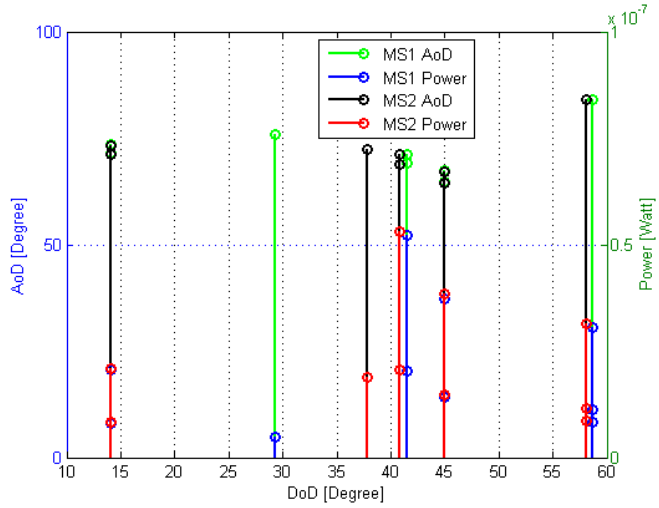

Fig.4.6 Amplitude and AoD of 10 strongest multipaths against DoD

The deep analysis of the results presented in Fig.4.6 for MS1 shows that at the base station with respect to strongest multipath component (41.5° of DoD), the closest and second closest unwanted multipaths are radiated at 45° and 29.30°, respectively. For MS2 with respect to strongest multipath component (40.87° of DoD), the closest and second closest unwanted multipaths are radiated at 37.81° and 45°, respectively. Therefore, it would be more appropriate for the base station using SPMA to serve MS1 using DoD of strongest multipath and MS2 using DoD of second strongest multipath.

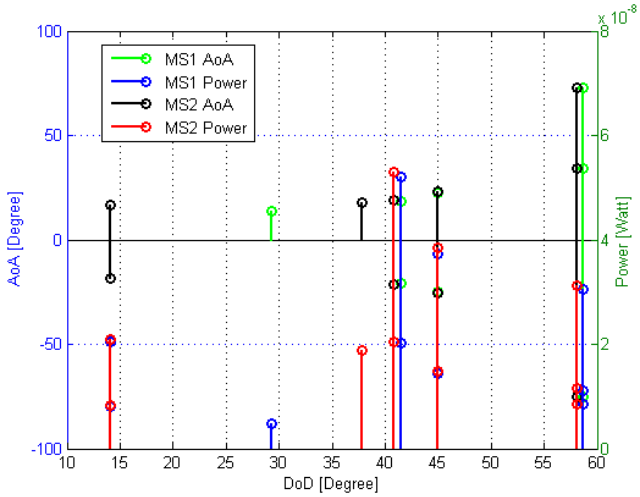

Fig.4.7 Amplitude and AoA of 10 strongest multipaths against DoD

Fig.4.7 shows the amplitude and angle of arrival (AoA) of the ten strongest multipath components of MS1 and MS2 against the direction of departure (DoD), at receiving end. For each multipath component at any DoD, there exist two AoA values; positive value representing a free space signal without hitting the ground, and a negative value representing a ground reflected path. In Fig.4.7, only the ten strongest multipath components are shown, therefore at some DoD instants AoA with negative values are missing. If a selected multipath for two mobile stations has very small separation in an azimuth plane, then a free space path can be selected for one mobile station and a ground reflected path for the other mobile station to keep the two multipaths independent from each other. The results presented in this section were taken from publication [P8].

5. SUMMARY AND CONCLUSIONS

Frequency spectrum is a scarce resource, and base stations have always limited radio resources. In cellular communication, efficient utilization of radio resources is clearly needed to be able to provide high system capacity, low probability of no data transfer, low speech blocking probability and enhanced user experience with minimum network deployment cost. Results presented in this thesis showed that UMTS900 deployment provides the solution to high deployment cost, and it not only gives better coverage in comparison with UMTS2100, rather if it is deployed as an overlay with UMTS2100 then it also helps in enhancing the network capacity, both for the voice traffic and data traffic.

In the first part of the thesis, a smart traffic handling is proposed for mixed traffic in a multilayer network. The analysis of the results presented in this thesis showed that a smart traffic handling scheme helps in balancing the load among the layers in multilayer network, and makes an efficient use of the capacity layers i.e., GSM1800 and UMTS2100 and coverage layers i.e., GSM900 and UMTS900. The idea of using GSM900 and UMTS900 as an overlay with GSM1800 and UMTS2100 as an underlay was maintained by smart traffic handling strategy, and the performance of smart traffic handling scheme improves with an additional layer of UMTS900. In UMTS system, load balancing and optimum distribution of traffic among different layers helps in keeping the NodeB power of the coverage layer at low level, which minimizes the interference to neighbour cells. Smart traffic handling scheme provides better system capacity with low speech blocking probability, and low probability of no data transfer in comparison with random layer selection strategy. The proposed power allocation scheme for HSDPA system presented in the thesis optimally utilizes the power resources to enhance the user throughput, especially for the cell edge users. It was also learned that DC-HSDPA with sophisticated power allocation scheme offers better

data rates compared to conventional DC-HSDPA without any power allocation strategy.

The simulation results presented in the second part of the thesis endorsed the fact that the use of adaptive MIMO switching leads to the efficient utilization of the dual-transmission antennas, and provides a better result than any other individual antenna transmission mode. A noticeable gain was observed by AMS in small cells as well as in large cells. LTE with AMS offers significant improvement in average cell throughput and probability of no data transfer compared to LTE with spatial multiplexing only. Performance of advanced antenna techniques like switched beam antenna and full adaptive beam antenna was also investigated in this thesis. It was found that macro cell capacity can be significantly improved by deploying smart antennas. A multiple switched beam antenna showed better performance compared with a single beam antenna, but inferior to an adaptive beam antenna.

This thesis provided performance comparison of traditional hexagon layout types for different order of sectorization with new alternative layouts based on regular tessellations. Novel "Snowflake" and "Flower" layouts were introduced in this thesis for 6-sector and 12-sector sites, respectively. A wide range of system simulations have been performed to analyze the performance of different network layouts at different intersite distances and antenna beamwidths. The post simulation analysis reveals that optimized network layouts offer better SINR and system throughput compared to traditional hexagonal layout. The simulation results revealed that the average cell SINR does not deteriorate much by having a higher order of sectorization, if antenna beamwidths are chosen accordingly. Higher order sectorization does not improve much the cell (sector) capacity, but definitely offers higher site capacity. It is also highlighted in this thesis that to avoid the deployment of small cells, higher order sectorization with optimized network layout can be considered as an alternate choice.

It is proposed in the third part of the thesis that to meet the requirement of 5G cellular network, a comprehensive and integrated "Single Radio" antenna design with centralized baseband processing is needed with extraordinary computational power. A novel single radio

antenna design with controlled emission should be able to adaptively adjust its beam, power, spectrum and capacity with respect to the user demand and changing environmental condition. A novel concept of Single Path Multiple Access (SPMA) was introduced for gaining a multifold increase in the capacity of a centralized macro site in cellular networks. The SPMA concept can also be used for fixed radio links (microwave links) for transmission between base stations and other network elements. The results obtained by accurate image based 3D ray tracing showed the requirements of antenna pattern to enable single and very narrow directed beam. Based on the propagation simulations, around 0.55° – 0.65° separation is needed in an azimuth plane between two independent multipaths for two users at geographical locations of 1m apart from each other in NLOS macro cellular environment. Similarly, 0.1° - 0.17° separation is needed in a vertical plane.

BIBLIOGRAPHY

[1] Cisco White Paper, "Cisco Visual Networking Index: Global Mobile Data Traffic Forecast Update, 2012-2017," February 2013.

[2] Holma, H., and Toskala, A. , "LTE for UMTS - OFDMA and SC-FDMA Based Radio Access", John & Wiley Sons, 2009.

[3] Wacker, A., Laiho-Steffens, J., Sipilä, K., and Heiska, K. , "he impact of the base station sectorisation on WCDMA radio network performance," in *50th IEEE Vehicular Technology Conference (VTC)* , pp. 2611-2615, 1999.

[4] Imbeni, D., Barta, J., Pollard, A., Wohlmuth, R., and Cosimini, P., "WCDMA 6-Sector Deployment – Case Study of a Real Installed UMTS-FDD Network," in *IEEE 63rd Vehicular Technology Conference (VTC-Spring)*, vol.2, pp.703-707, 7-10 May, 2006.

[5] Huang, H., Alrabadi, O., Samardzija, D., Tran, C., Valenzuela, R., and and Walker, S., "Increasing Throughput in Cellular Network with Higher-order Sectorization," in *ASILOMAR Conference on Signals, System and Computers* , pp. 630-635, 7-10 November, 2010.

[6] Hiltunen, K. , "Comparison of Different Network Densification Alternatives from the LTE Downlink Performance Point of View," in *IEEE Vehicular Technology Conference (VTC Fall)*, pp.1-5, 5-8 Sept, 2011.

[7] Yunas, S.F., Isotalo, T., and Niemela, J. , "Impact of Macrocellular Network Densification on the Capacity, Energy and Cost Efficiency in Dense Urban Environment," *International Journal of Wireless & Mobile Networks*, vol. 5, no. 5, October 2013.

[8] Hwang, I., Song, B, and Soliman, S.S., "A Holistic View on Hyper-Dense Heterogeneous and Small Cell Networks," *IEEE Communications Magazine*, vol. 51, no. 6, pp. 20-27, June 2013.

[9] Andrews, J.G., Claussen, H., Dohle, M., Rangan, S., and Reed, M.C. , "Femtocells: Past, Present, and Future," *IEEE Journal on Selected Areas in Communications*, vol. 30, no. 3, pp. 497-508, April 2012.

[10] Stevanović, I.V., Skrivervik, A., and Mosig, J. R. , "Smart antenna systems for mobile communications", Laboratoire

d'Electromagnetisme et d'Acoustique Ecole Polytechnique Federale de Lausanne, January, 2003.

[11] Larsson, E. G., Tufvesson, F., Edfors, O. and Marzetta, T. L. , "Massive MIMO for next generation wireless systems," *IEEE Communications Magazine,* vol. 52, no. 2, pp. 186-195, Febrauary 2014.

[12] Itkonen, J., Tuszon, B., and Lempiäinen, J., "Assessment of network layouts for CDMA radio access," *EURASIP Journal on Wireless Communications and Networking,* August 2008.

[13] Boccardi, F., Heath Jr, R.W., Lozano, A., Marzetta, T.L., and Popovski, P. , "Five Disruptive Technology Directions for 5G," *IEEE Communications Magazine,* vol. n, pp. 74-80, February 2014.

[14] Huawei Technologies, "5G: A Technology Vision," White Paper.

[15] Andrews, J.G. , "Seven Ways that HetNets Are a Cellular Paradigm Shift," *IEEE Communications Magazine* , vol. 51, no. 3, pp. 136-144, March 2013.

[16] Lohi, M., Weerakon, D., Aghvami, A.H., "Trends in Multi-Layer Cellular System De-sign and Handover Design," in *IEEE Wireless Communications and Networking Conference (WCNC)*, 1999.

[17] Lempiäinen, J., Manninen, M., "UMTS Radio Network Planning, Optimization and QoS Management", Kluwer Academic Publisher, 2003.

[18] Holma, H., Toskala, A., "WCDMA for UMTS", 2004: John Wiley & Sons.

[19] Laiho, J., Wacker, A., Novosad, T., "Radio Network Planning and Optimisation for UMTS", 2nd edition 2006: John Wiley & Sons.

[20] Sipila, K., Honkasalo, K.-C., Laiho-Steffens, J., and Wacker, A., "Estimation of capacity and required transmission power of WCDMA," in *IEEE 51st Vehicular Technology Conference*, vol.2, 2000, pp. 1002-1005.

[21] Nawrocki, M.J., Dohler, M., and Aghvami, A.H., "Understanding UMTS Radio Network Modelling, Planning and Automated

Optimisation", John Wiley & Sons, 2006.

[22] Braithwaite, C., Scott, M., "UMTS Network Planning and Development: Design and Implementation of the 3G CDMA Infrastructure", Elsevier, 2004.

[23] Sheikh, M.U., Lempiainen, J., "Impact of Smart Traffic Handling Scheme on Downlink Power of UMTS Base Station in Multilayer Network," in *IEEE 3rd International Congress on Ultra Modern Telecommunications and Control Systems and Workshops (ICUMT)*, Hunagry, October, 2011.

[24] Halonen, T., Romero, J., and Melero, J. , "GSM, GPRS and EDGE Performance, Evolution towards 3G/UMTS", John Wiley & Sons, 2nd edition, 2005.

[25] Türke, U, "Efficient Methods for WCDMA Radio Network Planning and Optimization," Dissertation Universitat Bremen, 2007.

[26] Mishra, A.R., "Fundamentals of Cellular Network Planning and Optimisation – 2G/2.5G/3G Evolution to 4G", John Wiley & Sons, 2004.

[27] Lodhi, A.; Hathi, N.; Gkekas, Y.; Nahi, P., "Coverage Comparison of UMTS Networks in 900 and 2100 MHz Frequency Bands," in *IET International Conference on Wireless, Mobile and Multimedia Networks*, pp.22-25, 11-12 Jan, 2008.

[28] Nokia Solution Networks white paper, "WCDMA Frequency Refarming: A Leap Forwards Ubiquitous Mobile Broadband Coverage".

[29] Holma, H., Ahonpää, T., and Prieur, E., "UMTS900 Co-Existence with GSM900," in *IEEE Vehicular Technology Conference (VTC)*, April 2007.

[30] QUALCOMM, "UMTS900 Overview & Deployment Guideline," Revision A, November 2006.

[31] UMTS Forum white paper, "Deployment of UMTS in 900 MHz band," 2006.

[32] Laiho, J., "Radio Network Planning and Optimisation for WCDMA",

Ph.D. dissertation, Helsinki University of Technology, 2002.

[33] Rappaport, T.S., "Wireless Communications - Principle and Practice", Prentice Hall, 2nd edition, 2002.

[34] Stallings, W., "Data and Computer Communications", 8th edition: Pearson Prentice Hall, 2006.

[35] Mehrotra, A., "GSM System Engineering", Artech House Inc., 1997.

[36] Wang, B., Pedersen, K.I., Kolding, T.E., and Mogensen, P.E., "Performance of VoIP on HSDPA," in *IEEE 61st Vehicular Technology Conference (VTC 2005-Spring)*, vol.4, pp. 2335- 2339, May-1 June, 2005.

[37] Kolding, T. E., Pedersen, K. I., Wigard, J., Frederiksen, F., and Mogensen, P. E., "High Speed Downlink Packet Access: WCDMA Evolution," in *IEEE Vehicular Technology Soceity (VTS) News*, vol. 50, No. 1, pp. 4-10, February 2003.

[38] Soldani, D., Li, M., and Cuny, R., "QoS and QoE Management in UMTS Cellular Systems", John Wiley & Sons Ltd, 2006.

[39] Nihtilta, T., and Haikola, V., "HSDPA MIMO System Performance in Macro Cell Network," in *IEEE International Sarnoff Symposium*, pp 1-4, New Jersey, USA, April, 2008.

[40] De Adrande, D.M., Klein, A., Holma, H., Viering, I., and Liebl, G. , "Performance Evaluation on Dual-Cell HSDPA Operation," in *IEEE 70th International Vehicular Technology Conference (VTC Fall)*, pp 1-5, Alaska, USA, 2009.

[41] Seidel, E., and Afzal, J., "White Paper – Dual Cell HSDPA and its Future Evolution," Novel Mobile Radio Research, January, 2009.

[42] Johansson, K., Bergman, J., Gerstenberger, D., Blomgren, M. and Wallen, A. , "Multi-Carrier HSPA Evolution," in *IEEE 69th Vehicular Technology Conference (VTC Spring)* , pp.1-5, 26-29 April, 2009.

[43] Mueckenheim, J., Brueck, S., and Schacht, M. , "A Model for HSDPA Cell Load and its Application," in *IEEE 6th International Conference on 3G and Beyond*, pp 1-5, London, United Kingdom,

2005.

[44] Seo, Y.I., and Sung, D.K., "Performance of VoIP in HSDPA based on an adaptive power allocation scheme," in *IEEE Wireless Communications and Networking Conference (WCNC) 2006*, vol.4, pp.2088-2093, 3-6 April, 2006.

[45] Sesia, S., Toufik, I., and Baker, M. , "LTE, The UMTS Long Term Evolution: From Theory to Practice", John Wiley & Sons, 1st edition 2009.

[46] Astely, D., Dahlman, E., Furuskar, A., Jading, Y., Lindstrm, M., and Parkvall, S. , "LTE: The Evolution of Mobile Broadband," *IEEE Communications Magazine*, vol. 47, pp. 44-51, April 2009.

[47] Dahlman, E., Parkvall, S., and Skold, J., "4G: LTE/LTE-Advanced for Mobile Broadband", Academic Press, 2011.

[48] Roessler. A, Rohde & Schwarz, "Understanding Downlink Power Allocation in LTE," Wireless Design and Development, [Online]. Available: http://www.wirelessdesignmag.com/blogs/2011/02/understanding-downlink-power-allocation-lte. [Accessed March 2014].

[49] Salo, J., Nur-Alam, M., and Chang, K., "Practical Introduction to LTE Radio Planning," European Communications and Engineering Ltd.

[50] 3GPP TS 36.213, "Evolved Universal Terrestrial Radio Access (E-UTRA): Physical Layer Procedures," Release 8, V8.4.0, 2008-09.

[51] Wang, L. C., Chawla, K., and Greenstein, L. J., "Performance Studies of Narrow-Beam Trisector Cellular Systems," *International Journal of Wireless Information Networks*, vol. 5, no. 2, pp. 89-102, 1998.

[52] Niemelä, J., Isotalo, T., and Lempiäinen, J., "Optimum Antenna Downtilt Angles for Macrocellular WCDMA Network," *EURASIP Journal on Wireless Communications and Networking*, vol. 5, 2005.

[53] Kraus, J. D., and Marhefka, R. J., "Antennas for all applications", McGraw-Hill, 3rd ed., 2001.

[54] Kumar, S., Kovacs, I. Z., Monghal, G., Pedersen, K. I., and

Mogensen, P. E., "Performance Evaluation of 6-Sector-Site Deployment for Downlink UTRAN Long Term Evolution," in *IEEE 68th Vehicular Technology Conference (VTC)* , pp. 1-5, 2008.

[55] Niemela, J., and Lempiainen, J., "Impact of Base Station Location and Antenna Orientation on UMTS Radio Network Capacity and Coverage Evolution," in *IEEE 53rd Vehicular Technology Conference (VTC-Spring)*, vol.4, pp. 2435-2439, 2001.

[56] Jankiraman, M., "Space-Time Codes and MIMO Systems", Artech House, 2004.

[57] Sheikh, M.U., Jagusz, R., Lempiäinen, J., "LTE performance with variable number of users per transmission time interval along with AMS," in *IEEE 3rd International Congress on Ultra Modern Telecommunications and Control Systems and Workshops (ICUMT)*, 2011.

[58] Molisch, A. F. , "Wireless communications", John Wiley & Sons Ltd, 2nd edition. UK 2011.

[59] Cabrera, D., and Rodriguez, J., "Switched beam smart antenna BER performance analysis for 3G CDMA cellular communication," in *Computer Research Conference (CRC)*, Puerto Rico, April, 2004.

[60] Bhobe, A.U., and Perini, P.L. , "An overview of smart antenna technology for wireless communication," in *IEEE Aerospace Conference*, vol.2, pp. 875-883, 2001.

[61] Rani, C.S., Subbaiah, P.V., and Reddy,K.C. , "Smart antenna algorithms for WCDMA mobile communication systems," *International Journal of Computer Science and Network Security (IJCSNS)*, vol. 8, no. 7, July,2008.

[62] Hossain, S., Islam, M.T., and Serikawal, S. , "Adaptive beamforming algorithms for smart antenna systems," in *International Conference on Control, Automation and Systems (ICCAS)* , pp. 412–416, 2008.

[63] Rani, C.S., Subbaiah, P.V., and Reddy, K.C. , "LMS and RLS Algorithms for smart antennas in a CDMA mobile communication environment," *International Journal of the Computer the Internet and Management (IJCIM)*, vol. 16, no. 2, p. , May-August, 2008.

[64] Engel, J.S., "The effects of cochannel interference on the parameters of a small cell mobile telephone system," *IEEE Transactions on Vehicular Technology*, vol. 8, no. 3, pp. 110-116, 1969.

[65] Sundberg, C.E., "Alternative cell configurations for digital mobile radio systems," *The Bell System Technical Journal*, vol. 62, no. 7, pp. 2037-2066, September, 1983.

[66] Palestini, V., "Evaluation of overall outage probability in cellular system," in *IEEE 39th Vehicular Technology Conference (VTC)*, pp. 625-630, 1-3 May, 1989.

[67] Palestini, V., "Alternative frequency plans in hexagonal-shaped cellular layouts," in *IEEE 3rd International Symposium on Personal, Indoor and Mobile Radio Communications (PIMRC)*, pp. 585-590, 19-21 October, 1992.

[68] Suzuki, K., Niikura, E., and Morita. N., "A new method which optimizes frequency reuse in cellular radio systems," in *IEEE Vehicular Technology Conference*, vol. 34, pp. 322-327, 1984.

[69] Lee, W.C.Y., "Elements of cellular mobile radio systems," *IEEE Transactions on Vehicular Technology*, vol. 35, no. 2, pp. 48-56, 1986.

[70] Chheda,A., and Bassirat, F., "Enhanced Cellular Network Layout for CDMA Networks having Six-Sectored Cells," U.S.Patent 5960349, 28th September 1999.

[71] Gershman, A. B., and Sidiropoulous, N. D. , "Space Time Processing for MIMO Communications", John & Wiley Sons , 2005.

[72] Andrews, J. G., Buzzi, S., Choi, W., Hanly, S. V., Lozano, A., Soong, A. K., and Zhang, J. C., "What Will 5G Be?," *IEEE Journal on Selected Areas in Communications*, vol. 32, no. 6, p. 1065–1082, June 2014.

[73] Osseiran, A., Boccardi, F., Braun, V., Kusume, K., Marsch, P., Maternia, M., Queseth, O., Schellmann, M., Schotten, H., Taoka,H., Tullberg, H., Uusitalo, M.A., Timus, B., and Fallgren, M., "Scenarios for 5G mobile and wireless communications: the vision of the METIS project," *IEEE Communications Magazine IEEE*, vol. 52, no.

5, pp. 26-35, May 2014.

[74] NTT DoCoMo, ""“5G Radio Access: Requirements, Concept and Technologies”," White paper, 2014.

[75] Dahlman, E., Mildh, G., Parkvall, S., Peisa, J., Sachs, J., and Selén, Y., ""5G radio access”," *Ericsson Review,* vol. 91, no. 6, p. 42–48, 2014.

[76] Gomez-Diaz, J. S., and Perruisseau-Carrier,J. , "Microwave to THz properties of graphene and potential antenna applications," in *International Symposium on Antennas and Propagation (ISAP)* , pp.239-242, 29 October 2012 - 02 November 2012.

[77] Schurig, D., et al. , "Metamaterial Electromagnetic Cloak at Microwave Frequencies," *Science,* vol. 314, p. 977–980, November, 2006. DOI: 10.1126/science.1133628.

[78] Jornet, J.M. and Akyildiz, I.F. , "Graphene-based nano-antennas for electromagnetic nanocommunications in the terahertz band," in *4th European Conference on Antennas and Propagation (EUCAP)* , April, 2010.

[79] Llatser, I., Kremers, C., Chigrin, D.N., Jornet, J.M., Lemme, Cabellos-Aparicio, A., and Alarcon, E., "Characterization of graphene-based nano-antennas in the terahertz band," in *6th European Conference on Antennas and Propagation (EUCAP)* , pp.194-198, 26-30 March, 2012.

[80] Weldon, J., Jensen, K. and Zettl, A. , "Nanomechanical radio transmitter," Physica Status Solidi B, vol. 245, no. 10, pp. 2323-2325, Sept 2008 .

[81] Zhu, F., Lin,Q. , and Hu, J., "A directive patch antenna with a metamaterial cover," in *Proc. Asia-Pacific Microwave Conference Proceedings (APMC)*, vol.3, pp. 4-7, Dececember 2005.

[82] Jun, H. , Chun-seng, Y. , and Qing-chun, L. , "A new patch antenna with meta material cover," *Journal of Zhejiang University Science A* , 2005, Doi:10.1631/jzus.2006.A0089..

[83] Son, H.W., and Myung, N.H., "A deterministic ray tube method for microcellular wave propagation prediction model," *IEEE*

Transactions on Antennas and Propagation, vol. 47, no. 8, pp. 1344-1350, August, 1999.

[84] Schettino, D.N., Moreira, F.J.S., and Rego, C.G. , "Efficient Ray Tracing for Radio Channel Characterization of Urban Scenarios," *IEEE Transactions on Magnetics,* vol. 43, no. 4, pp. 1305-1308, April, 2007.

[85] Soni, S. and Bhattacharya, A. , "An efficient two-dimensional ray-tracing algorithm for modeling or urban microcellular environment," *International Journal of Electronics and Communications (AEU),* vol. 66, no. 6, pp. 439-447 , June 2012.

[86] Huawei Technologies , "“5G: A Technology Vision”," White Paper.

PUBLICATION	P1

Sheikh, M.U., and Lempiäinen, J., "UMTS900 Deployment with Different Call Handling Strategies", in *Proc. 6th IEEE International Symposium on Wireless Communication System (ISWCS)*, Tuscany, Italy, pp. 590-594, 7-10 September 2009.

UMTS900 Deployment with Different Call Handling Strategies

Muhammad Usman Sheikh, Jukka Lempiäinen

Department of Communication Engineering, Tampere University of Technology
P.O. Box 553, FIN–33101, Tampere, Finland
Muhammad.sheikh@tut.fi
Jukka.lempiainen@tut.fi

Abstract— **The target of this paper is to investigate different traffic handling strategies to increase the capacity of the network. Impact of deploying UMTS900 with other GSM900/1800 and UMTS2100 layer was also observed in terms of capacity of the network. Number of mobile users is increasing enormously, and it is expected that the demand for data services and different kind of multimedia services will grow with accelerated pace. UMTS2100 has been deployed to meet the requirement of data services. But due to higher frequency band of operation, signals at higher frequencies experience more path loss. Therefore, to provide better coverage to indoor data users more sites of UMTS2100 are required. UMTS900 deployment provides the solution for high deployment cost, and it provides the better coverage as compared to UMTS2100. The deployment of UMTS900 as an overlay with UMTS2100 also helps in enhancing the network capacity, both for the voice traffic and data traffic.**

A position and service based call handling scheme is proposed in this paper. Results of this paper show that by adopting proposed traffic handling strategy, capacity of the network can be increased.

***Index Terms*— Traffic handling strategy, UMTS900 deployment, Radio propagation, Frequency coordination**

I. INTRODUCTION

Study has revealed that in recent years, there is a significant increase in the number of users of the third generation WCDMA radio access technology. For mobile communication, WCDMA has been the widely adopted third generation air interface technology. It is expected that the trend of adopting WCDMA as radio access technology will continue to exhibit rapid growth. The target of the radio network planner is to provide the maximum coverage with the minimum number of sites and to ensure the good quality of the services. In this way cellular operator not only minimize the capital investment of the network but also bring down the operational cost of network.

Better propagation, coverage and low cost capital investment make UMTS900 deployment attractive [1]. In the existing UMTS2100 deployed area, UMTS900 can serve as an overlay to provide continuous indoor coverage to data users. Aspects regarding co-location, interference from other system, intra-operator and inter-operator interference, handovers and traffic load sharing must be considered while deploying UMTS900 system. Spectrum available for UMTS900 deployment is already occupied by GSM900, it has made the UMTS900 deployment challenging as the spectrum needs to be shared between UMTS900 and GSM900. In this kind of multilayer network, reframing part of the GSM900 band for UMTS900 requires some additional efforts in GSM frequency planning. In densely populated areas, city centers, or in metropolitan areas GSM1800 and UMTS2100 can be deployed as capacity layer and GSM900 and UMTS900 layers as coverage layer to provide better coverage [2], [3].

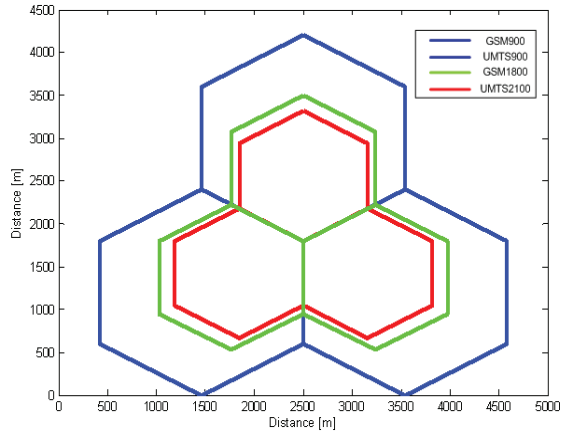

Fig.1. Hexagon shape cells with different cell boundaries.

Special attention was given on the deployment of UMTS900 network. Emphasis was given on the ways to improve and optimize coverage and to enhance capacity. The main purpose of this paper is to investigate different call handling strategies as a way to increase the total traffic handling capacity of the network. This paper presents the analysis of three different traffic handling schemes with respect to their maximum traffic handling capacity. The main parameters for capacity calculation are the blocking probability, required service quality, and the maximum number of users in an area. The studies for this paper are carried out by performing simulations on MATLAB.

The rest of the paper is organized as follows. In section II a brief description of parameters defining system capacity is presented. Section III deals with traffic handling strategies. Section IV and V is about simulation environment, simulation

parameters, simulation results and their analysis. Finally, Section VI concludes the paper.

II. Parameters Defining System Capacity

In this section, brief description of parameters affecting the capacity calculations of GSM and UMTS system are presented.

A. GSM Capacity

Capacity planning is an important process in network planning as it defines the maximum number of transceivers required at each base station and indicates the maximum traffic handling capacity of each site. The frequency reuse factor is defined as the maximum number of base stations that can be implemented before the allocated frequency band can be reused. Frequency reuse factor along with total available frequencies defines the maximum number of transceivers at each BS and hence defines the maximum capacity of site. With small reuse factor high capacity can be achieved but small reuse factors leads to high interference in system. Each transceiver has 8 time slots also known as channels. One broadcast channel (BCCH) is assumed in each sector and single standalone dedicated control channel (SDCCH) for a pair of TRX. Signaling between mobile station and base station also requires channel and remaining channels are used for carrying traffic known as traffic channels (TCH).

B. Load Equations in UMTS

The load equation approach is commonly used to compute the capacity of UMTS network in UL and DL direction. In load equations, different factors are taken into considerations which influence the capacity of network like activity factor in speech and data services, required E_b/N_0, own cell and other cell interference, number of hand overs in DL direction etc.

The main objective of capacity planning is to limit the interference from other cells to an acceptable level. Upper bound of the capacity is referred as pole capacity (N_{pole}), it defines the maximum number of allowed users in UMTS cell. Pole capacity of single UMTS cell in DL direction can be computed with the formula presented in equation (1) [4].

$$N_{pole\_DL} = \frac{W/R_b}{E_b/N_0 * v * [1-\delta] + i} \quad (1)$$

N_{pole_DL} is the pole capacity in downlink direction, W is the spreading bandwidth of the system, which is fixed by the UMTS standard at 3.84 MHz, R_b is the bit rate of offered service, E_b/N_0 is the quality requirement, v is the activity factor, δ is the measure of orthogonality between the codes in DL direction, and i is the interference factor defined as the ratio between other cell interference to own cell interference.

Pole capacity is obtained by assuming infinite transmission power of UE and interference at NodeB approaches to infinity whereas in practical system, both UE transmission power and NodeB receiver acceptable interference is limited. Thus practical cell capacity (N_{User}) is defined as the percentage of the pole capacity and that percentage is referred as loading (η), as shown in equation (2) [4].

$$N_{User} = N_{pole} * \eta \quad (2)$$

According to [5] and [6], the down link loading factor (η_{DL}) can be expressed as

$$\eta_{DL} = \sum_{j=1}^{N} \frac{(E_b/N_0)_j}{\frac{W}{R_j}} * v_j * [(1-\delta) + i_j] \quad (3)$$

C. Power Sharing in UMTS

Total available power at the base station is one of the limiting factors of downlink capacity which is known as the soft limit. There are hard limits as well like number of orthogonal codes etc., but they are not considered here. Total power needs to be shared among common control channels (CCCHs), synchronization channels (SCHs), pilot channel (CPICH), and dedicated traffic channel (DCH). Therefore, all channels' power contributes to limit the capacity in DL direction. Total time average DL transmit power (P_{Total}) is given by equation (4) [6].

$$P_{Total} = P_{CPICH} + P_{CCCH} + P_{Sync} + P_{DCH} \quad (4)$$

CPICH and CCCHs are transmitted with fixed power but the activities of CCCHs are fixed only when the traffic in a cell is constant. With a change in a load of the cell, activities of CCCHs are also changed, because if there are more call attempts in the cell then there will be more signalling required for call establishment. Therefore total power of CCCHs fluctuates with the change in loading of a cell. Total power at the base station of the cell can be computed by the formula presented in equation (5) [7].

$$P_{Total} = \frac{\eta_{DL} * P_{CCCH} + N \sum_{j=1}^{N} \frac{(E_b/N_0)_j}{\frac{W}{R_j}} * v_j * L_j}{1-\eta_{DL}} + P_{CPICH} \quad (5)$$

In equation (5), N is the total thermal noise power and L_j is the path loss of jth user between NodeB antenna and user equipment. User located near the NodeB experiences less path loss than the user located at the cell edge and therefore requires less transmission power from the base station. The dedicated channels for traffic obey power control routines and their power requirement depends upon the service profile.

D. Frequency Coordination Between UMTS900 and GSM900

UMTS was initially deployed around 2 GHz spectrum. But, better propagation, coverage and low cost capital investment make UMTS900 deployment quite attractive. The spectrum

available for UMTS900 deployment is already in use by GSM900, it has made the UMTS900 deployment challenging as the spectrum needs to be shared between UMTS900 and GSM900. In this kind of multilayer network, reframing part of the GSM900 band for UMTS900 requires some additional efforts in GSM frequency planning. Amount of spectrum for UMTS900 should be minimized so that the remaining spectrum can be used by GSM900. The nominal channel bandwidth for UMTS system is 5 MHz [3].

In coordinated deployment, GSM900 and UMTS900 are located on the same location and also perform site sharing. Adjacent channel interference is less significant in coordinated deployment, since UMTS900 and GSM900 are co-located. 3GPP recommends a carrier separation of 2.8 MHz between UMTS900 and GSM900 carrier for uncoordinated deployment [2]. However, by coordinated deployment, carrier spacing can be pushed smaller than 2.8 MHz. For deploying UMTS900 in co-existence with GSM900, the suggested frequency plan is sandwich type deployment as shown in Fig.2. In sandwich type deployment, UMTS900 carriers are placed in between GSM900 carriers of same operator and thus provide isolation between operators. In this way interference on adjacent band networks is minimized [2], [3].

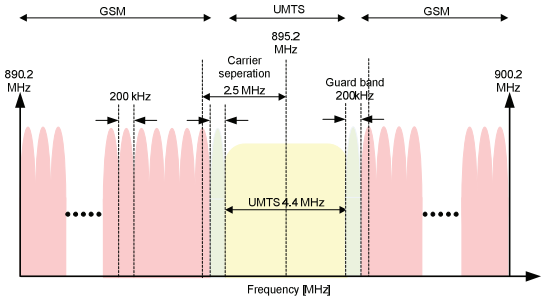

Fig.2. Frequency band division between UMTS900 and GSM900

In 10 MHz band, 5.2 MHz is reserved for GSM900 frequencies and 4.4 MHz for UMTS900 and rest of the available spectrum is used for placing guard bands. Guard bands of 200 kHz are placed at the starting and ending of UMTS900 band. The carrier seperation of 2.5 MHz between GSM900 and UMTS900 is suggested.

III. Traffic Handling Strategies

In this section three different traffic handling strategies are presented. Traffic handling scheme is set of rules according to which user is connected to any of available network layer.

A. Scheme I

All network layers i.e. GSM900/1800 and UMTS900/2100 have some maximum limit to handle traffic. This call handling strategy is very random. For speech users, on the basis of available service it can connect to any system either GSM or UMTS. Data users can only be connected to UMTS layer. User equipment chooses randomly any available layer to connect to it, and if that layer has already reached its maximum traffic handling capacity then user equipment will not search for another layer to connect and that user will be blocked.

B. Scheme II

This call handling scheme is very similar to the first one. Layer selection is also random but in this case if the first selected layer has already reached its maximum limit then, user equipment will again look for another available layer, but the reselection of other layer is again random. On the basis of available services UE will try to connect to next layer, and this procedure of reselection continues until it tries to connect all layers.

C. Scheme III

This smart call handling strategy is compact and organized one and is based on the location of the user, distance of the user from the base station and the required service type. Primarily, GSM layer is meant for speech user and UMTS layer is meant for data users. But if GSM layers reach their maximum limit then UMTS layer can also be utilized to serve speech user. Users are connected to corresponding layer on the basis of their position; if the speech user is near the base station then it is forced to connect to GSM1800 layer, as GSM1800 layer serves as capacity layer and in case if GSM1800 has reached its maximum limit, then user tries to connect to GSM900 layer. GSM900 layer serves as coverage layer for the speech users. In the case of UMTS900 deployment, UMTS2100 serves as capacity layer for data user and UMTS900 serves as coverage layer.

IV. Simulation Parameters And Environment

In this section, details about simulation environment, simulation procedure and simulation parameters are given.

A. Simulation Procedure

MATLAB was used for performing the simulation of different call handling strategies with different layers of the network e.g. GSM900/1800 and UMTS900/2100. The Okumura Hata model was used as the radio wave propagation model. The capability of each mobile to make connection to the network is calculated through iterative process. Terminals types with voice service of 12.2 kbps and data services of 384 kbps at the application layer were created. In case, where UMTS900 was deployed, users with different services e.g. voice and data were homogeneously distributed over the whole area. But, for the case without the deployment of UMTS900, distribution of data users were restricted to an area defined by the pilot coverage of UMTS2100. For GSM users, numbers of available time slots were the blocking factor whereas for UMTS, maximum downlink and uplink transmission power and cell loading were the limiting factor for finding the maximum handling capacity of the network. For UMTS base station, transmit power for each link between the base station and the user equipment is calculated on the basis of path loss between them. On the basis of traffic handling scheme, speech and data users were connected to

GSM and UMTS layers. A flow of simulation procedure in MATLAB is presented in Fig.3.

Simulation scenarios were divided into two main categories. In the simulations of first category, operator was assumed to have three mobile communication systems; GSM900/1800 and UMTS2100 and in second category impact of UMTS900 system was also included.

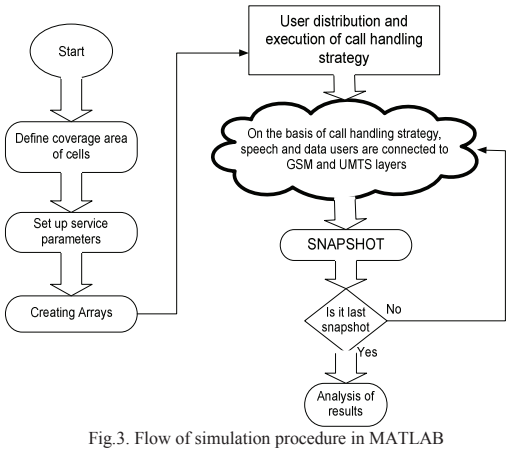

Fig.3. Flow of simulation procedure in MATLAB

B. User Distribution

Users were distributed homogenously over the area under consideration independent of the clutter information. Number of users in the cell has uniform distribution. Minimum number of speech users and data users in cell is nine and one respectively, and maximum number of users in cell depends on the blocking probability. Users in cell were uniformly distributed between the minimum and maximum number of users in cell. Similarly location of user is random, and has flat distribution over the coverage area of the cell. Total number of users per site was kept constant in each snapshot, but number of users per cell was random.

C. Simulation Parameters

General simulation parameters regarding UMTS and GSM systems are presented in Table I and Table II respectively [6].

TABLE I
GENERAL UMTS SIMULATION PARAMETERS

Parameter	Unit	Value
Downlink		
Speech E_b/N_O	dB	8
Speech activity factor		0.6
Data E_b/N_O	dB	2.5
Data activity factor		1.0
Noise figure	dB	4
BS TX P_{max}	dBm	43
Max BS TX power per connection	dBm	33
CPICH TX power	dBm	33
P_CCPCH power	dBm	30
S_CCPCH power	dBm	27
P_SCH power	dBm	30
S_SCH power	dBm	27
Max power for DCH	dBm	41.75
Uplink		
Speech E_b/N_O	dB	5
Speech activity factor		0.6
Data E_b/N_O	dB	0.5
Data activity factor		0.75
Other		
Interference factor		0.6
Orthogonality		0.65
Speech blocking probability	%	2
Data blocking probability	%	10

TABLE II
GENERAL GSM SIMULATION PARAMETERS

Parameter	Unit	Value
Max GSM900 TRXs (with UMTS900)	No.	3
Max GSM900 capacity (with UMTS900)	Channels	20
Max GSM900 TRXs (without UMTS900)	No.	4
Max GSM900 capacity (without UMTS900)	Channels	27
Max GSM1800 capacity	Channels	27

Simulations were done with different systems, and with different system settings. In Table 2, maximum GSM capacity represents number of channels available for traffic. There were total of 50 absolute radio frequency channel numbers (ARFCNs) in 10 MHz band, but due to deployment of UMTS900 only 26 ARFCNs were left for GSM900. Thirteen GSM900 carriers are present before and thirteen are present after UMTS900 as shown in Fig.2

V. SIMULATION RESULTS AND ANALYSIS

Fig.4. shows the distribution of users in the cells, and also shows the connectivity of users to different cellular layers using scheme I without UMTS900. It can be observed that in absence of UMTS900, data users were restricted to an area defined by the pilot coverage of UMTS2100, as data users were not able to make connection to GSM layer. Speech users connecting to different layers were spread over whole site area. With UMTS2100 layer only, there is large gap between the coverage of speech service and data service. Therefore, to provide continuous coverage to data users with UMTS2100 only, more sites are required.

Fig.5. shows the users distribution and their connectivity to cellular layers using scheme I with UMTS900 deployment. Due to the better coverage provided by UMTS900 for data users, the distribution of data user is not restricted to only coverage area of UMTS2100 now. Speech users connected to UMTS layers were found over whole site area. However, in case where UMTS900 was not present, speech users connecting to UMTS layer were restricted to 40% of the site area and in 60% of area they were only able to connect to GSM layers. Additional UMTS900 layer over large area helps in enhancing the network capacity.

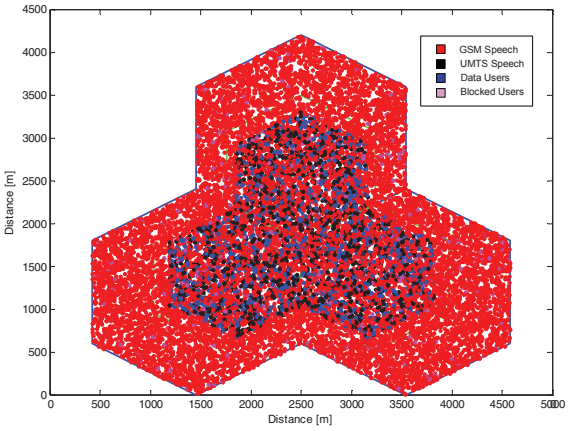

Fig.4.Distribution of users in cells (Scheme I without UMTS900)

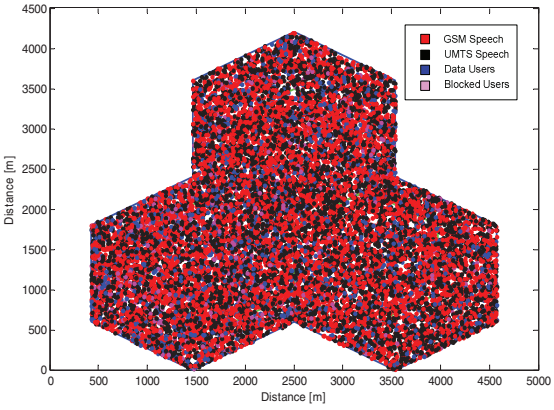

Fig.5. Distribution of users in cells (Scheme I with UMTS900)

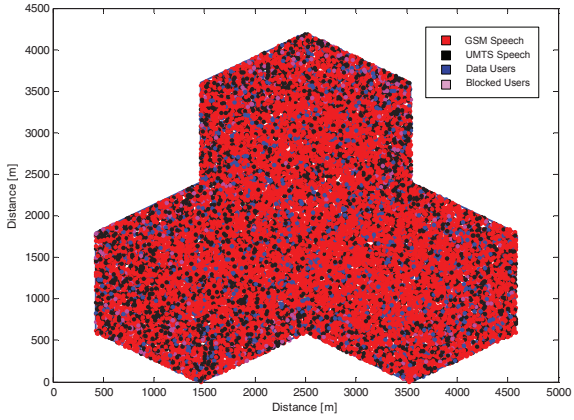

Fig.6. Distribution of users in cells (Scheme III with UMTS900)

Fig.6. shows the distribution of users, and indicates the user connectivity to different layers using scheme III along with UMTS900. It can be seen that in coverage area of GSM1800, only few speech users were connected to UMTS layers. Most of the blocked users were located between cell edges of GSM1800 and GSM900, as in that area only coverage layers were present i.e. GSM900 and UMTS900.

Results presented in Table III shows UMTS900 deployment not only improved the coverage but also helped in enhancing the network capacity. For the network without UMTS900, change in call handling strategy improves network capacity considerably. If UMTS900 is deployed with bad call handling scheme even then the capacity of the network increases but only with a small margin. Therefore to take the full advantage of UMTS900, it should be deployed with smart strategy.

TABLE III
MAXIMUM SUPPORTED USERS BETWEEN DIFFERENT SCHEMES

CASE	Speech users per site	Speech users per cell	Data users per site	Data users per cell
NO_UMTS900_SchemeI	74	42	9	5
NO_UMTS900_ SchemeII	76	45	9	5
NO_UMTS900_ SchemeIII	104	57	9	5
UMTS900_ SchemeI	76	44	11	7
UMTS900_ SchemeII	91	51	13	7-8
UMTS900_ SchemeIII	146	92	17	9-10

VI. CONCLUSION

The analysis of results shows that by deploying UMTS900 without any proper traffic handling scheme, capacity of the network increased by a small margin. The capacity of the network can be enormously increased by adopting a sophisticated call handling strategy based on the location of the user and required service type. To increase a capacity for speech users along with data users, results of simulations suggest, that UMTS900 should be implemented along with smart call handling scheme.

ACKNOWLEDGEMENT

Authors would like to thank Tampere University of Technology, FINLAND for funding the work.

REFERENCES

[1] Holma, H., Ahonpää, T., and Prieur, E., "*UMTS900 Co-Existence with GSM900"*, Vehicular Technology Conference, April 2007.
[2] UMTS Forum white paper, "*Deployment of UMTS in 900 MHz band*", 2006.
[3] QUALCOMM, "*UMTS900 Overview & Deployment Guideline*", Revision A, November 2006.
[4] QUALCOMM, *"Air Interface Cell capacity of WCDMA Systems"*, Revision B, May 22, 2007.
[5] Holma, H., Toskala, A., *"WCDMA for UMTS"*, John Wiley & Sons, 2004.
[6] Lempiäinen, J., Manninen, M., *"UMTS Radio Network Planning, Optimization and QoS Management"*, Kluwer Academic Publisher, 2003.
[7] Nawrocki, M.J., Dohler, M., and Aghvami, A.H., *"Understanding UMTS Radio Network Modelling, Planning and Automated Optimisation"*, John Wiley & Sons, 2006.

PUBLICATION	P2

Sheikh, M.U., and Lempiäinen, J., "Assessment of Smart Traffic Handling Schemes in Multimode Multiband Cellular Network" in *Wiley's Journal on Wireless Communication and Mobile Computing*, vol. 11, pp: 1618-1627, December 2011.
DOI: 10.1002/wcm.1210

PUBLICATION	P3

Sheikh, M.U., and Lempiäinen, J., "Impact of Penalty Time on Multilayer Network Along with UMTS900 Deployed with Smart Traffic Handling Scheme", in *Proc. IEEE Student Conference on Research and Development (SCOReD)*, Serdang, Malaysia, pp. 12-15,16-18 November, 2009.

Impact of Penalty Time on Multilayer Network along with UMTS900 Deployed with Smart Traffic Handling Scheme

Muhammad Usman Sheikh, Jukka Lempiäinen

Department of Communication Engineering, Tampere University of Technology
P.O. Box 553, FIN–33101, Tampere, Finland
Muhammad.sheikh@tut.fi
Jukka.lempiainen@tut.fi

Abstract— **The target of this paper is to analyze the impact of penalty time in second generation system in terms of capacity. GSM uses time slots (channels) for carrying traffic, therefore impact of penalty time was only observed in GSM system not in UMTS system. Impact of smart traffic handling scheme was also observed in terms of blocking probabilities. Due to better signal propagation condition at 900 MHz band, it is of keen interest to deploy UMTS900 with other GSM900/1800 and UMTS2100 layer. Handovers are needed to support multilayer and multimode networks e.g. using UMTS and GSM networks together. In this paper, change in overhead traffic caused by additional UMTS900 layer was also analyzed. Extensive number of handovers causes loss in network traffic handling capacity. A compact and organized smart traffic handling is given in this paper which is based on the location of the user, distance of the user from the base station and required service type. The concept of overlay – underlay configuration was also exploited in smart traffic handling scheme.**

***Index Terms*— Penalty time, Blocking probability, Traffic handling scheme, UMTS900 deployment, Radio propagation, Frequency planning**

I. INTRODUCTION

Number of mobile users is increasing enormously, and it is expected to grow with accelerated pace. GSM being the classical mobile communication system does not provide high data services and still it is being used mainly for providing services to speech users. UMTS2100 has been deployed to meet the requirement of data services. To provide coverage equal to GSM900's speech users, far more number of UMTS2100 sites are required, hence it increases the deployment cost of network. UMTS900 gives better coverage and provides a solution with low capital investment

In order to meet the high demand of services e.g. speech services and data services concept of multilayer cellular system was introduced in [2]. In multilayer network the coverage area of GSM900/1800 and UMTS900/2100 overlaps over each other. To meet the requirement of increasing traffic in hot spot areas overlay – underlay configuration is implemented [3]. The goal is to create a seamless network, where GSM and UMTS networks are integrated into a single network. Thus, fast and efficient handovers between the layers are needed [2], [3].

Main emphasis was given on finding the impact of penalty time. The percentage of traffic loss due to penalty time was observed. Impact of additional UMTS900 layer was also observed as it was supposed that addition of layer will cause more handovers and thus increase the penalty traffic. This paper also presents the analysis of two different traffic handling schemes, with and without UMTS900 layer with respect to blocking probability in the network. All simulations of this paper were done on MATLAB.

II. TRAFFIC HANDLING SCHEMES AND SIMULATION PARAMETERS

In this section two different traffic handling schemes are presented. This section also deals with the simulation environment and parameters

A. Case1: Random Layer Selection

This call handling scheme is based on random selection of layers. Speech users, on the basis of available service can be connected to any system either GSM or UMTS. Data users can only be connected to UMTS layer. User equipment chooses randomly any available layer to connect to it, and if that layer has already reached its maximum traffic handling, then user equipment again look for another available layer, but the reselection of other layer is again random. This procedure of reselection continues until it tries to connect all layers.

B. Case2: Smart Traffic Handling Scheme

This smart call handling strategy is based on the location of the user, distance of the user from the base station and the required service type. Speech users are forced to connect to GSM layers first. But if GSM layers reach their maximum limit then UMTS layer can also be utilized to serve speech user. Users are connected to corresponding layer on the basis of their position; if the speech user is near the base station then it is forced to connect to GSM1800 layer. If GSM1800 has reached its maximum limit, then user tries to make connection to GSM900 layer. GSM900 layer serves as coverage layer for the speech users. Similarly, UMTS2100 serves as capacity layer for data user and UMTS900 serves as coverage layer.

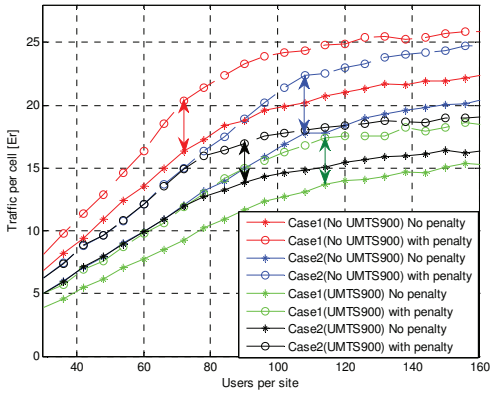

Fig.3. Difference of traffic with penalty and without penalty for GSM900

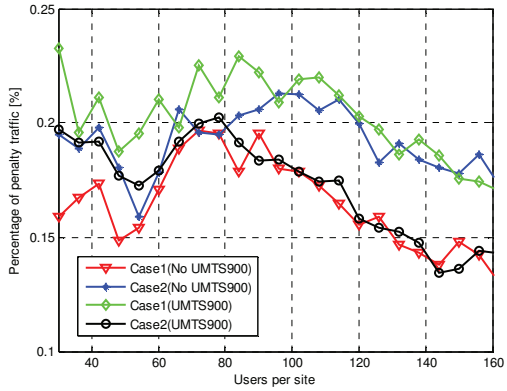

Fig.4. Percentage of penalty traffic in GSM900 layer

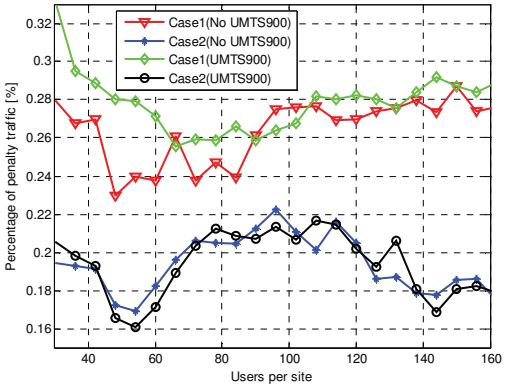

Fig.5. Percentage of penalty traffic in GSM1800 layer

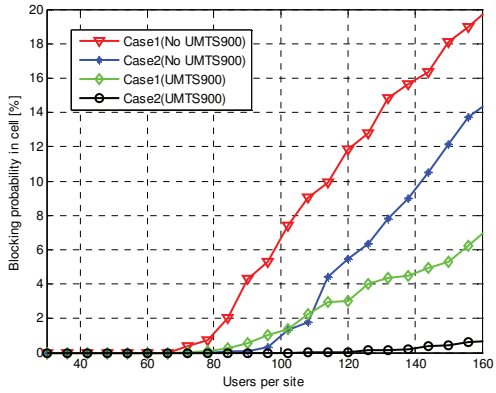

Fig.6. Speech blocking probability in cell

III. Simulation Results and Analysis

Fig.3 shows the difference between traffic without penalty and traffic including penalty time in GSM900 for different cases. Coloured two headed arrows represent the traffic difference in erlangs for their respective cases. It can also be seen from Fig.3 that for case2, loading of GSM900 layer with/without UMTS900 is identical till 72 users per site. Afterward case2 without UMTS900 has more traffic channels available for GSM900 and therefore is more loaded compared with case2 with UMTS900. Fig.4 also shows that by adopting smart traffic handling scheme, percentage of penalty traffic can also be reduced. Fig.4 also supports deployment of UMTS900 with smart traffic handling scheme. Fig.5 presents the results of penalty traffic in GSM1800 layer. Intelligent traffic scheme performs substantially better for GSM1800. Fig.6 shows blocking probability for speech users in a cell. In terms of blocking probability, top notch performance was shown by smart traffic handling scheme with UMTS900.

IV. Conclusion

The analysis of results shows, that there is overhead traffic caused by penalty time. Overhead traffic increases with the increase in users per cell due to more handovers, but the percentage of penalty traffic to total traffic reduces with increase in traffic. Addition of UMTS900 layer in multilayer network increases overhead traffic but if UMTS900 is deployed with smart traffic handling scheme then penalty traffic can be sufficiently reduced. Intelligent traffic handling scheme with UMTS900 improves speech blocking probability remarkably.

References

[1] Holma, H., Ahonpää, T., and Prieur, E., "*UMTS900 Co-Existence with GSM900"*, Vehicular Technology Conference, April 2007.

[2] Lohi, M., Weerakon, D., Aghvami, A.H., "*Trends in Multi-Layer Cellular System Design and Handover Design*", Wireless Communications and Networking Confierence,1999.WCNC. 1999 IEEE.

[3] Lempiäinen, J., Manninen, M., *"Radio Interface System Planning for GSM/GPRS/UMTS"*, Kluwer Academic Publisher, 2001.

[4] QUALCOMM, *"UMTS900 Overview and Deployment Guideline"*, Revision A, November, 2006.

[5] Sheikh, M.U., Lempiäinen, J., *"UMTS900 Deployment with Different Call Handling Strategies"*, IEEE International Symposium on Wireless Communication Systems. 2009. ISWCS'09 (Accepted, To be published in September, 2009.

PUBLICATION	P4

Sheikh, M.U., Jagusz, R., and Lempiäinen J., "Performance Evaluation of Adaptive MIMO Switching in Long Term Evolution", in *Proc. IEEE 7th International Wireless Communication and Mobile Computing (IWCMC'11) Conference*, Istanbul, Turkey, pp. 866-870, 4-8 July 2011.

Performance Evaluation of Adaptive MIMO Switching in Long Term Evolution

Muhammad Usman Sheikh[1], Rafał Jagusz[1,2] , Jukka Lempiäinen[1]

[1] *Department of Communication Engineering, Tampere University of Technology, Finland*
[2] *West Pomeranian University of Technology Faculty of Electrical Engineering, Szczecin, Poland*
Muhammad.Sheikh@tut.fi, Rafal.Jagusz@tut.fi, Jukka.Lempiainen@tut.fi

***Abstract*— In a race towards 4G technologies, future cellular network like Long Term Evolution (LTE) is competing with high data rates and improved spectrum efficiency. The target of this paper is to evaluate performance of Adaptive MIMO Switching (AMS) in LTE in terms of cell throughput and throughput gain with respect to other antenna configuration. The impact of different intersite distance on the performance of AMS was also investigated in this paper. The assessment was based on simulations using analytical channel model. Kronecker channel model without any Channel State Information (CSI) at transmitter was used for the simulation purposes. Adaptive MIMO switching works on the principle of switching among transmit diversity, receive diversity, and spatial multiplexing in accordance to SINR level. Simulation results reveal that significant improvement in cell throughput can be achieved by applying AMS technique. However, utilization of standard MIMO transmission techniques also improves channel capacity.**

***Keywords*— Adaptive modulation and coding, Adaptive MIMO switching, Long term evolution, Channel capacity**

I. INTRODUCTION

Cellular networks with Single-Input-Single-Output (SISO) systems offer limited channel capacity. Nowadays, interactive services are able to produce sufficient network traffic to create bottlenecks at radio interface. Multi Input Multi Output (MIMO) stands for multiple number of antennas at transmitter and receiving side. In transmit diversity multiple antennas are used at transmitting side; in receive diversity multiple antennas are used at receiver side. Transmit and receive diversity helps in improving the signal to interference noise ratio, but it does not directly improves the throughput [1]. Spatial multiplexing is another form of MIMO system, in which independent data stream are sent on each transmit antenna, roughly doubling the throughput.

LTE system is categorized as an evolved cellular network and MIMO is important feature of LTE system. LTE uses Orthogonal Frequency Division Multiple Access (OFDMA) in downlink and Single Carrier-Frequency Division Multiple Access (SC-FDMA) in uplink direction [2]. Mentioned access schemes can significantly improve spectral efficiency, but multiple antenna transmission further improves the spectral efficiency. LTE can be considered as a system with high spectral efficiency as a result of flexible radio interface [3].

In this paper MIMO transmission modes can be distinguished as transmit diversity with single receiving antenna (TD), receive diversity using Maximum Ratio Combining (MRC), and spatial multiplexing (SM) with equal number of multiple antennas at transmitting and receiving side. Transmit diversity is a basic MIMO setup, where each antenna is transmitting the same copy of data [2]. In MRC, the signals from the independent channel are combined at the receiver. Each branch signal is multiplied by weight factor such that branch with strong signal is further amplified, while weak signals are attenuated to provide better SINR. Third case is of SM, it means that each antenna is transmitting independent and different data stream. With SM data rates can be improved with higher efficiency comparing with TD and MRC [2].

This paper provides comparison between different transmission modes with different modulation and coding schemes. Emphasis was given on finding the average cell throughput in LTE, with different transmission modes. Performance of AMS with different intersite distance was investigated. Aim of this paper was to highlight the gain achieved by AMS. Research work of this paper was carried out by performing simulations in MATLAB environment.

The rest of the paper is organized as follows. Section II deals with LTE system features. In section III, detail about Shannon capacity, channel model along with channel capacity is presented. Description of simulation environment and simulation parameters is given in section IV. Section V is about simulation results and their analysis. Finally section VI concludes the paper.

II. LTE SYSTEM FEATURES

In this section, brief description of adaptive modulation and coding schemes, multiple antenna configuration, LTE physical layer, and adaptive MIMO switching is presented.

A. LTE Physical Layer

Essential improvement introduced in LTE system are new system access techniques i.e. OFDMA and SC-FDMA adopted in downlink and uplink directions, in reference to prior cellular system. It supports different bandwidth ranging from 1.25MHz to 20MHz, while sub-carrier spacing of 15 kHz remains constant [2]. Flexible bandwidth deployment made LTE system an attractive choice for the operators. Radio resources are being assigned to users dynamically which leads to higher flexibility.

Radio resources are allocated in reference to user demand. Resource block is considered as grid in time and frequency domain. Smallest data unit which can be allocated to a single user is a pair of resource block. Resource Block (RB) consists of 12 consecutive subcarriers in frequency domain for half ms in time domain. The transmission time interval (TTI) is one ms for LTE. There is parallel transmission of data with multiple subcarriers in downlink direction [3], [4].

In uplink transmission, as mentioned previously, SC-FDMA is used. This approach sustains low level of Peak to Average Power Ratio (PAPR) [4]. MU-MIMO transmission can be used in uplink direction as virtual multiple antenna transmission.

B. Adaptive Modulation and Channel Coding Rate

The data rate is adjusted by changing the modulation scheme and the channel coding rate. The process of adjusting the modulation scheme and coding rate is adaptive to instantaneous channel condition. Modulation and coding schemes used in LTE system have direct impact on the amount of transmitted data. Straightforward way to provide high data rates over band limited system is to use high order modulation. In downlink direction three main modulation schemes are in use: QPSK, 16QAM and 64QAM with certain channel coding rate. In uplink direction 64QAM is supported by only category V user equipment [2]. Coding rate shows the amount of bits used for channel coding purpose. Lower order modulation scheme e.g. QPSK is more robust to the errors comparing with higher order modulation schemes. Therefore, higher order modulation such as 64QAM can be employed only when the channel conditions are good and have high signal to interference noise ratio. Modulation and coding schemes with their respected spectral efficiency used for the simulation purpose of this paper are presented in Table I.

TABLE I. MODULATION AND CHANNEL CODING RATE

Modulation Scheme	Channel Coding Rate	Spectral Efficiency [bps/Hz]
QPSK	1/3	0.67
QPSK	1/2	1.0
QPSK	2/3	1.33
QAM16	1/2	2.0
QAM16	2/3	2.67
QAM16	5/6	3.33
QAM64	2/3	4.0
QAM64	5/6	5.0

C. Multiple Antenna Configurations

Adaptive modulation and coding schemes, reduced transmission time interval (TTI) and advanced medium access technique helps in improving the spectral efficiency of LTE system. Still, spectral efficiency of the system can be further improved by multi antenna technique (MIMO). Previously advanced reception and transmission diversity techniques were implemented in UMTS. Reception diversity with single transmitting antenna is known as Single Input Multiple Output (SIMO) system [1]. Transmission with multiple antennas on transmitting end and single antenna at receiving end is known as Multiple Input Single Output (MISO) system, which is an example of transmit diversity [1]. Interference between the antennas can be significantly reduced by applying spatial separation between antennas. Spatial separation between the antennas may decrease the correlation factor between the received signals coming from different antennas. In this paper, MIMO system with the same number of antennas on each transmitting and receiving side are considered as MIMO with spatial multiplexing (SM).

D. Adaptive MIMO Switching

To cope with increasing user demand of throughput, additional advanced antenna techniques are required from cellular systems. Adaptive MIMO switching (AMS) is a scheme of switching among different antenna transmission mode to maximize the user throughput with improved coverage and quality of service (QoS) [4]. In radio environment, channel conditions are continuously changing, transmission mode is selected by switching from diversity to spatial multiplexing or vice versa to provide maximum throughput. The target of AMS is to efficiently utilize the radio resources, maximizing the spectral efficiency. When the user experiences high signal to interference noise ratio e.g. near the eNodeB, spatial multiplexing is used and diversity techniques are used for the users at cell edge or with low SINR value. SINR threshold value for switching between the transmission modes depends upon the throughput [4].

III. CHANNEL CAPACITY

This section deals with capacity formulation for different antenna transmission modes.

A. Shannon Capacity

Shannon's capacity mathematical formula presented in equation (1) is the basis for the research work of this paper. Shannon capacity theorem defines the theoretical upper bound for the maximum rate of data transfer considering white Gaussian noise. It states that channel capacity is proportional to the bandwidth W, and a logarithmic function of signal to noise power ratio SNR. It also shows that data rates are limited by the noise power [6].

$$C = W * log_2(1 + SNR) \quad (1)$$

If we consider bandwidth equals to 1 Hz, then equation (1) gives us the spectral efficiency of the channel as bits per second per hertz (bps/Hz). Shannon provided upper bound for capacity with respect to additive white Gaussian noise (AWGN) however practical channels differ much from the characteristics of AWGN channel. Shannon's formula needs to be reconsidered for Rayleigh fading channel. Actual capacity of network is always less than Shannon capacity [6].

B. Kronecker Channel Model

Kronecker channel model is analytical channel model and belongs to the family of random channel matrix model. This model is applied to radio channels where Channel State Information (CSI) is not known at the transmission side. Propagation mechanism in the Kronecker model considers signal scatters located in the vicinity of transmitter and receiver [5]. Rayleigh fading is often used to model the non line of sight (NLOS) channel assuming scatters near the transmitter and receiver. Channel matrix is modelled by the Kronecker product of transmit and receive covariance matrix. MIMO channel can be modelled by Kronecker as given in equation (2) [5].

$$H = R_R^{1/2} * H_{IID} * (R_T^{1/2})^T \quad (2)$$

In equation (2), R_T and R_R are the transmit and receive covariance matrices respectively, $(.)^T$ performs the transpose operation of matrix. H_{IID} is a random fading MIMO channel matrix whose entries are independent and identically distributed (i.i.d). Each entry has Gaussian distribution with zero mean and unit variance. Kronecker model is inaccurate compare to Weichselberger model but simpler regarding computation [5].

C. Channel Capacity for Transmission Modes

In random matrix models all the factors affecting the input output relationship of the MIMO system are put together in random matrix H. Factors like fading, interference between transmit and receive antennas, constructive and destructive interference caused by physical obstacles are taken into account while modelling the channel. Without CSI at transmitter, assuming equal power at all transmitting antennas, MIMO channel capacity can be given by the equation (3)

$$C_{Gen} = \min(M_T, N_R) * log_2 det\left(I_{N_R} + \frac{E_x}{M_T \sigma^2} H R_{xx} H^H\right) \quad (3)$$

In equation (3), C_{Gen} represents capacity of general MIMO channel when CSI is unknown at the transmitter. Total average energy at the transmitter side is denoted by E_x, and it is equally divided among all transmit antennas. M_T and N_R represents number of transmission and receive antennas respectively. H represents random channel matrix where H^H is Hermitian's transposition of matrix H. I_{N_R} refers to identity matrix, whereas R_{xx} stands for covariance matrix at transmitter. Average Gaussian noise power is expressed by σ^2. Assuming perfect flat channel, with unity covariance matrix and total transmission power is equally divided among all transmit antennas, equation (3) can be transformed for different transmission mode as [7]

$$C_{SISO} = C_{MISO} = log_2 det\left(1 + \frac{E_x}{\sigma^2}\right) \quad (4)$$

$$C_{SIMO} = log_2 det\left(1 + \frac{E_x * N_R}{\sigma^2}\right) \quad (5)$$

$$C_{MIMO_{nxn}} = n * log_2 det\left(1 + \frac{E_x}{n * \sigma^2}\right) \quad (6)$$

From equation (4) it can be seen that MISO system does not offer any increase in capacity, because there is no diversity at the receiver. At one time only one data pipe is active, and transmission power is equally divided among all transmit antennas [7]. However, MRC helps in improving the SINR which practically increases channel capacity as seen in equation (5). Equation (6) shows that ideally capacity can be doubled compare to SISO system by increasing 3 dB transmission power in case of 2 transmit and receive antennas. In equation (6), n is the number of transmit and receive antennas [7].

IV. Simulation Environment and Simulation Parameters

MATLAB was used as simulation tool for performing simulations for the research work of this paper. Impact of different antenna transmission modes over the throughput of LTE system with different intersite distance was analyzed. These simulations were done with seven sites, with three cells on each site. Single site was interfered by six other sites. Users with full traffic buffer were assumed i.e. they always have data to transmit. Every user tries to get as much throughput as possible. Cell resources were equally divided among all active users in cell, leaving no unused resources at any TTI. Therefore cell loading of 100% was assumed along with 100% other cell loading in neighboring cells. Number of users supported in any TTI was fixed, and users were homogenously distributed over the cell area. Location of users was random, with flat distribution over the coverage area of the cell. COST231 Hata model was used as radio propagation model for calculating the path loss between the user and the eNodeB. Only modulation and coding schemes presented in Table I were assumed for simulation purpose. General parameters of LTE used for the simulation are presented in Table II.

TABLE II. General LTE Simulation Parameters

Parameter	Unit	Value
Downlink		
Area type		Urban
Operating frequency band	MHz	2600
Bandwidth	MHz	20
Carrier spacing	kHz	15
Total resource block (RB)	No.	100
Transmission power	dBm	43
Antenna gain	dBi	18
Antenna height	m	25
Cyclic prefix		Normal
Number of users per TTI	No.	5
Cell loading	%	100
UE noise figure	dB	8
Data activity factor		1

V. Simulation Results and Analysis

In Fig.1 required SINR value against spectral efficiency per antenna for different antenna configuration is shown. For more than one antenna at transmit side, same modulation and coding scheme was assumed for all antennas. SIMO and MISO are providing receive and transmit diversity respectively. MIMO2x2 and MIMO4x4 are working on the principle of spatial multiplexing. It can be seen that SIMO system performs best in low SINR condition among all other antenna configurations. MISO system performs very similar to SISO system as total transmission power was divided between the transmit antennas; therefore advantage of channel gain is not significant. MIMO 4x4 has highest SINR requirement and works well in good SINR condition. In adaptive MIMO switching, different antenna configuration is selected on the basis of achieved maximum throughput.

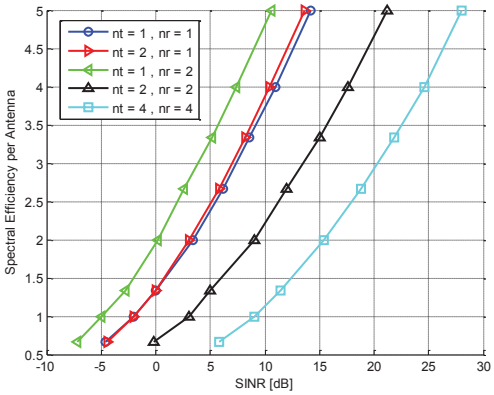

Fig.1. Required SINR for different MCS with different transmission modes

In Fig.2 average cell throughput against intersite distance for different antenna configuration is shown. It can be seen that the average cell throughput achieved by using AMS is better than average cell throughput by any individual antenna configuration. In Fig.2 AMS2x2 considers adaptive MIMO switching with maximum two antennas at transmitting and receiving side, with AMS4x4 maximum of 4 transmit and receive antennas were considered. Average cell throughput achieved by SIMO system was found similar to MIMO2x2, while keeping the total transmission power fixed and constant in both cases. In Fig.2 highest cell throughput was achieved with lowest intersite distance. By analyzing the results presented in Fig.2 it was found that by increasing the intersite distance average cell throughput is decreased.

In Fig.3 relative throughput gain for different antenna configurations against intersite distance is shown. Relative throughput gain with respect to single input and single output (SISO) system is plotted in Fig.3. It was found that although average cell throughput achieved by AMS decreases with increasing intersite distance as shown in Fig.2, but relative throughput gain increases with increasing intersite distance. It can be seen by adopting spatial multiplexing with two transmit and receive antennas (MIMO2x2), relative throughput gain does not improve by 100% with respect to SISO system. Only 20% gain was observed by adopting spatial multiplexing for MIMO2x2 with 1000m intersite distance. With AMS2x2 and AMS4x4 relative gain of 50% and 75% can be achieved respectively at 1000m intersite distance. It was found that AMS performs better with large intersite distance

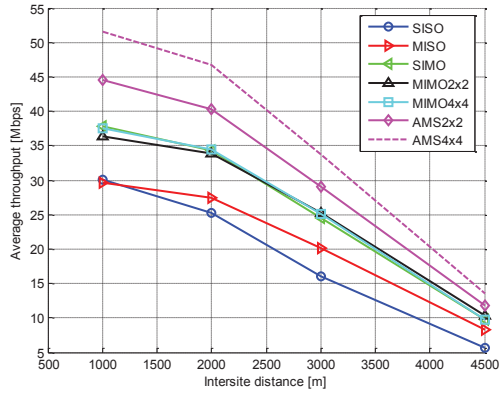

Fig.2. Average throughput of cell against ISD for different transmission mode

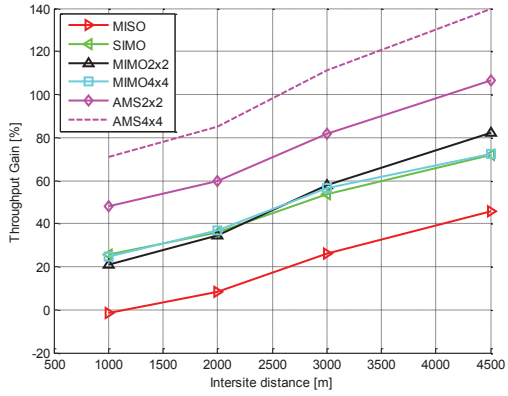

Fig.3. Relative throughput gain against ISD for different transmission mode

Fig.4 shows the cumulative distribution functions (CDF) of cell throughput for different intersite distances, achieved by using adaptive MIMO switching (AMS) with maximum two antennas at transmitting and receiving side in LTE system. There is high probability of no data transfer with large intersite distance, because of limited transmission power at eNodeB for downlink direction. Better results are achieved with smaller intersite distance. Probability of having cell throughput above 50Mbps is 34%, 23%, 9.5% and 1.5% with 1000m, 2000m, 3000m and 4500m correspondingly. Mean value of cell throughput with AMS for different intersite distance can be seen from Fig.4

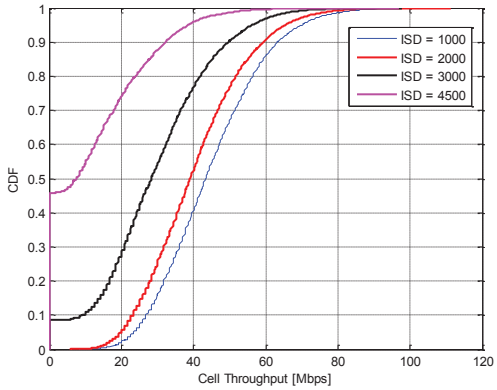

Fig.4. CDF plot of AMS 2x2 throughput for different ISD

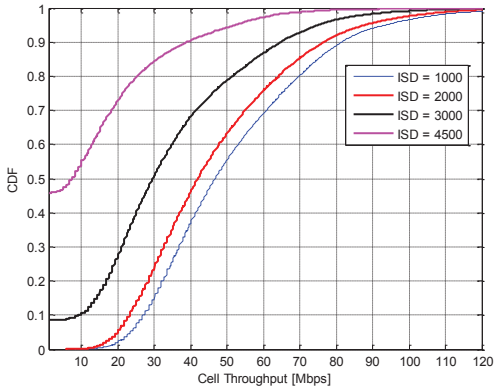

Fig.5. CDF plot of AMS 4x4 throughput for different ISD

Fig.5 shows the cumulative distribution functions (CDF) of cell throughput for different intersite distances, achieved by using adaptive MIMO switching (AMS) with maximum four antennas at transmitting and receiving side in LTE system. By comparing results presented in Fig.4 and Fig.5 it was found that upper part of CDF curves of throughput with different intersite distances shifts to right in Fig.5, which shows enhanced throughput results with AMS4x4 compare to AMS2x2. Performance of AMS4x4 is similar to AMS2x2 in low SINR condition, actual throughput gain from AMS4x4 is attain in good SINR condition.

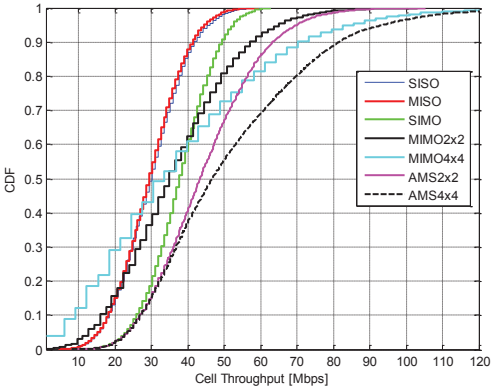

Fig.6. CDF of throughput with 1000m ISD for different transmission mode

Fig.6 shows the cumulative distribution functions (CDF) of cell throughput with 1000m intersite distance for different antenna configuration in LTE system. CDF of cell throughput for MISO system seems to follow the similar behaviour when compared with SISO system. But performance of SIMO was found better. It can be seen that the activation of adaptive MIMO switching enhances the cell throughput significantly. Effective utilization of spatial multiplexing in good SINR condition and exploiting diversity techniques in bad SINR condition improves the overall cell throughput by adaptive MIMO switching. Probability of having cell throughput above 30Mbps is 57% with MIMO4x4, whereas probability of having cell throughput above 30Mbps is 86% with adaptive MIMO switching. Similarly, probability of having throughput above 70Mbps is only 12%, 5.5%, and 20%with MIMO4x4, AMS2x2 and AMS4x4 respectively.

VI. Conclusion

Adaptive modulation and coding scheme along with multiple antennas transmission improves spectral efficiency, but the analysis of results shows that average cell throughput can be further enhanced by adopting adaptive MIMO switching. Significant improvement in cell throughput was observed with AMS. It was found that average cell throughput decreases but the relative throughput gain achieved by AMS increases with the increase in intersite distance. A noticeable gain was observed by AMS in small cells as well as in large cells. AMS efficiently utilizes the radio resources, and improves the overall spectral efficiency of LTE system.

Acknowledgement

Authors would like to thank Tampere University of Technology, Finland and European Communications Engineering Ltd for supporting this research work.

References

[1] M., Jankiraman, *"Space-Time Codes and MIMO Systems"*, Artech House, 2004

[2] S. Sesia, I. Toufik, M. Baker., *"LTE, The UMTS Long Term Evolution: From Theory to Practice"*, John Wiley & Sons, 1st edition 2009.

[3] D. Astely, E. Dahlman, A. Furusk¨ar, Y. Jading, M. Lindstrm, and S. Parkvall, "*LTE: The Evolution of Mobile Broadband*", IEEE Communications Magazine, vol. 47, pp. 44-51, April 2009.

[4] H. Holma., A. Toskala., "*LTE for UMTS - OFDMA and SC-FDMA Based Radio Access*", John & Wiley Sons, 2009.

[5] A. B. Gershman., and N. D. Sidiropoulous., *"Space Time Processing for MIMO Communications"*, John & Wiley Sons, 2005.

[6] J.G. Proakis, "*Digital Communications"*, McGraw-Hill, New York, 2001.

[7] A.J. Paulraj, D.A. Gore, R.U. Nabar, H. Bölcksei "*An overview of MIMO Communications – A Key to Gigabit Wireless*", Proceedings of the IEEE, vol. 92 no. 2, pp. 198-218, February 2004

PUBLICATION	P5

Sheikh, M.U., and Lempiäinen J., "Performance Analysis of Dual-Cell HSDPA plus MIMO and LTE along with Adaptive MIMO Switching at Cellular Level", *in Elsevier Journal on Physical Communication (Special Issue),* vol. 9, pp. 288-298, December 2013.
DOI: 10.1016/j.phycom.2012.07.002

PUBLICATION	P6

Sheikh, M.U., and Lempiäinen J., "A Flower Tessellation for Simulation Purpose of Cellular Network with 12-Sector Sites" in *IEEE Wireless Communications Letters*, vol.2, no.3, pp.279-282, June 2013.
DOI: 10.1109/WCL.2013.022213.120861

A Flower Tessellation for Simulation Purpose of Cellular Network with 12-Sector Sites

Muhammad Usman Sheikh, Student Member IEEE & Jukka Lempiäinen, Senior Member IEEE
Department of Communication Engineering, Tampere University of Technology
P.O.Box 553, FIN-33101, Tampere Finland
Muhammad.Sheikh@tut.fi, Jukka.Lempiainen@tut.fi

Abstract— This paper presents a novel network tessellation for 12-sector site deployment called "Flower" topology for use in cellular network simulations. The aim of this paper is to study the impact of higher order sectorization and perform a comparison of different network tessellations for Dual Cell HSDPA (DC-HSDPA) network. Throughput and Signal to Interference plus Noise Ratio (SINR) at different Intersite Distance (ISD) were used as merits of performance. It was found that at 1000m ISD, flower topology for 12-sector sites offers 7.2% and 210% relative throughput gain with respect to traditional hexagon layout for 12-sector and 3-sector sites deployment, respectively.

Index Terms— Dual cell high speed downlink packet access, Sectorization, Network tessellation, Network capacity, Intersite distance

1 INTRODUCTION

In future, new advanced mobile services with different Quality of Service (QoS) and high data rate requirement will demand a high capacity from cellular network. Spectral efficiency of a system can be increased by employing spatial multiplexing through multiple antennas [1]. However, the successful reception of dual stream transmission requires good SINR condition, Performance of spatial multiplexing transmission is not homogeneous over the entire cell area in macrocellular environment [1]. Idea of Dual-Cell HSDPA (DC-HSDPA) was floated by 3GPP in

Release 8, to provide homogeneous capacity gain for each user over cell dominance area. In DC-HSDPA, two single carriers of HSDPA each of 5MHz is aggregated, and simultaneously the resources of both carriers are allocated to single user with the help of joint scheduler [2].

Mobile operators generally use macro cells with wide beam antennas for umbrella coverage, but future capacity demands cannot be fulfilled by using them only. The spectral efficiency of a system can be improved through "Sectorization", dividing the site coverage area spatially into multiple sectors and reusing the radio resources in each sector [3]. Normally, single site is divided into 3 sectors, having equally spaced antennas in azimuth plane with difference of 120^0. In this paper, 6-sector and 12-sector site deployment is referred as an example of higher order sectorization. In order to avoid the installation of new sites due to high operational costs, and to improve the capacity of cellular network, implementing high order sectorization within the existing site can be considered as a possible cost effective solution [4].

For initial site selection plan in cellular network system simulations, regular network tessellations are used. Regular network layout is based on geometric shapes, fulfilling the criterion of providing continuous coverage. Network tessellation is defined by the location of sites, order of sectorization, azimuth direction, and beamwidth of antenna. Earlier studies showed the network layouts based on hexagon for 3-, 6-, and 12-sector sites deployment [5-6]. The performance of cloverleaf layout for 3-sector site was found better than hexagonal layout [5]. However, for higher order of sectorization, cloverleaf layout cannot be used and new tessellation is needed to combat the problem of interference. The results presented in [5-6] indicate that 6-sector traditional hexagon tessellation offers better coverage and enhanced capacity compared to 3-sector site deployment. An optimum tessellation for 6-sector site is presented in [7], in which

antenna of each sector is oriented in such a way that they are not facing each other. The authors of this paper call that layout as “Snowflake” layout.

The impact of higher order sectorization has been previously studied in [3-7], however no study on optimum network tessellation for 12-sector is available in open literature. This paper introduces a novel network layout called “Flower” tessellation for 12-sector site deployment, and also presents the performance analysis of enhanced tessellation for 6-sector site given in [7]. The target of this research work is to learn about the possible gain of using higher order sectorization in macrocellular environment. This paper highlights the advantage of adopting optimum network tessellation, and presents the performance comparison of traditional hexagonal layout with cloverleaf, snowflake and flower topology for 3-, 6-, and 12-sector sites respectively. The research work of this paper was done by performing simulations in MATLAB environment.

II THEORY

This section deals with the theoretical aspects sectorization, network tessellation, and antenna selection for sectors.

A. High order sectorization

For a macrocellular network without extensive capacity demand, 3-sector site is a practical solution. However, for the case of high capacity requirement, 3-sector sites are not able to fulfil the purpose and new sectors needs to be added. Adding another carrier in the same sector is not a viable solution for the mobile operators having only one carrier. High order sectorization is a promising technique for enhancing the site capacity without building additional sites and is therefore a good solution for hot spot areas [6]. Six-sector sites and 12-sector sites are example of high order sectorization. Performance of high sectorization depends upon the half power beamwidth of the antenna in horizontal plane, with optimum beamwidth antenna 6-sector site not

only provide better coverage but also provide significant capacity enhancement compared to 3-sector sites [8].

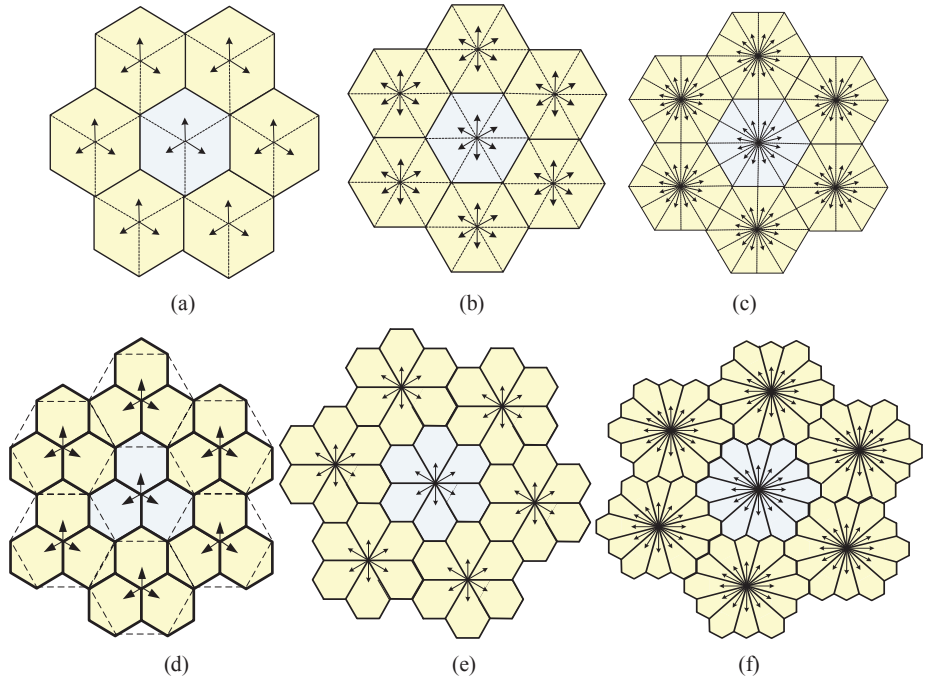

Fig.1. Cellular network layouts. (a) 3-sector hexagon, (b) 6-sector hexagon, (c) 12-sector hexagon, (d) 3-sector cloverleaf, (e) 6-sector snowflake, and (f) 12-sector flower layout

B. Introduction to cellular network layouts

To learn about the system behavior in different radio conditions, preliminary cellular system performance is evaluated through link and system level simulation ns. For making a nominal plan of sites for simulation purpose, it is generally assumed that the sites have regular network layout. Tessellations use geometric shapes i.e. hexagon, triangle, square etc. to create a continuous plane and a regular grid like structure. These tessellations can be used as a basis for selecting the position of nominal sites [5].In literature, there are several definitions for the regular layout, but the most commonly used shape for cellular network is “Hexagon”. Hexagonal layout for 3-, 6-, and 12-sector site is shown in Fig.1 (a-c) respectively Cloverleaf layout for 3-

sector site shown in Fig.1(d) was presented in [5], and was found better then 3-sector hexagonal layout. To enhance the performance of 6-sector site, an optimized network layout is presented in [7], in which sectors do not face each other and hence reduce the impact of other cell interference. Authors of this paper call the tessellation for six-sector site presented in [7] as "Snowflake" topology. Fig.1(e) shows the orientation of sectors and site location of snowflake topology. Finally, a novel tessellation for 12-sector site is shown in Fig.1(f). This layout for 12-sector site is named as "Flower" topology due to shape of the site dominance area.

C. Antenna selection and its beamwidth

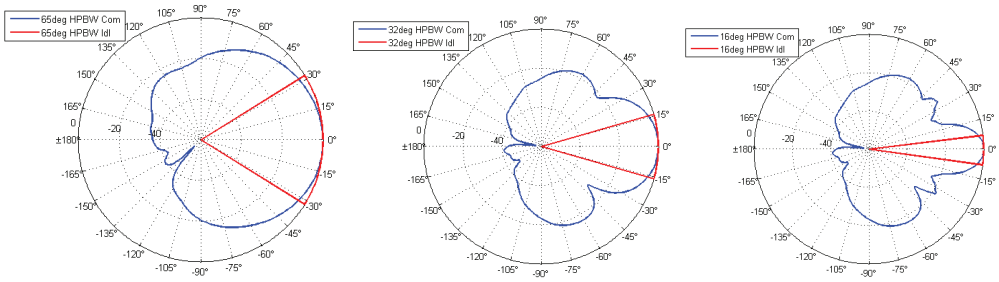

Fig.2. Radiation patterns of ideal and commercial antennas. (a) 65^0, (b) 32^0, and (c) 16^0 HPBW antenna

Antenna configuration i.e. height, azimuth, beamwidth and radiation pattern has deep impact on cell capacity, and therefore selection of optimum antenna is of much importance [8]. Ideal sectored antenna has flat response within the sector and zero response outside the sector. For ideal sectored antenna there is no overlapping between the sectors of same site and hence there is no intersector interference [3]. Practically it is not possible to achieve ideal sector response, and each sector receives co-channel interference from the neighbour sectors of the same site as well as from other sites. Wide HPBW of antenna leads to large sector overlapping and will cause interference leakage to neighbour cell, which in turn will reduce the system capacity. Fig.2(a-c) depict the ideal sector response and the radiation pattern of commercially available 65^0, 32^0, and 16^0 HPBW antennas, respectively. For the research work of this paper, HPBW of antennas were

scaled proportionally to the number of sectors per site i.e. 3-. 6-, and 12-sector sites were implemented with 65^0, 32^0, and 16^0 HPBW antennas, respectively.

III System Simulations and results Analysis

A single site in the middle interfered by two tiers of interferers i.e. 18 sites at equal intersite distance was considered for simulation purpose. All sites are assumed to have same antenna height and equal maximum transmit power. The scenario studied assumes macrocellular urban environment with data users having full traffic buffer, homogeneously distributed over the whole cell area. Flat terrain was assumed and Okumura-Hata path loss model was used for estimating the path loss between the user and NodeB, and lognormal distribution with 6dB standard deviation was used to model shadowing. Code orthogonality factor is modelled with Gaussian curve having maximum value of 0.97 at site location and 0.7 at cell edge, instead of average orthogonality factor value. Out of total 16 codes, maximum of 15 codes are available for allocating to the users at physical layer level. The simulator supports multiple users (5 users) per TTI with code multiplexing, and allocates equal number of codes to the active users in cell.

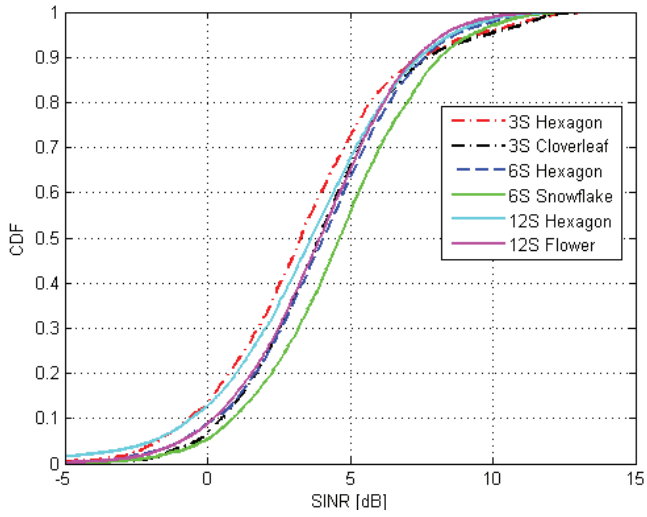

Fig.3. CDF of cell SINR at 1000m ISD with 5 users per TTI.

Fig.3 shows the CDF of cell SINR value for DC-HSDPA system with 5 users per TTI at 1000m ISD. In each iteration of Monte Carlo simulation, average SINR value over the cell is obtained by adding the linear SINR value of each user then dividing the sum by the number of users served per TTI. As seen from the results in Fig.4, the contribution of lower SINR level (less than 0dB) is over 13% by 3- and 12-sector hexagon layout, however with cloverleaf and flower layout it is brought down to 7% and 9%, respectively. It can be seen that improvement in cell SINR is not proportional to increasing order of sectorization. Migrating from 3-sector to 6-sector improves the cell SINR but shifting from 6-sector to 12-sector strategy deteriorates cell SINR. It was found that 6-sector deployment with snowflake topology outperforms and offers highest mean cell SINR of approximately 4.6dB and gives a gain of around 0.6dB compared to 6-sector hexagon tessellation. Similarly, improvement in cell SINR is also evident by cloverleaf and flower layout for 3- and 12-sector sites respectively, compared to traditional hexagon layout.

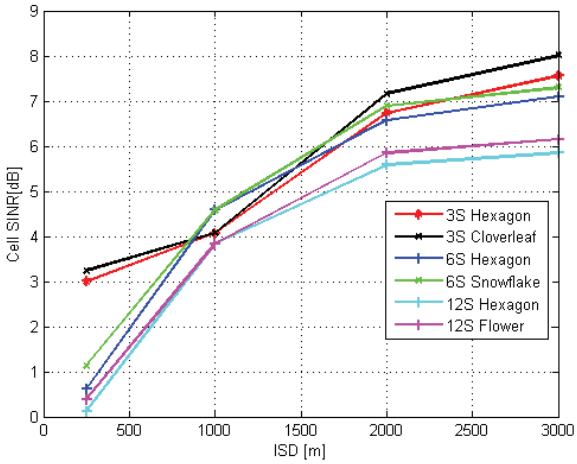

Fig.4. Mean cell SINR of different layouts against intersite distance.

Fig.4 shows the attained mean cell SINR for different network layouts against different intersite spacing. The trend of the curves shows that cell SINR improves by increasing the intersite distance. Small intersite distance corresponds to small cells, where high interference is caused by

the near located neighbor cells and limits the user SINR. Irrespective of the ISD, 12-sector layout offers lowest cell SINR.

TABLE I. STATISTICAL ANALYSIS OF ACHIEVED THROUGHPUT

	Mean cell throughput (Mbps)	*Relative cell throughput gain (%)*	*Mean site throughput (Mbps)*	*Relative site throughput gain (%)*
ISD = 250 meter				
3S Hexagon	7.93	**0**	23.79	**0**
3S Cloverleaf	8.13	**2.52**	24.39	**2.52**
6S Hexagon	6.25	**-21.19**	37.50	**57.62**
6S Snowflake	6.74	**-15.06**	40.44	**69.99**
12S Hexagon	5.85	**-26.23**	70.20	**195.23**
12S Flower	6.15	**-22.44**	73.80	**210.21**
ISD = 1000 meter				
3S Hexagon	9.86	**0**	29.58	**0**
3S Cloverleaf	10.90	**10.55**	32.70	**10.55**
6S Hexagon	10.74	**8.93**	64.44	**117.85**
6S Snowflake	11.72	**18.86**	70.38	**137.93**
12S Hexagon	10.05	**1.92**	120.60	**307.7**
12S Flower	10.77	**9.23**	129.24	**336.92**
ISD = 2000 meter				
3S Hexagon	14.54	**0**	43.62	**0**
3S Cloverleaf	15.49	**6.53**	46.47	**6.53**
6S Hexagon	14.38	**-1.1**	86.28	**97.79**
6S Snowflake	15.10	**3.86**	90.60	**107.29**
12S Hexagon	12.84	**-11.7**	154.08	**253.23**
12S Flower	13.67	**-5.99**	164.04	**276.06**
ISD = 3000 meter				
3S Hexagon	15.48	**0**	46.44	**0**
3S Cloverleaf	16.58	**7.11**	49.74	**7.11**
6S Hexagon	15.01	**-3.03**	90.06	**93.92**
6S Snowflake	15.63	**0.97**	93.78	**101.93**
12S Hexagon	13.15	**-15.05**	157.8	**239.8**
12S Flower	14.06	**-9.17**	168.72	**263.31**

The results presented in Fig.5 highlights the gain of adopting proper network layout and spotlight the advantage of using higher order sectorization. It was found that at a small ISD i.e. 250m, impact of network layout is less significant, but the benefit of using optimum layout becomes prominent at large intersite spacing. Maximum gain of optimized network layouts for 3-, 6-, and 12-sector sites was found at 1000m ISD. It was learned that cloverleaf layout provides approximately 10.5%, snowflake offers 9% and flower layout tenders approximately 7.2% better throughout compared to hexagon layout for 3-, 6- and 12-sector sites respectively. Statistical

analysis of sector and site throughput along with relative gain with respect to 3-sector hexagon layout is presented in Table I.

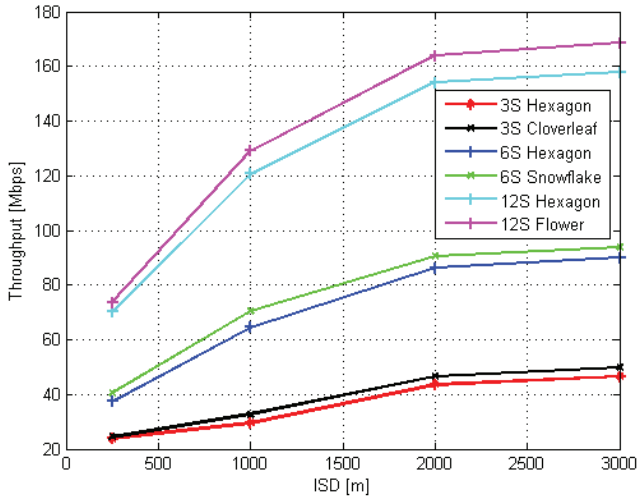

Fig.5. Mean site throughput for different layouts against intersite distance.

IV Conclusion

This paper introduced a regular network layout called flower tessellation for 12-sector site deployment, and provides the performance comparison of cloverleaf and snowflake topology with hexagon layout. Post simulation analysis reveals that optimized network layouts offer better system throughput compared to traditional hexagon layout. For the purpose of cellular network simulations, flower topology can be considered as a basis for selecting a site location and sector azimuth direction, due to its enhanced performance in offering better SINR and throughput. The relative capacity gain of cloverleaf topology is about 2.5-10.5%, of snowflake topology 4-9%, and of flower layout is approx. 5-7.2% over hexagon layout, depending on intersite spacing. Simulation results show that adding a new sector at small ISD degrade the cell quality. To avoid the deployment of small cells, high order sectorization with optimized network layout can be considered as an alternate choice.

ACKNOWLEDGMENTS

Authors would like to thank Tampere University of Technology and European Communications Engineering (ECE) Ltd. and Tampere Doctoral Program of Information Science and Engineering (TISE) for supporting the research work of this paper.

REFERENCES

[1] Nihtilta, T., and Haikola, V. *"HSDPA MIMO System Performance in Macro Cell Network",* IEEE International Sarnoff Symposium. April, 2008, pp 1-4, New Jersey, USA.

[2] Bonald, T., Elayoubi, S.E., El Falou, A., Landre, J.B., *"Radio Capacity Improvement with HSPA+ Dual-Cell"*, IEEE International Conference on Communications (ICC), 2011, pp.1-6, 5-9 June 2011.

[3] Huang, H., Alrabadi, O., Samardzija, D., Tran, C., Valenzuela, R., and and Walker, S., "*Increasing Throughput in Cellular Network with Higher-order Sectorization",* ASILOMAR Conference on Signals, System and Computers, pp. 630-635, 7-10 November 2010.

[4] Kumar, S., Kovacs, I. Z., Monghal, G., Pedersen, K. I., and Mogensen, P. E.,*"Performance Evaluation of 6-Sector-Site Deployment for Downlink UTRAN Long Term Evolution",* IEEE 68th Vehicular Technology Conference (VTC), 2008-Fall., pp. 1-5.

[5] Itkonen. J., Tuzson. B., Lempiäinen. J., *"Assessment of Network Layouts for CDMA Radio Access"*, EURASIP Journal on Wireless Communications and Networking, 2008.

[6] Imbeni. D., Barta. J., Pollard. A., Wohlmuth. R., and Cosimini. P., *"WCDMA 6-Sector Deployment – Case Study of a Real Installed UMTS-FDD Network"*, IEEE 63rd Vehicular Technology Conference (VTC), Spring-2006, vol.2, pp.703-707, 7-10 May 2006

[7] A. Chheda, F. Bassirat, *"Enhanced Cellular Network Layout for CDMA Networks having Six-Sectored Cells"*, U.S.Patent 5960349, 28th September 1999.

[8] Niemela. J. and Lempiainen. J., *"Impact of Base Station Location and Antenna Orientation on UMTS Radio Network Capacity and Coverage Evolution",* IEEE 53rd Vehicular Technology Conference (VTC), Spring-2001, vol.4, pp. 2435-2439, 2001.

PUBLICATION	P7

Sheikh, M.U., Lempiäinen J., and Ahnlund, H., "Advanced Antenna Techniques and High Order Sectorization with Novel Network Tessellation for Enhancing Macro Cell Capacity in DC-HSDPA Network", in *AIRCC International Journal of Wireless & Mobile Networks (IJWMN)*, vol. 5, no. 5, pp. 65-84, October 2013.
DOI: 10.5121/ijwmn.2013.5505

ADVANCED ANTENNA TECHNIQUES AND HIGH ORDER SECTORIZATION WITH NOVEL NETWORK TESSELLATION FOR ENHANCING MACRO CELL CAPACITY IN DC-HSDPA NETWORK

Muhammad Usman Sheikh[1], Jukka Lempiainen[1] and Hans Ahnlund[2]

[1]Department of Communications Engineering, Tampere University of Technology
[2]European Communications Engineering Ltd, Tekniikantie 12, Espoo Finland

ABSTRACT

Mobile operators commonly use macro cells with traditional wide beam antennas for wider coverage in the cell, but future capacity demands cannot be achieved by using them only. It is required to achieve maximum practical capacity from macro cells by employing higher order sectorization and by utilizing all possible antenna solutions including smart antennas. This paper presents enhanced tessellation for 6-sector sites and proposes novel layout for 12-sector sites. The main target of this paper is to compare the performance of conventional wide beam antenna, switched beam smart antenna, adaptive beam antenna and different network layouts in terms of offering better received signal quality and user throughput. Splitting macro cell into smaller micro or pico cells can improve the capacity of network, but this paper highlights the importance of higher order sectorization and advance antenna techniques to attain high Signal to Interference plus Noise Ratio (SINR), along with improved network capacity. Monte Carlo simulations at system level were done for Dual Cell High Speed Downlink Packet Access (DC-HSDPA) technology with multiple (five) users per Transmission Time Interval (TTI) at different Intersite Distance (ISD). The obtained results validate and estimate the gain of using smart antennas and higher order sectorization with proposed network layout.

KEYWORDS

System capacity, Sectorization, Advanced antenna techniques, Switched beam antenna, Adaptive antenna, Dual Cell High Speed Downlink Packet Access.

1. INTRODUCTION

Rising trend of packed switched traffic and high capacity requirement in mobile networks have urged the researchers to think about new antenna designs and possible network layouts for future cellular networks. Current and future capacity demands of next generation mobile networks cannot be achieved by using traditional macro cells only. It has been noted several times that macro cells are not able to offer high data rates homogeneously over the entire cell area, and most of the network capacity is lost due to interference coming from the neighbor cells. The increasing demand of new advanced mobile services with different Quality of Service (QoS) requirement in cellular systems has led to the development and evolution of new technologies. Concepts of micro cells and femto cells have been proposed to improve the system capacity in high density traffic areas [2]. However, to reduce the fixed costs such as electricity, transmission, rentals etc., adding new cells and sites should be avoided. Maximum capacity utilization of macro cells should be

DOI : 10.5121/ijwmn.2013.5505

guaranteed by adopting new network tessellation and by employing possible advanced antenna solutions, including smart antennas. Smart antennas have gained enormous popularity in the last few years, and have been able to grab the attention for its ability to improve the performance of cellular systems [3].

Moreover, cell and system capacities are related to network layout, antennas deployment techniques, orientation and beamwidth of antennas. Directional antennas with optimum electrical or mechanical tilt are used to get required coverage with minimum interference [2]. Antenna configuration i.e. antenna height, azimuth, radiation pattern and beamwidth has deep impact on cell capacity [4– 6]. Different network tessellations have been compared in [7], and it was noted that for 3-sector sites, cloverleaf layout offers the lowest interference level, and thus should have the best cell and system capacity for macro cells. Thus, cloverleaf is a good basis for nominal planning of mobile networks with 3-sector sites. However, for higher order of sectorization, cloverleaf layout cannot be used and new tessellation is needed to combat the problem of interference. Base station antenna configuration needs to be optimized to attain minimum inter cell interference [1], [8]. The conventional cellular concept approach uses fixed beam position with wide beamwidth. Whereas, advanced approach of smart antenna employs multiple narrow beams and beam steering for each user in a cell. Adaptive algorithms form the heart of antenna array processing network. The processor based on different beamforming algorithms does the complex computation for beamforming [9]. Achieved user SINR and user throughput strongly relies on interference management and inter-cell interference avoidance [10]. Handovers between cells due to mobility of user, and software features have their own impact on cell capacity. However, this research work does not deal with these issues.

Over the last decade, services like multimedia messaging, video streaming, video telephony, positioning services and interactive gaming have become an integral part of everyday life. These services are the driving force in reshaping the cellular technologies. Universal Mobile Telecommunication System (UMTS) has been the most popular choice for 3G mobile communication systems, but UMTS had challenges in meeting the requirement of high data rate services. High Speed Downlink Packet Access (HSDPA) was for first time introduced in Release 5 of 3GPP specifications [8], [10]. The evolution of HSDPA continued and later in Release 8, the concept of Dual Cell HSDPA was floated in which the radio resources of two adjacent HSDPA carriers were aggregated with the help of joint scheduler. The main target of DC-HSDPA was not only to improve the user's throughput in the close vicinity of base station rather it also enhances the user's throughput homogeneously over whole cell area. DC-HSDPA offers theoretical peak data rate of 42 Mbps, improved spectral efficiency, and enhanced user experience with low delays or latency [8], [11].

In this paper user's SINR value, average SINR over the cell, mean cell throughput, mean site throughput, user's throughput and user's probability of no data transfer will be taken as merits of performance. Statistical analysis with 10^{th}, 50^{th}, 90^{th} percentile, and mean value is also presented in this paper. The rest of the paper is organized as follows. Section II deals with theoretical aspects of cell capacity. Section III explains different antenna techniques. Description of simulation tool and environment, simulated cases, and simulation parameters is presented in section IV. Simulation results and their analysis are given in section V. Finally, section six concludes the paper.

2. CELLULAR THEORY

2.1. Interference and Cell Capacity

Theoretical maximum cell capacity can be estimated by Shannon capacity equation (bits/s) for Additive White Gaussian Noise (AWGN) channel as given in equation (1), [1], [4]

$$C = Wlog_2\left(1 + \frac{S}{N}\right) = Wlog_2\left(1 + {E_bR}/{N_0W}\right) \qquad (1)$$

where W is the bandwidth available for communication, S is the received signal power which can be denoted as energy per information bit E_b, multiplied with the information rate R. A variable N is the noise power impairing the received signal. The noise power can be defined as noise spectral density N_0 multiplied with the transmission bandwidth W. Signal to Noise ratio (S/N) can be extended to Signal to Interference plus Noise Ratio (SINR) by including interference from own cell and also co-channel interference coming from neighbor cells. HSDPA is a WCDMA based network, and the total interference is a sum of three interference sources; own (serving) sector signals, other site/sector signals, and thermal noise. In downlink direction, the total interference I_{DL} for any particular user at a given location is given by equation (2), [8]

$$I_{DL} = I_{other} + I_{own} + P_N \qquad (2)$$

$$I_{other} = \sum_{i=1}^{k} \frac{Pt_i}{L_i} \qquad (3)$$

$$I_{own} = \frac{(Pt_S - S_j)}{L_S} * (1 - \alpha) \qquad (4)$$

In equation (2), P_N is a thermal noise power. In equation (3), I_{other} is the total received power from other sectors of the network, and is a sum of other cells interfering sources. Pt_i is a total transmit power and L_i is a path loss for i^{th} neighbor cell. In equation (4), I_{own} is the total received interference from own sector, where Pt_S and L_S are the total transmit power and path loss respectively of serving cell. Where S_j is the received power of HS-PDSCH of the j^{th} user from the serving NodeB. α denotes orthogonality factor. Orthogonality is a measure for level of interference caused by own sector signals. For perfectly orthogonal DL channelization codes α is equals to 1. In HSDPA technology, code orthogonality is partly lost ($\alpha < 1$) in wireless radio environment due to multipath propagation [8], [12]. The ratio of I_{other}/I_{own} is a commonly used measure of sector overlap and interference in the network layout. The SINR represents the quality of the received signal. In the downlink direction the receiver input, SINR is defined as

$$SINR_{DL} = \frac{S_j}{I_{other} + I_{own} + N} \qquad (5)$$

2.2. Network layouts and inter cell interference

In initial nominal plan for mobile network, regular network layouts are used for guidance on selection of nominal site location, order of sectorization, and azimuth direction. There is triangular, square, and hexagonal tessellation for 3-sector site, but the most commonly used tessellation is cloverleaf layout as shown in [7]. These tessellations are chose to form continuous coverage of the mobile network. In Fig1a, cloverleaf layout is shown, that is formed by using hexagonal geometry of cell. In cloverleaf layout, all the interfering sites of the first tier of

interferer are pointing at the null of serving site. Authors of this paper propose a name "Snow Flake" layout for the enhanced cellular network tessellation for six sector site presented in [13]. Snow flake tessellation is shown in Fig1b. This paper presents a novel network layout for 12-sector site, as shown in Fig.1c and calls it as "Flower" layout. SINR calculations include own cell and neighbor cell interference as given in equation (5). These interferences are related to propagation loss i.e. path loss L_S and L_i between serving NodeB and interfering NodeBs respectively. Especially inter cell interference depends heavily on chosen network layout i.e. how base stations are deployed in a network, antenna configuration, and azimuth. Network layout has significant impact on interference management and hence on capacity of macrocellular network. One way to compare different network layouts or different antenna configurations is to compare the interference coming from neighbor cells to serving cells. It has been shown in [7] that for 3-sector sites, cloverleaf is the most defensive for interference and thus provides high capacity gain. In this article, for 3-sector sites only cloverleaf layout is considered for network simulations.

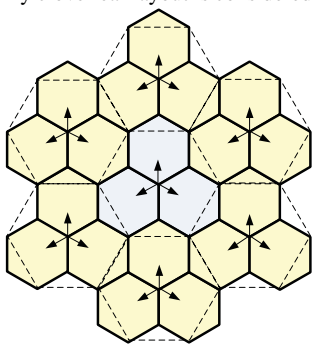

Fig.1. (a) 3-sector "Cloverleaf" layout

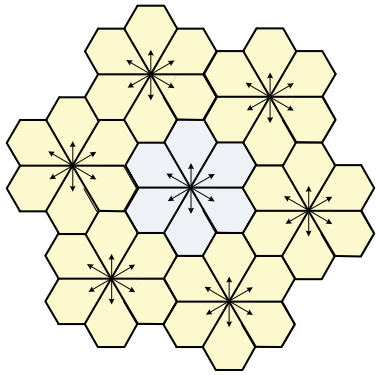

Fig.1. (b) 6-sector "Snow Flake" layout

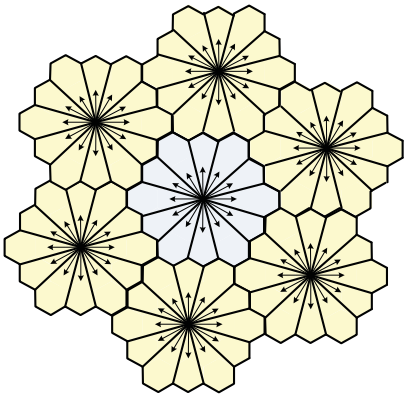

Fig.1. (c) 12-sector "Flower" layout

3. ANTENNA THEORY

The functionality of antenna depends on number of factors including physical size of an antenna, impedance (radiation resistance), beam shape, beam width, directivity or gain, polarization etc [14]. By definition, an antenna array consists of more than one antenna element. The radiation pattern of an antenna array depends on number of antenna elements used in array. The more elements there are, the narrower beam can be formed. Planar arrays are capable of making a narrow beam in horizontal as well as in vertical plane. Therefore, planar array beams are also called "Pencil Beams". Smart antennas with ability of beam steering can be constructed by adding "Intelligence" to planar arrays. Smart antenna improves the coverage of cell by concentrating more power in a narrow beam, enhances the cell capacity and offers increased data rates by offering high signal to interference plus noise ratio [15]. By avoiding interference and increasing signal power, smart antenna improves link quality and helps in combating large delay dispersion [16].

In the research work of this paper, three different type of antenna were taken into account i.e.1) Conventional 65^0 wide beam antenna, 2) Switched beam smart antenna and 3) Full adaptive beam antenna.

3.1. Conventional wide beam antenna

In traditional cellular networks, three-sectored approach with 65^0 wide beam antenna has been in used for long time due to lower interference compared to 120^0 wide beam antenna. To further improve the performance of fixed wide beam antenna, electrical or mechanical tilting can be used [6]. Base station antennas can be dropped down to building walls but then the propagation environment is not any more related to macro cells, rather shifts to micro cell environment. Other possibility is to modify and narrow the radiation pattern with the help of antenna arrays.

3.2. Switched beam smart antenna

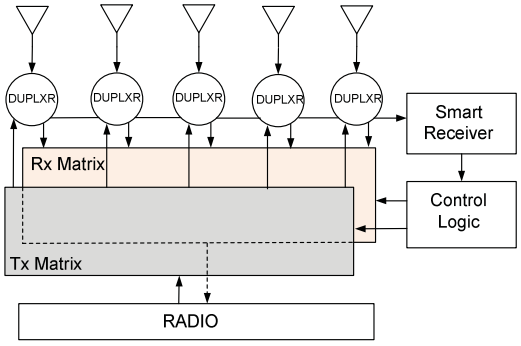

Fig.2. Block diagram of switched beam smart antenna system

Switched beam antenna approach is the extension of conventional cellular sectorisation method, in which single 120^0 wide macro sector is divided into several micro sectors. A switched beam antenna is a combination of multiple narrow beams in predetermined directions, overlapping over each other. It covers the desired cell area with finite number of narrow fixed beams, where each beam can serve a single user or multiple users [3]. Switched beam antenna does not steer or adapt the beam with respect to the desired signal. In this type of antenna, a RF switch connected to fixed beams controls the beam selection based on the beam-switching algorithm. A switch selects the "Optimum" beam to provide service to mobile station. The optimum beam here refers to the beam that offers the highest SINR value. In some cases, maximum received power for the user can be used as a beam selection criterion. During user mobility, switched beam antenna tracks the user and continuously updates the beam selection to ensure high quality of service [17]. The general block diagram of switched beam smart antenna system is shown in Fig.2 [18].

It consists of an array of antennas that divides the macro sector into several micro sectors. A precise switched beam antenna can be implemented by using "Butler Matrices" [16], [18]. It uses a smart receiver for detecting and monitoring the received signal power for each user at each antenna port. Based on the measurement made by the smart receiver and beam selection algorithm, the control logic block determines the most favorable beam for specific user. The RF switch part governed by the control logic (brain of switched beam antenna) activates the path from the selected antenna port to the radio transceiver. Switched beam antenna offers higher directivity with less interference and thus provides gain over conventional antenna. Theoretically, gain of using switched beam antenna over conventional wide single beam antenna is directly proportional to the number of beams. For a given sector containing U beams, resultant increased gain is given by equation (6) [18]. Switched beam approach is simpler and easier to implement compared to fully adaptive beam approach.

$$Gain = 10\text{Log}(U) \qquad (6)$$

An example of the horizontal radiation pattern of 65^0, 32^0, and 16^0 HPBW antenna is depicted in Fig.3a, 3b and 3c respectively. Radiation pattern of seven switched beam antenna with each beam of 8^0 HPBW is shown in Fig.3d.

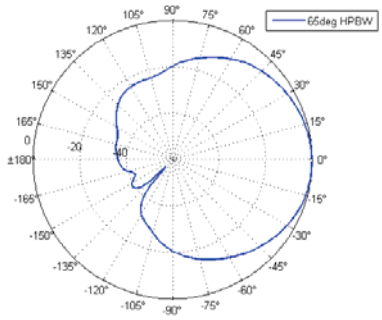

Fig.3. (a) Radiation pattern of conventional 65^0 beamwidth antenna used in 3-sectored site

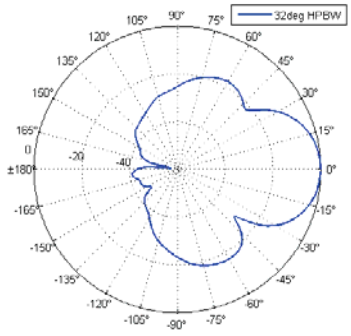

Fig.3. (b) Radiation pattern of narrow 32^0 beamwidth antenna used in 6-sectored site

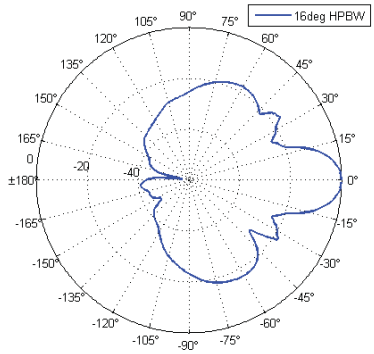

Fig.3. (c) Radiation pattern of narrow 16^0 beamwidth antenna used in 12-sectored site

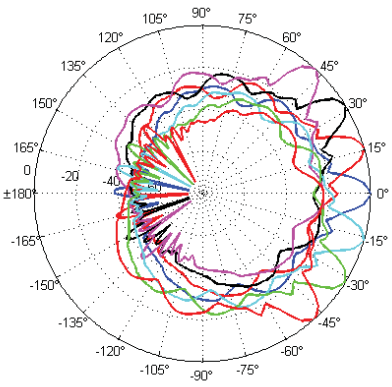

Fig.3. (d) Radiation pattern of switched beam antenna with seven beams of 8^0 HPBW

3.3. Full adaptive beam antenna

Adaptive antenna exploits the array of antenna elements to achieve maximum gain in desired direction while rejecting interference coming from other directions. Adaptive antennas are more complex than multi beam switched antennas. While butler matrices are operating on the RF domain, adaptive antennas use a linear combination of signals, and process them in the baseband. Adaptive antenna can steer its maxima and nulls of the array pattern in nearly any direction in response to the changing environment [16]. The basic idea behind adaptive antenna is the same as in switched beam antenna i.e. to maximize the SINR values. While the multiple switched beam antennas have a limited selection of directions to choose the best beam, an adaptive antenna can freely steer its beam in correspondence to the location of user. Smart antenna employs Direction of Arrival (DOA) algorithm to track the signal received from the user, and places nulls in the direction of interfering users and maxima in the direction of desired user [19]. On the other hand, since adaptive antennas needs more signal processing, multiple switched beam antennas are easier to implement and have the advantage of being simpler, and less expensive compared to adaptive antennas. The overall capacity gain of smart antennas is expected to be in the range of 100% to 200%, when compared with conventional antennas [3].

Beam forming algorithms used in adaptive antennas are generally divided into two classes with respect to the usage of training signal i) Blind Adaptive algorithm and ii) Non-Blind Adaptive algorithm [20]. In a non-blind adaptive beam forming algorithm, a known training signal d(t) is sent from transmitter to receiver during the training period. The beamformer uses the information of the training signal to update its complex weight factor. Blind algorithms do not require any reference signal to update its weight vector; rather it uses some of the known properties of desired signal to manipulate the weight vector. Fig.4 shows the generic beam forming system based on non-blind adaptive algorithm, which requires a training (reference) signal [19].

The output of the beamformer at time n, $y(n)$, is given by a linear combination of the data at the k antenna elements. The baseband received signal at each antenna element is multiplied with the weighting factor which adjusts the phase and amplitude of the incoming signal accordingly. The sum of this weighted signal results in the array output $y(n)$. On the basis of adaptive algorithms, entries of weight vector $\boldsymbol{w}$ are adjusted to minimize the error $e(n)$ between the training signal $d(n)$ and the array output $y(n)$. The output of the beamformer $y(n)$ can be expressed as given in equation (7), [20]

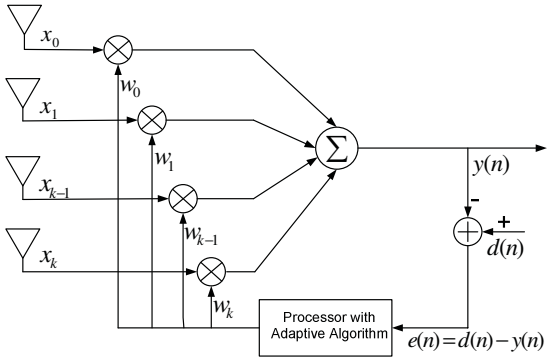

Fig.4. Block diagram of adaptive beamforming system

$$y(n) = \boldsymbol{w}^H(n)\boldsymbol{x}(n) \qquad (7)$$

$$\boldsymbol{w}(n) = [w_1(n)\ \ w_2(n) \ldots\ldots w_{k-1}(n)\ \ w_k(n)] \qquad (8)$$

$$\boldsymbol{x}(n) = [x_1(n)\ \ x_2(n) \ldots\ldots\ldots x_{k-1}(n)\ \ x_k(n)] \qquad (9)$$

$$e(n) = d(n) - y(n) \qquad (10)$$

where $\boldsymbol{w}(n)$ is the weight vector with $w_k(n)$ a complex weight for kth antenna element at time instant n, and $[.]^H$ denotes Hermitian (complex conjugate) transpose. $x_k(n)$ is the received baseband signal at kth antenna element [9], [20]. Least Mean Square (LMS), Normalized Least Mean Square (NLMS), Recursive Least Squares (RLS), and Direct Matrix Inversion (DMI) are examples of non-blind adaptive algorithm, whereas Constant Modulus Algorithm (CMA) and Decision Directed (DD) algorithms are examples of blind adaptive algorithm [9], [19-20]. These beamforming algorithms have their own pros and cons as far as their computational complexity, convergence speed, stability, robustness against implementation errors and other aspects are concerned.

4. SYSTEM SIMULATIONS

4.1. Simulation Environment

MATLAB was used as a simulation tool for carrying a campaign of simulations. Monte Carlo type of simulation was done with 5000 iterations with multiple users. It was aimed to model a network as realistic as possible. All system simulations for three sectored sites were done with macro cell cloverleaf layout. Snow flake and flower tessellation was selected for 6-sector 12-sector sites respectively. Base station grid of 19 sites was built, where single middle site in the middle has six sites in the first tier of interferer, and 12 sites in the second tier of interferer. All the interfering sites were at equal Intersite Distance (ISD) as shown in Fig.5(a,b,c), with same site parameters. Base station antenna height was set to 25m, which is typical value in city centre areas where 5-7 floor buildings exists. Power required for common pilot channel and signaling was taken into account. Frequency band of 2100MHz was used in simulations because DC-HSDPA system was selected as an example technology. Simulations were done with flat terrain, and Okumura-Hata model was used for calculating path loss between user and NodeB. Fading component is modelled with log normal distribution having zero mean and 5dB of standard deviation. Orthogonality factor used in equation (4) for computing own cell interference follows

Gaussian curve with maximum of 0.97 at site location and 0.7 at cell edge.

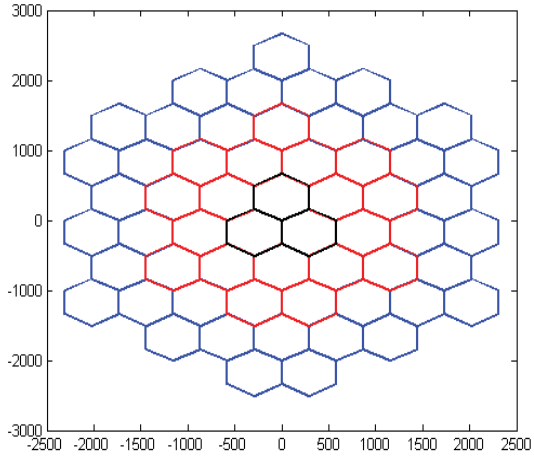

Fig.5. (a) Grid of nineteen 3-sector sites used in simulation with clove-leaf topology

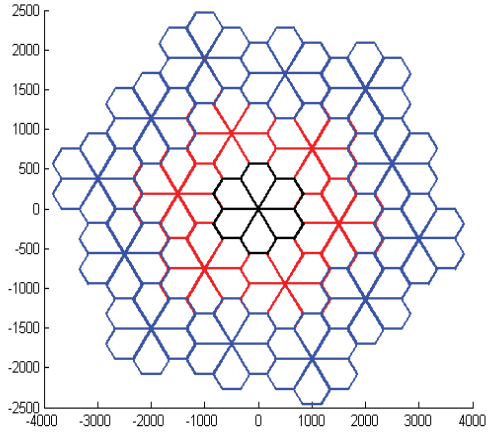

Fig.5. (b) Grid of nineteen 6-sector sites used in simulation with snow flake topology

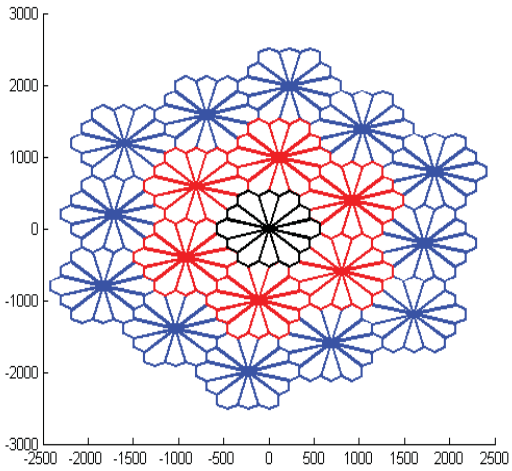

Fig.5. (c) Grid of nineteen 12-sector sites used in simulation with flower topology

4.2. Simulation cases and simulation procedure

Following three cases were considered for simulations.

- **3 Sector:** It is the most common scenario in which each site has three sectors and every sector has single 65^0 half power beamwidth antenna. This acts a reference case for comparing with higher order sectorization and advanced antenna case. Fig.3a shows the radiation pattern of an antenna used for simulations, with no electrical or mechanical tilt, and with maximum antenna gain of 15.39dB.
- **6 Sector:** It is the case in which each site has six sectors, and every sector has single 32^0 half power beamwidth antenna. Fig.3b shows the radiation pattern of an antenna used for simulations, with no electrical or mechanical tilt, and with maximum antenna gain of 18.20dB.
- **12 Sector:** In this case, each site comprises of 12 narrow sectors, and every sector has 16^0 HPBW antenna. Fig.3c shows the radiation pattern of an antenna used for simulations, with no electrical or mechanical tilt, and with maximum antenna gain of 21.15dB.
- **7 Switched beams:** This case represents multiple fixed switched beam scenario, where single sector is covered by seven potential narrow beams. Each narrow beam has eight degree HPBW with a spacing of 16^0 between the beams as shown in Fig.3d. Only that beam which has smallest deviation angle with respect to its main beam for user becomes active for that particular user. No down tilting was assumed, and each beam has maximum antenna gain of 23.55dB.
- **Adaptive beam:** In this last scenario, adaptive antennas are used to form an accurate beam for each individual user. In this scenario, narrow beam of six degree in the horizontal plane is steered precisely to the serving user, keeping user in the middle of the beam for maximum gain. Adaptive antenna have maximum gain of 24.5dB.

Key parameters related to DC-HSDPA systems used in simulations are presented in Table I. For each iteration, 5 users with full traffic buffer in each cell were created. Users were homogenously spread over the whole cell area on the flat terrain. In this simulation, DC-HSDPA serves five code multiplexed users per Transmission Time Interval (TTI). Out of total 16 codes, maximum of 15 codes were available for High Speed Physical Downlink Shared Channel (HS-PDSCH). Total

transmission power for HS-PDSCH and available codes were equally distributed among the five users in each TTI. In the serving cell to compute the received signal value, Okumura-Hata model was used to calculate the path loss between the user and serving NodeB. Simulator supports Adaptive Modulation and Coding (AMC), and in these simulations eight different Modulation and Coding Schemes (MCS) were considered with 64QAM 5/6 coding rate as highest and QPSK 1/2 coding rate as lowest possible MCS. As throughput is the function of SINR, hence later SINR information was employed to compute each user throughput. Cell throughput in each TTI is the sum of individual users' throughput. Post processing of data was done to get the results in refined form.

Table I. General DC-HSDPA simulation parameters

Parameter	*Unit*	*Value*
DC-HSDPA Downlink		
Users per TTI	No.	5
Operating frequency band	MHz	2100
Bandwidth	MHz	5 + 5
Chip rate	Mcps	3.84
Total HS-PDSCH Codes	No.	15
Max HS-PDSCH power	dBm	41.63
HS-SCCH power	dBm	26
Processing gain	dB	12.04
HSDPA loading	%	70
Interference margin	dB	5.2
UE noise figure	dB	8.0
Downlink activity factor		1.0

5. SIMULATION RESULTS AND ANALYSIS

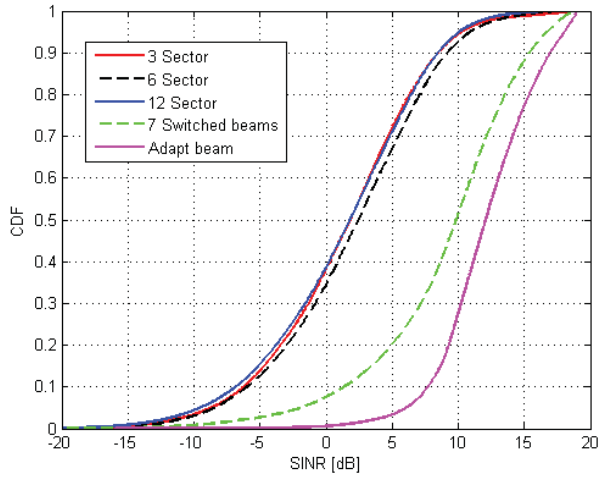

Fig.6. CDF plot of user SINR with 5 users per TTI at 1000m ISD

Fig.6 shows the Cumulative Distribution Function (CDF) of the user SINR with 5 users per TTI at 1000m ISD for different cases. Clearly switched beam antenna shows better performance in terms of offering higher SINR compared to 65^0, 32^0, and 16^0 wide beam antenna used in 3-sector, 6-sector and 12 sector sites respectively. But adaptive beam antenna outperforms and shows superior performance compared to all other cases. By analyzing the curves shown in Fig.6 it can be deduced that adaptive and switched beam antennas served the purpose of improving user experience by reducing the interference and enhancing the received SINR. The CDF curve of SINR for the case of adaptive beam is on the extreme right position, indicating that the SINR for the users is improved on average. It is also important to note that the average user SINR does not deteriorate by increasing the order of sectorization and almost similar performance is shown by 3-sector, 6 sector and 12-sector sites. However, 6-sector site offers slightly better performance compared to 3 and 12-sector sites. Adaptive beam antenna performed well in the close vicinity of the NodeB as well as near the cell edge, as 80% of the samples are concentrated in a narrow range of 9.12dB, starting from 7.72dB to 16.84dB of user SINR. But for other traditional antenna cases, eighty percent of SINR values has wide span and spread over the range of around 14.96dB, starting from -6.3 to 8.66dB. Statistical analysis of user SINR is presented in Table II.

Table II. Statistical Analysis of User SINR

	10 percentile user SINR (dB)	***50 percentile user SINR (dB)***	***90 percentile user SINR (dB)***	***Mean user SINR (dB)***	***STD user SINR (dB)***	***Relative SINR gain (dB***
3-Sector	-6.22	1.83	8.51	1.44	5.89	0
6-Sector	-5.99	2.44	9.22	1.98	5.96	0.54
12-Sector	-6.87	1.78	8.50	1.23	6.05	-0.21
7 Switched beam	1.36	9.83	15.41	8.94	5.72	7.50
Adaptive beam	7.72	12.10	16.97	12.07	3.73	10.63

Relative SINR gain shown in Table II is the relative gain in dB with respect to the mean SINR value of 3-sector case. It was learned that adaptive and switched beam antennas offer 10.63dB and 7.50dB respectively better user SINR compared to traditional wide antenna used in 3-sector site at 1000m intersite distance.

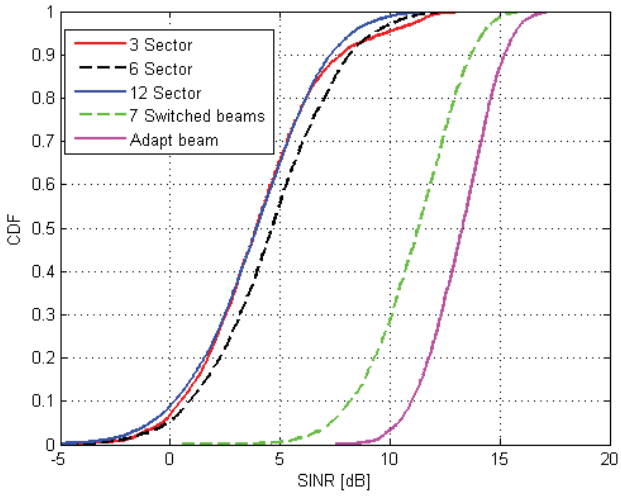

Fig.7. CDF plot of cell SINR with five users per TTI at 1000m ISD

Fig.7 shows the cumulative distribution function of SINR value averaged over the whole cell with 5 users per TTI at 1000m ISD for different simulated cases. Averaged SINR value over the whole cell area in each iteration of Monte Carlo simulation was obtained by adding the linear SINR value of each user and then divide the sum by number of users served per TTI. It can be seen that 6-sector deployment helps in improving the cell SINR by a small margin of 0.51dB only compared to 3-sector deployment, but a significant improvement of 7.02dB and 9.11dB is witnessed in case of switched beam and adaptive beam case respectively. Smart antennas not only improve the user experience rather they improve the overall cell SINR as well. It is also evident that the multiple switched beam antenna offers improvement in SINR but the difference is smaller compared to adaptive antenna. Statistical analysis of cell SINR is given in Table III.

Table III. Statistical Analysis of SINR over whole Cell

	10 percentile cell SINR (dB)	***50 percentile cell SINR (dB)***	***90 percentile cell SINR (dB)***	***Mean cell SINR (dB)***	***STD cell SINR (dB)***	***Relative SINR gain (dB***
3-Sector	0.49	3.91	7.79	4.07	2.94	**0**
6-Sector	0.91	4.63	8.14	4.58	2.85	**0.51**
12-Sector	0.21	3.94	7.31	3.84	2.80	**-0.23**
7 Switched beam	8.19	11.28	13.68	11.09	2.14	**7.02**
Adaptive beam	10.96	13.29	15.21	13.18	1.63	**9.11**

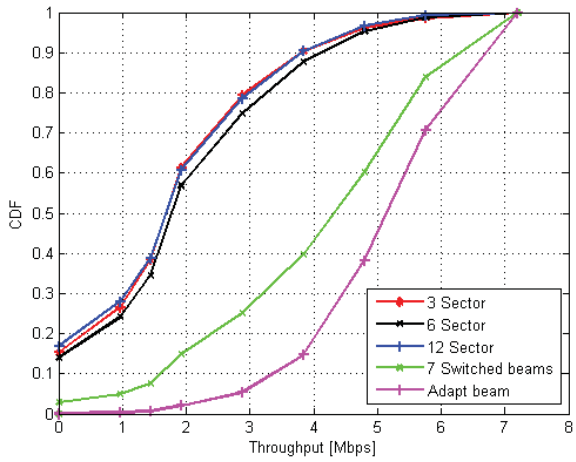

Fig.8. CDF plot of user throughput with 5 users per TTI at 1000m ISD

Fig.8. shows the CDF of the user throughput of DC-HSDPA network with 5 users per TTI at 1000m ISD for different antenna solutions. Eight marks on CDF plots represent eight different MCS. As equal codes and equal power was distributed among the users, therefore high throughput samples show that high modulation and coding scheme was used by the user. High MCS are less robust against interference and thus have high requirement of SINR. It is interesting to note that around 4.5% of the users were able to adapt 64QAM in 3-, 6-, and 12-sector case, whereas this number was raised to 39.98% and 61.8% by switched and adaptive beam antennas respectively. As seen from the results, more than 85% of the samples with adaptive beam were obtained with three highest MCS. Samples of zero throughputs in CDF plots represent the users with no data transfer due to very low SINR. It was also noted that single wide beam antenna keeps the probability of no data transfer at almost 15%. Whereas, switched beam antenna and adaptive beam antenna show remarkable improvement in probability of no data transfer and kept it at negligible level of 2.88% and 0.16% respectively. These results clearly indicate the impact of advanced antenna techniques in improving the user experience, when other cells are heavily loaded and are severely interfering the serving cell.

Fig.9 shows the CDF of cell throughput achieved by using DC-HSDPA with equal power and equal codes allocation for different network tessellation and antenna techniques. Cell throughput in each TTI was computed by summing the individual throughput of the served users. Like in previous results, case adaptive beam lead the comparison and shows extra ordinary performance compared to other network tessellations and antenna types in terms offering higher cell throughput. Almost identical cell throughput is achieved in 3-sector and 12-sector case, but 6-sector offers slightly better capacity. High SINR values showed in Fig.7 is translated into high throughput values in Fig.9. Adaptive beam antenna exhibits better performance and offers 27.99Mbps of average cell throughput compared to 22.81Mbps by switched beam case. 10 percentile cell throughput shows that 90% of the cell throughput samples with adaptive beam were above 24Mbps, and with switched beam 90% of the samples were above 17.28Mbps. Relative throughput gain is the relative gain in percentage value compared to 3-sector case. In [9], it was expected to get 100-200% improvement in cell capacity by smart adaptive antennas, and the results shown in Fig.9 are in line with the expectation. Adaptive beam shows a significant

relative gain of 156.7%, however switched beam have relative gain of 109.27%. Statistical analysis of cell throughput is shown in Table IV.

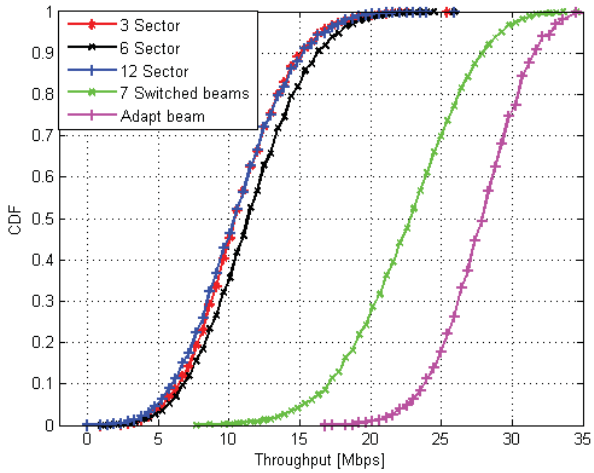

Fig.9. CDF plot of cell throughput with five users per TTI at 1000m ISD

Table IV. Statistical Analysis of Cell Throughput

	10 percentile cell throughput ***(Mbps)***	*50 percentile cell throughput* ***(Mbps)***	*90 percentile cell throughput* ***(Mbps)***	*Mean cell throughput* ***(Mbps)***	*STD cell throughput* ***(Mbps)***	*Relative throughput gain* ***(%)***
3-Sector	6.72	10.56	15.36	10.90	3.40	**0**
6-Sector	7.20	11.52	16.32	11.72	3.67	**7.52**
12-Sector	6.24	10.56	15.36	10.77	3.59	**-1.20**
7 Switched beams	17.28	23.04	28.32	22.81	4.23	**109.27**
Adaptive beam	24.0	28.32	31.68	27.99	3.03	**156.70**

Fig.10 shows the mean cell throughput of the DC-HSDPA cell with five users per TTI against the intersite distance for different cases. The trend of the sectored antenna cases and switched beam antenna case show that average cell throughput increases by increasing the intersite distance. Small intersite distance corresponds to small cells; hence, the high interference coming from the neighbor cells limit the cell throughput. The variations in the cell throughput for all cases except the adaptive antenna case were caused by the fact that larger the intersite distance, smaller will be the impact of interfering cells and hence larger will be the achieved average cell throughput. However, for adaptive antenna case cell throughput is inversely proportional to the intersite distance. The results show that a deployment of smart antennas significantly enhances the average cell throughput irrespective of the ISD. The highest cell throughput was achieved with adaptive beam antenna at small ISD of 250m. However, the worst capacity is offered by 12-sector antenna at 3000m ISD. It means higher order of sectorization not necessarily offers better cell throughput.

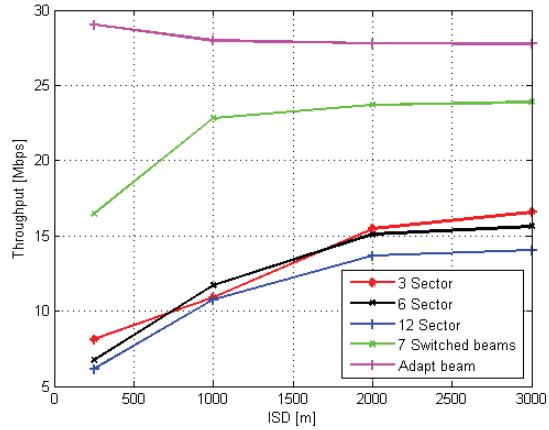

Fig.10. Mean cell throughput with five users per TTI against ISD

Fig.11 shows the achieved mean site throughput for DC-HSDPA system against the intersite distance for different cases. As seen in Fig.11, applying higher order sectorization and deploying advance antenna techniques provides significant throughput gain over traditional 3-sector site topology. Relative site throughput gain for 6-sector and 12-sector topology is higher at large intersite distances than small ISD. With respect to the reference case of 3-sector site at 1000m ISD, when intersite distance is reduced to 250m (small cell) for 3-sector site, mean site throughput is reduced by 25.41%. However, a relative throughput gain of approximately 23.67% and 125.69% is achieved by 6-sector and 12-sector sites respectively at 250m ISD, which is comparatively small compared to 164.04% and 401.65% by 6 and 12-sector sites respectively at 2000m ISD. Adaptive antenna beam outperformed at 250m ISD and was found more effective at small ISD. More detailed analysis of site throughput and the relative gain is presented in Table V. Relative gains shown in Table V are with respect to reference case 3-sector site at 1000m ISD. Negative value of gains means inferior performance.

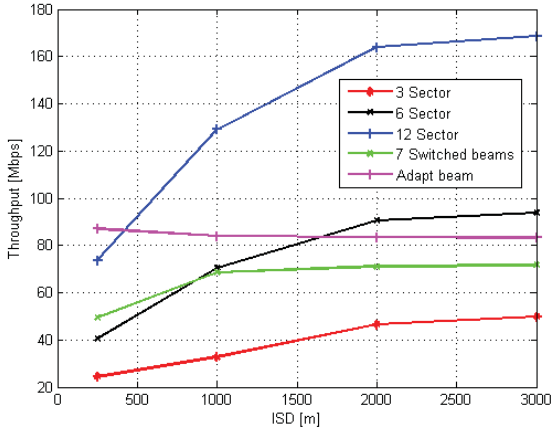

Fig.11. Mean site throughput with five users per TTI against ISD

Table V presents the average downlink throughput and relative sector (cell) gain with respect to 3-sector at 1000m ISD (reference case).

Table V. Statistical Analysis of Cell Throughput

	Mean cell throughput ***(Mbps)***	*Relative cell throughput gain (%)*	*Mean site throughput* ***(Mbps)***	*Relative site throughput gain (%)*
ISD = 250 meter				
3-Sector	8.13	**-25.41**	24.39	**-25.41**
7 Switched beams	16.48	**51.20**	49.44	**51.20**
Adaptive beam	29.01	**166.15**	87.03	**166.15**
6-Sector	6.74	**-38.17**	40.44	**23.67**
12-Sector	6.15	**-43.57**	73.80	**125.69**
ISD = 1000 meter as reference				
3-Sector	10.90	**0**	32.70	**0**
7 Switched beams	22.81	**109.27**	68.43	**109.27**
Adaptive beam	27.98	**156.70**	83.94	**156.70**
6-Sector	11.72	**7.52**	70.38	**115.23**
12-Sector	10.77	**-1.20**	129.24	**295.23**
ISD = 2000 meter				
3-Sector	15.49	**42.11**	46.47	**42.11**
7 Switched beams	23.71	**117.53**	71.13	**117.53**
Adaptive beam	27.80	**155.05**	83.40	**155.05**
6-Sector	15.10	**38.53**	90.60	**177.06**
12-Sector	13.67	**25.41**	164.04	**401.65**
ISD = 3000 meter				
3-Sector	16.58	**52.11**	49.74	**52.11**
7 Switched beams	23.89	**119.17**	71.67	**119.17**
Adaptive beam	27.75	**154.58**	83.25	**154.58**
6-Sector	15.63	**43.39**	93.78	**186.79**
12-Sector	14.06	**28.99**	168.72	**415.97**

6. CONCLUSION

In this article, we investigated advance antenna techniques along with different network tessellations including cloverleaf topology for 3-sector sites, snow flake topology for 6-sector sites and proposed a novel flower topology for 12-sector sites in DC-HSDPA network. Impact of intersite distance on the performance of higher order sectorization and on the performance of adaptive and switched beam antenna was also taken into account. A comprehensive set of simulation results were demonstrated together with a performance analysis. Post simulation analysis confirms that the capacity gain achieved by higher order sectorization and switched beam antenna increases by increasing the ISD. However, adaptive beam antenna also significantly improves the cell SINR and cell throughput, but adaptive antenna is more effective in small cells compared to large ISD. The simulation results revealed that the average cell SINR does not deteriorate much by having higher order sectorization, however 6-sector site provides around 0.5dB better cell SINR compared to 3-sector site. At 1000m ISD, the cell SINR is improved by approximately 7.02dB and 9.11dB when switched beam and adaptive beam antennas were used respectively compared to traditional 3-sector site with 65^0 beamwidth antenna. Significant improvement was also witnessed in terms of average cell throughput, it was found that the average cell throughput increased by 109.3% with multiple switched beam antenna, and 156.7%

with adaptive beam antenna compared to 3-sector site at 1000m ISD. Adaptive beam antenna outperformed and offered high SINR, high throughput with low probability of no data transfer. Multiple switched beam antenna showed better performance compared to single beam antenna but inferior to adaptive beam. Three-sector and higher order sectorization offer almost 15% of probability of no data transfer for the user at 1000m ISD. Switched beam antenna helps in improving the probability of no data transfer and kept it at almost 2.88%, but adaptive antenna significantly improved probability of no data transfer and brought it down to 0.16% at 1000m ISD. Simulation results revealed that the user experience and the macro cell capacity can be significantly improved by deploying smart antennas. Higher order sectorization does not improve much the cell (sector) capacity, but definitely offers higher site capacity. Especially at large ISD, high order sectorization is more effective and significantly increases the site capacity. To avoid the deployment of small cells, usage of adaptive and switched beam antennas or higher order sectorization can be considered as an alternate choice.

The results were obtained by using semi-statistic simulations with Okumura-Hata propagation model, and thus may cause offset type of error in all results. However, the obtained results are still comparable with each other to show capacity improvements. For future work, it would be interesting to see the performance of fixed switched beam antenna with narrower and even more number of beams in a cell, as in this paper seven beams of 8^0 were considered in each cell.

ACKNOWLEDGEMENTS

Authors would like to thank Tampere University of Technology, European Communications Engineering (ECE) Ltd. and Tampere Doctoral Program of Information Science and Engineering (TISE) for supporting the research work of this paper.

REFERENCES

[1] W.C.Y. Lee, “Mobile communications design fundamentals”, John Wiley & Sons, Inc., 1993.
[2] L. C. Wang, K. Chawla, L. J. Greenstein, “Performance Studies of Narrow-Beam Trisector Cellular Systems,” International Journal of Wireless Information Networks, Vol. 5, No. 2, 1998, pp. 89-102.
[3] I.V. Stevanović, A. Skrivervik, J. R. Mosig, “Smart antenna systems for mobile communications”. Laboratoire d'Electromagnetisme et d'Acoustique Ecole Polytechnique Federale de Lausanne, January 2003.
[4] A. Wacker, J. Laiho-Steffens, K.Sipilä, K. Heiska, “The impact of the base station sectorisation on WCDMA radio network performance,” in Proc. 50th IEEE Vehicular Technology Conference, 1999, pp. 2611-2615.
[5] B. C. V. Johansson, S. Stefansson, “Optimizing Antenna Parameters for Sectorized W-CDMA Networks,” in Proc. IEEE Vehicular Technology Conference, 2000, pp. 1524-1531.
[6] J. Niemelä, T. Isotalo, J. Lempiäinen, “Optimum Antenna Downtilt Angles for Macrocellular WCDMA Network,” EURASIP Journal on Wireless Communications and Networking, vol. 5, 2005.
[7] J. Itkonen, B. Tuszon, J. Lempiäinen, “Assessment of network layouts for CDMA radio access”, EURASIP Journal on Wireless Communications and Networking, Volume 2008
[8] J. Lempiäinen, M. Manninen, “Radio interface system planning for GSM/GPRS/UMTS”, Kluwer Academic Publishers. 2001.
[9] C.S. Rani., P.V. Subbaiah., K.C. Reddy, “LMS and RLS Algorithms for smart antennas in a CDMA mobile communication environment”. International Journal of the Computer the Internet and Management (IJCIM), Vol.16 No.2, May-August 2008.
[10] E. Dahlman, S. Parkvall, J. Skold, "3G Evolution: HSPA and LTE for mobile broadband", Academic press, First edition, 2007.
[11] K. Johansson, J. Bergman, D. Gerstenberger, M. Blomgren, A. Wallen, "Multi-carrier HSPA evolution", Vehicular Technology Conference, 2009. VTC Spring 2009. IEEE 69th , pp.1-5, 26-29 April 2009.

[12] D. Soldani, M. Li, and R. Cuny, "QoS and QoE management in UMTS cellular systems". John Wiley & Sons Ltd, 2006.
[13] A. Chheda, F. Bassirat, " Enhanced cellular network layout for CDMA networks having six-sectored cells ", U.S.Patent 5960349, 28th September 1999.
[14] J. D. Kraus, R. J. Marhefka, "Antennas for all applications". 3rd ed. 2001, McGraw-Hill.
[15] R. Kawitkar, "Issues in deploying smart antennas in mobile radio networks," Proceedings of World Academy of Science, Engineering and Technology Vol.31, July 2008, pp. 361-366, ISSN 1307-6884.
[16] A. F. Molisch, "Wireless communications". 2nd edition. UK 2011, John Wiley & Sons Ltd.
[17] D. Cabrera, J. Rodriguez, "Switched beam smart antenna BER performance analysis for 3G CDMA cellular communication", Computer Research Conference CRC2004, Puerto Rico, April 2004.
[18] A.U. Bhobe, P.L. Perini, "An overview of smart antenna technology for wireless communication", IEEE Aerospace Conference, Vol.2, pp. 875-883, 2001.
[19] C.S. Rani., P.V. Subbaiah., K.C. Reddy, "Smart antenna algorithms for WCDMA mobile communication systems", International Journal of Computer Science and Network Security (IJCSNS), Vol.8 No. 7, July 2008.
[20] S. Hossain, M.T. Islam, S. Serikawal, "Adaptive beamforming algorithms for smart antenna systems", International conference on control, automation and systems, ICCAS 2008. p. 412–416.

Authors

Muhammad Usman Sheikh was born in Rawalpindi, Pakistan, in 1983. He received the B.S. degree in Electrical Engineering (Telecommunication) from COMSATS Institute of Information Technology, Islamabad, Pakistan, in 2006. He received the M.S. degree in Radio Frequency Electronics from Tampere University of Technology (TUT), Finland, in 2009. Currently, he is working towards the Dr. Tech. degree. His main research interests are radio network planning aspects of GSM/UMTS/LTE networks and traffic handling in the multilayer networks. He is student member of IEEE.

Jukka Lempiäinen was born in Helsinki, Finland, in 1968. He received an MSc, Lic Tech, Dr Tech. all in Electrical Engineering, from Helsinki University of Technology, Espoo, Finland, in 1993, 1998 and 1999, respectively. He is a Senior Partner and the President of European Communications Engineering Ltd. He has altogether more than ten years experience in GSM based mobile network planning and consulting. Currently, he is also a part-time Professor of the Telecommunications (Radio Network Planning) at Tampere University of Technology, Finland. He has written two international books about GSM/GPRS/UMTS cellular radio planning, several international journal and conference papers and he has three patents. He is URSI National Board Member, Finland.

Hans Ahnlund was born in Porjus, Sweden in 1968. He received his M.Sc. (EE) degree from Lund University of Technology in 1994. He is Vice President and board member of European Communications Engineering. He is one of the authors of the book 'UMTS Radio Network Planning, Optimization and QoS Management'. He holds two patents in the wireless technology sector.

PUBLICATION	P8

Sheikh, M.U., and Lempiäinen J., "Will New Antenna Materials Enable Single Path Multiple Access (SPMA)?", *in Springer Journal on Wireless Personal Communications*, vol. 78, no. 2, pp. 979-994, September 2014.
DOI: 10.1007/s11277-014-1796-x.

Tampereen teknillinen yliopisto
PL 527
33101 Tampere

Tampere University of Technology
P.O.B. 527
FI-33101 Tampere, Finland

ISBN 978-952-15-3402-7
ISSN 1459-2045